

Diaphragms arrangement:

- 1 @ each end of beam
- 2 @ quarter points
- 2 @ center of span (11 ft apart)

TPT= 104,500 lb/diaphragm

TPT= 104,500 lb/diaphragm

TPT= 104,500 lb/diaphragm

CL

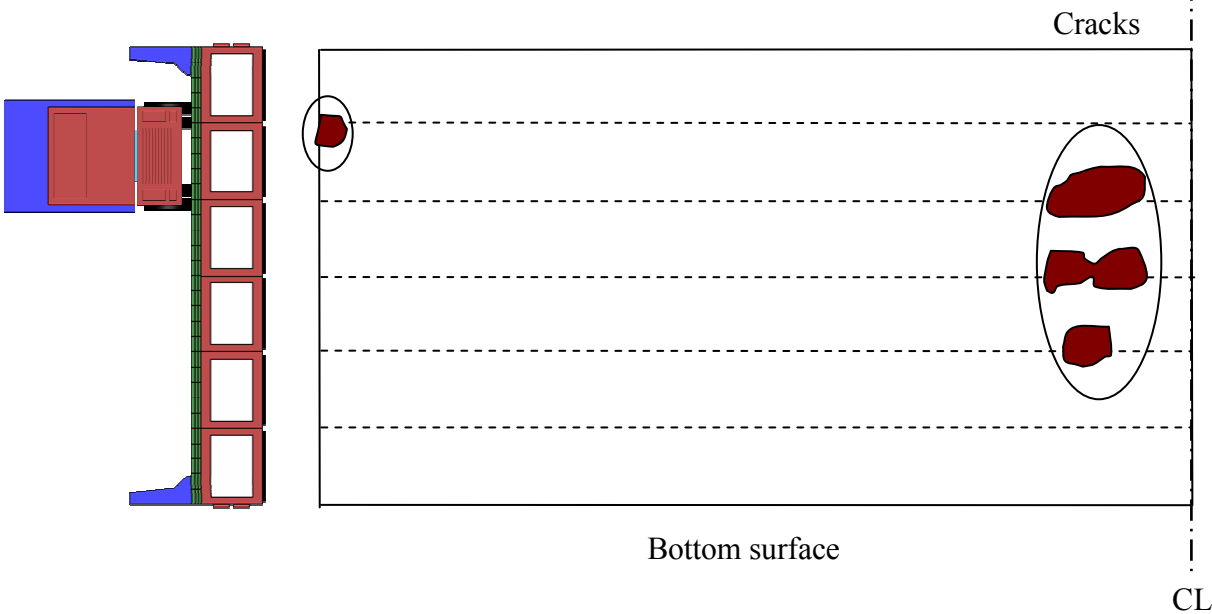
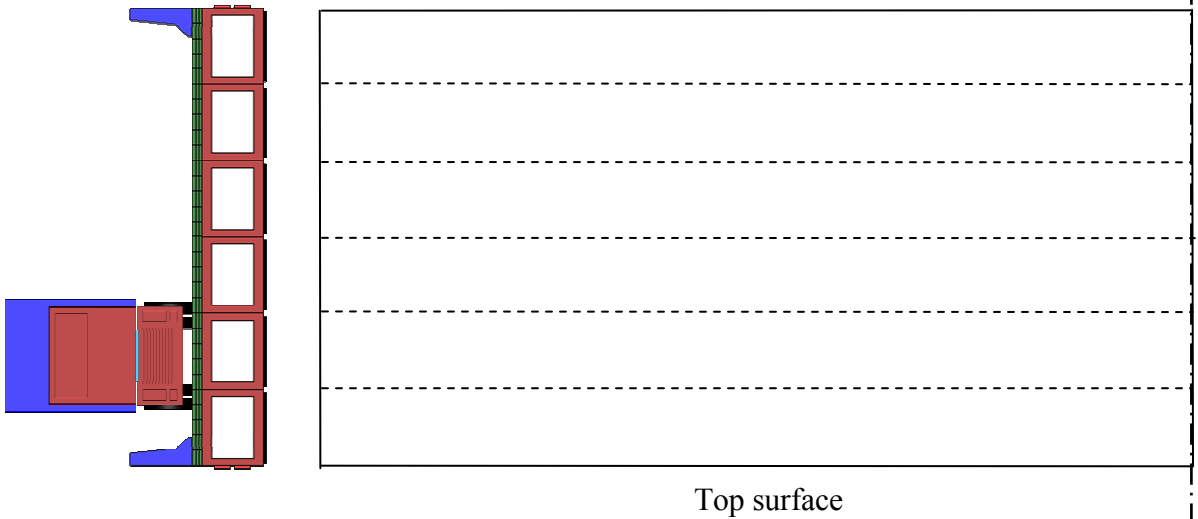


Figure 4.2-21 Crack development in the slab after applying equivalent AASHTO HS-25 truck.

Diaphragms arrangement:

- 1 @ each end of beam
- 2 @ quarter points
- 2 @ center of span (11 ft apart)

TPT= 104,500 lb/diaphragm

TPT= 104,500 lb/diaphragm

TPT= 104,500 lb/diaphragm

CL

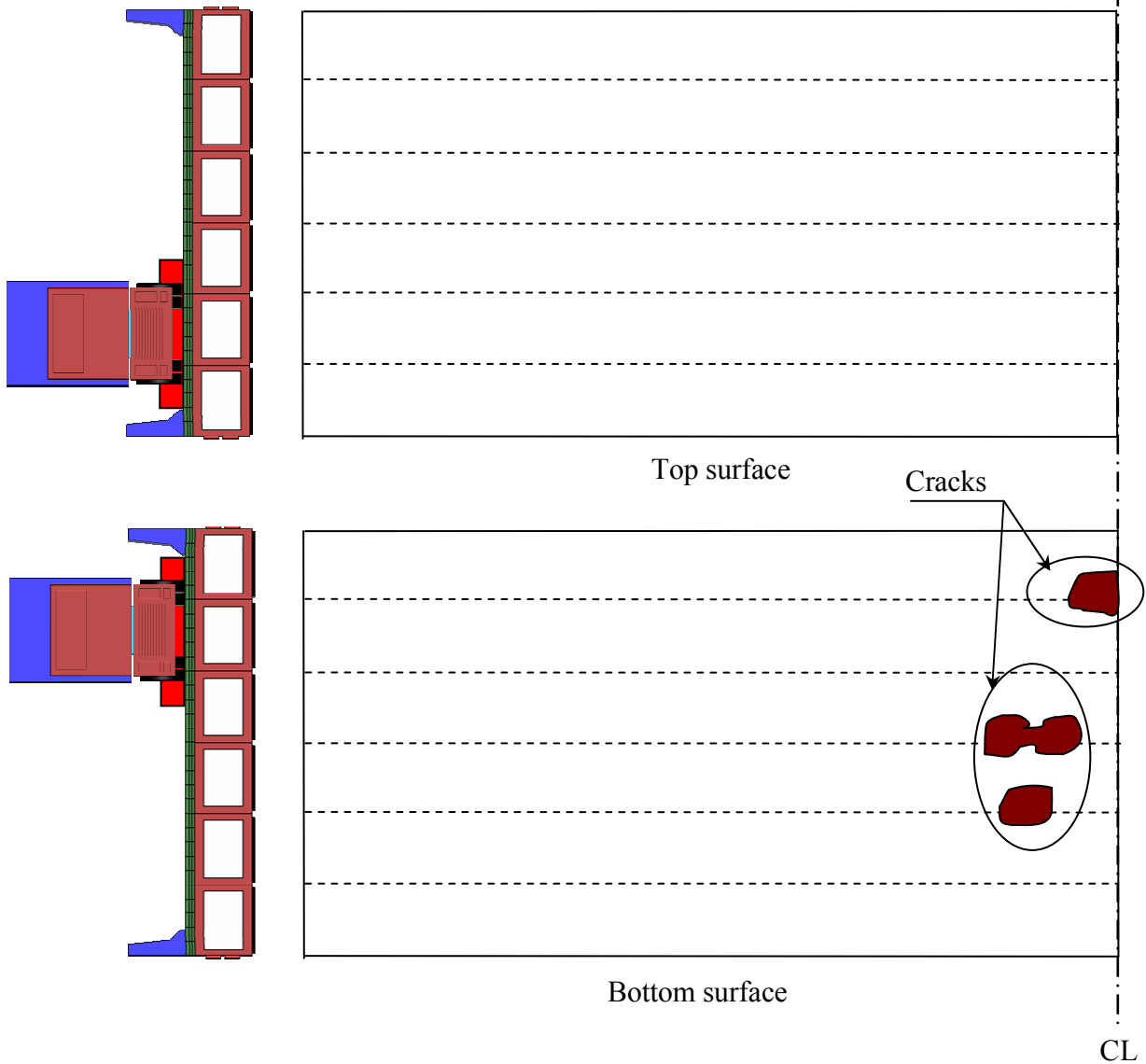


Figure 4.2-22 Crack development in the slab after applying equivalent AASHTO HL-93 load.

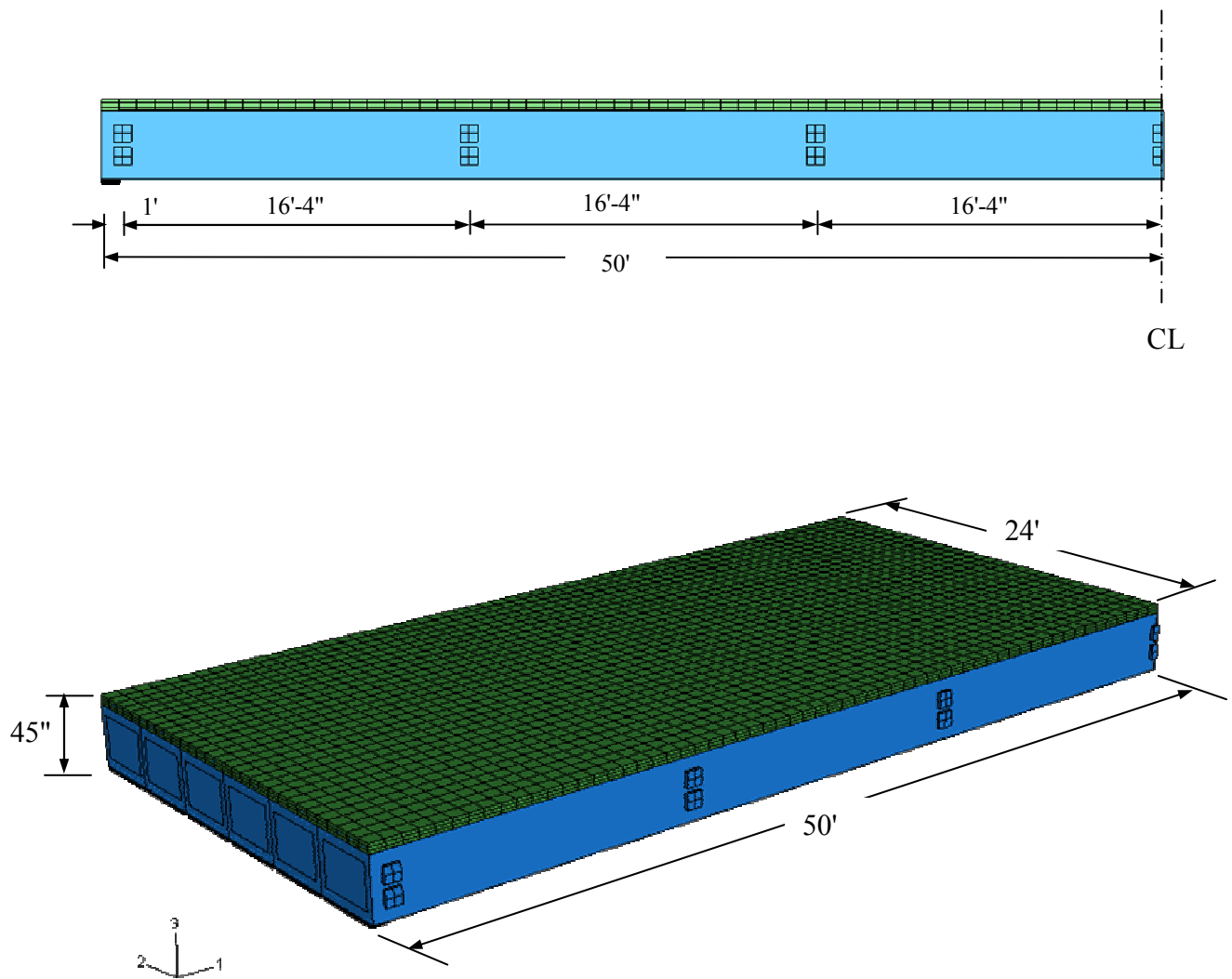


Figure 4.2-23 Assembly for modified 100 ft span bridge model.

Table 4.2-3 Maximum principal stress in the deck slab of 100 ft span bridge model under service loads.

Model	No. of Diaphragms	TPT Force lb/diaphragm	MP Positive Gradient (psi)	MP LL+ IM (psi)	
				HS-25 truck	HL-93 load
Span = 100 ft Width = 24 ft	6	104,000	254	N/A (cracks)	N/A (cracks)
	6	150,000	247	N/A (cracks)	N/A (cracks)
	7	150,000	234	353	351

- MP: Maximum principal stresses
- LL: Live load
- IM: Impact allowances
- N/A: Not available

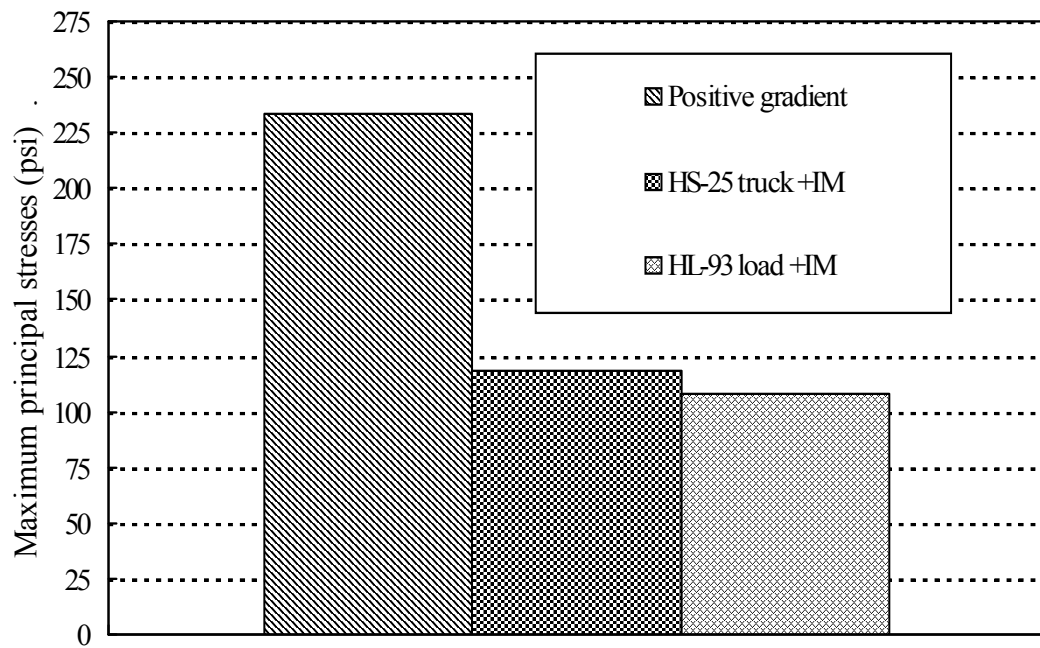


Figure 4.2-24 Service loads contribution in deck slab principal stresses (Case of seven diaphragms, TPT =150,000 lb/diaphragm).

4.2.4.4 124 ft Span Bridge Model

This FE model simulated a bridge with span of 124 ft and width of 24 ft. Half of the span was modeled, and equivalent loads were used to simulate the live loads. The ratio used to transfer the AASHTO HS-25 truck load effect to its equivalent of the lane load was $M_{truck} = 1.36 M_{lane}$. Similarly, the ratio used to transform the truck effect to the tandem effect in AASHTO HL-93 load was $M_{truck} = 1.30 M_{tandem}$.

The first model was provided with a TPT arrangement that conformed to the MDOT Specifications (2006), which require seven diaphragms for this span (Figure 4.2-25); two diaphragms at the ends and five equally spaced diaphragms in-between. To satisfy the flexural requirements, the box-beam depth was determined to be 54 in. Two transverse strands were provided per diaphragm, with each transverse strand prestressed with a force equal to 52,250 lb (total of 104,500 lb/diaphragm).

Applying the positive temperature gradient increased the longitudinal compressive stresses in the slab top and bottom surfaces. In the transverse direction, the compressive stresses increased to 610 psi at the slab ends, while the majority of the slab experienced compressive stresses in the range of 272 and 347 psi. At the same time, high transverse tensile stresses of about 251 psi developed in the slab bottom surface. Similarly, the maximum principal stresses increased to 285 psi (tension) at the slab bottom surface, while the top surface experienced maximum principal stresses averaging zero psi. The deck slab experienced cracks, as shown in Figure 4.2-26 and Figure 4.2-27 after applying equivalent AASHTO HS-25 truck load and equivalent AASHTO HL-93 load, respectively.

To prevent the crack development, the TPT force level was increased from 104,500 lb/diaphragm to 150,000 lb/diaphragm, without changing the number of diaphragms or their arrangement. No cracks developed after applying the positive temperature gradient; yet, the cracks developed when applying live loads.

Without changing the diaphragms number, a TPT force equal to 200,000 lb/diaphragm was applied. Increasing the TPT level did not eliminate the development of the deck cracks and it was considered impractical to apply TPT force larger than 200,000 lb/diaphragm. Therefore, the remaining option was to increase the number of diaphragms to nine instead of seven

(Figure 4.2-28); two at the ends and seven equally spaced in-between. The new arrangement was examined first with a TPT force equal to 100,000 lb/diaphragm.

When applying equivalent AASHTO HS-25 truck, few cracks developed in the slab bottom surface. Similar cracks developed also when applying AASHTO HL-93 load. However, from the stress distribution and the crack pattern, it was evident that some increase in the TPT force would eliminate the crack development. Therefore, the final trial was to apply TPT force of 150,000 lb/diaphragm.

By applying equivalent AASHTO HS-25 truck load, the maximum principal stresses reached 351, and the slab did not crack. The slab did not experience cracks under equivalent AASHTO HL-93 load either. Accordingly, by applying post-tensioning force of 150,000 lb/diaphragm at nine diaphragms, the model was able to support equivalent AASHTO HS-25 truck or AASHTO HL-93 loads along with 100% of positive temperature gradient without developing any longitudinal cracks in the deck slab. Hence, this TPT arrangement was considered sufficient. A summary for the aforementioned investigation is presented in Table 4.2-4. In addition, the contribution of each load type in the developed maximum principal stresses in the deck slab is shown in Figure 4.2-29.

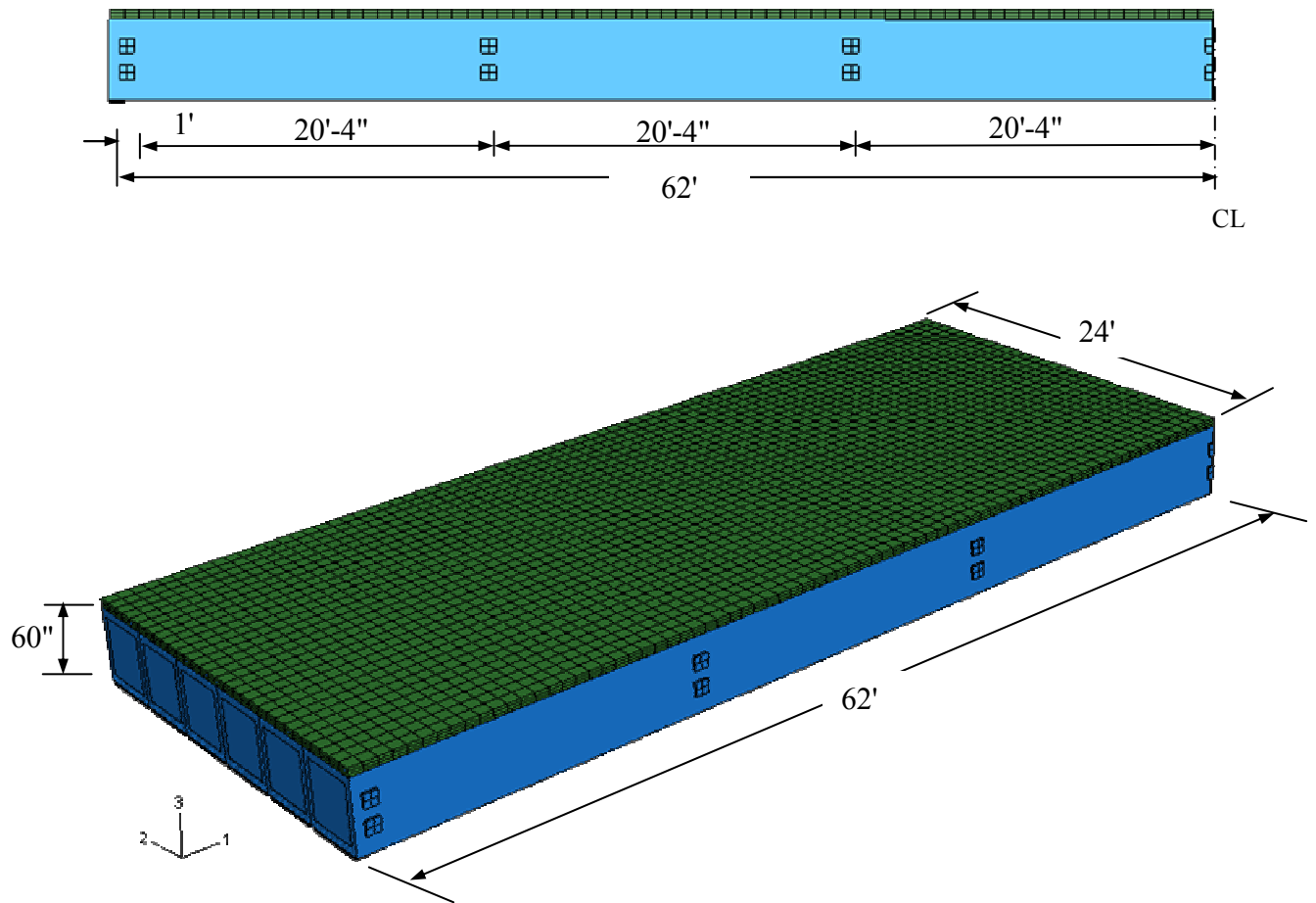


Figure 4.2-25 Assembly of 124 ft span bridge model.

Diaphragms arrangement:

1 @ each end of beam
5 @ equally spaced in-between

TPT= 104,500 lb/diaphragm
TPT= 104,500 lb/diaphragm

CL

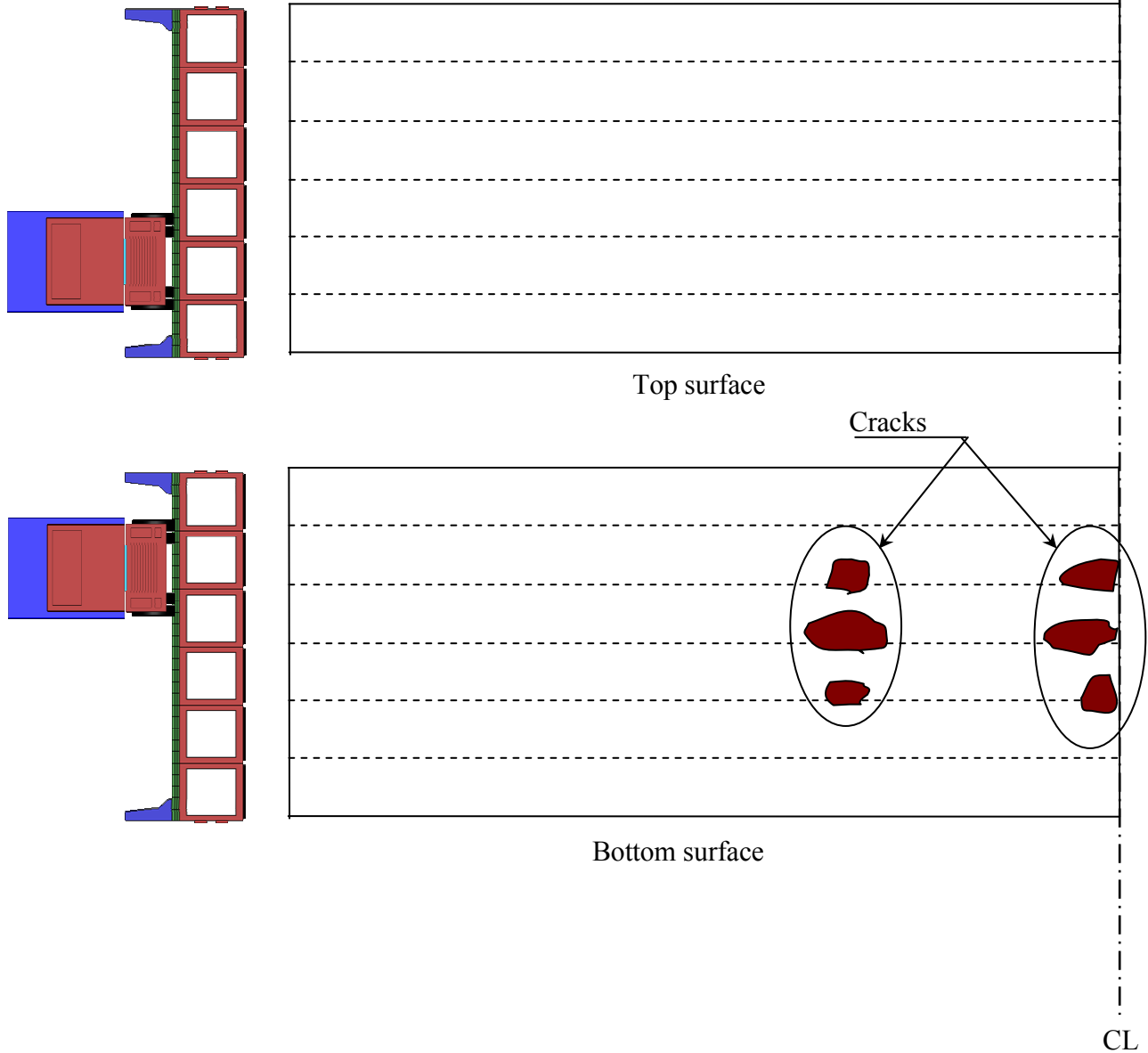


Figure 4.2-26 Crack development in the slab after applying equivalent AASHTO HS-25 truck.

Diaphragms arrangement:

1 @ each end of beam

TPT= 104,500 lb/diaphragm

5 @ equally spaced in-between

TPT= 104,500 lb/diaphragm

CL

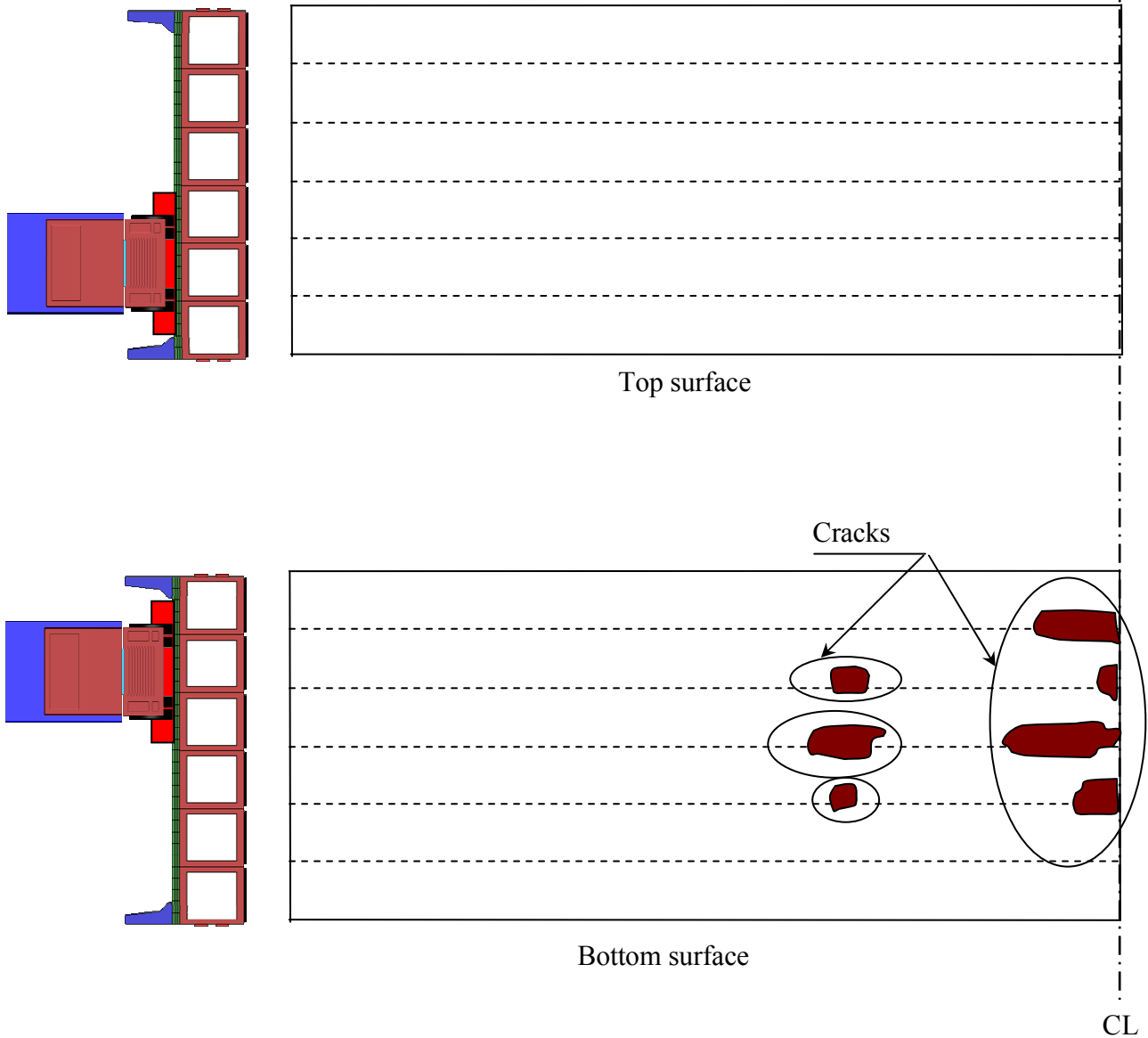


Figure 4.2-27 Crack development in the slab after applying equivalent AASHTO HL-93 load.

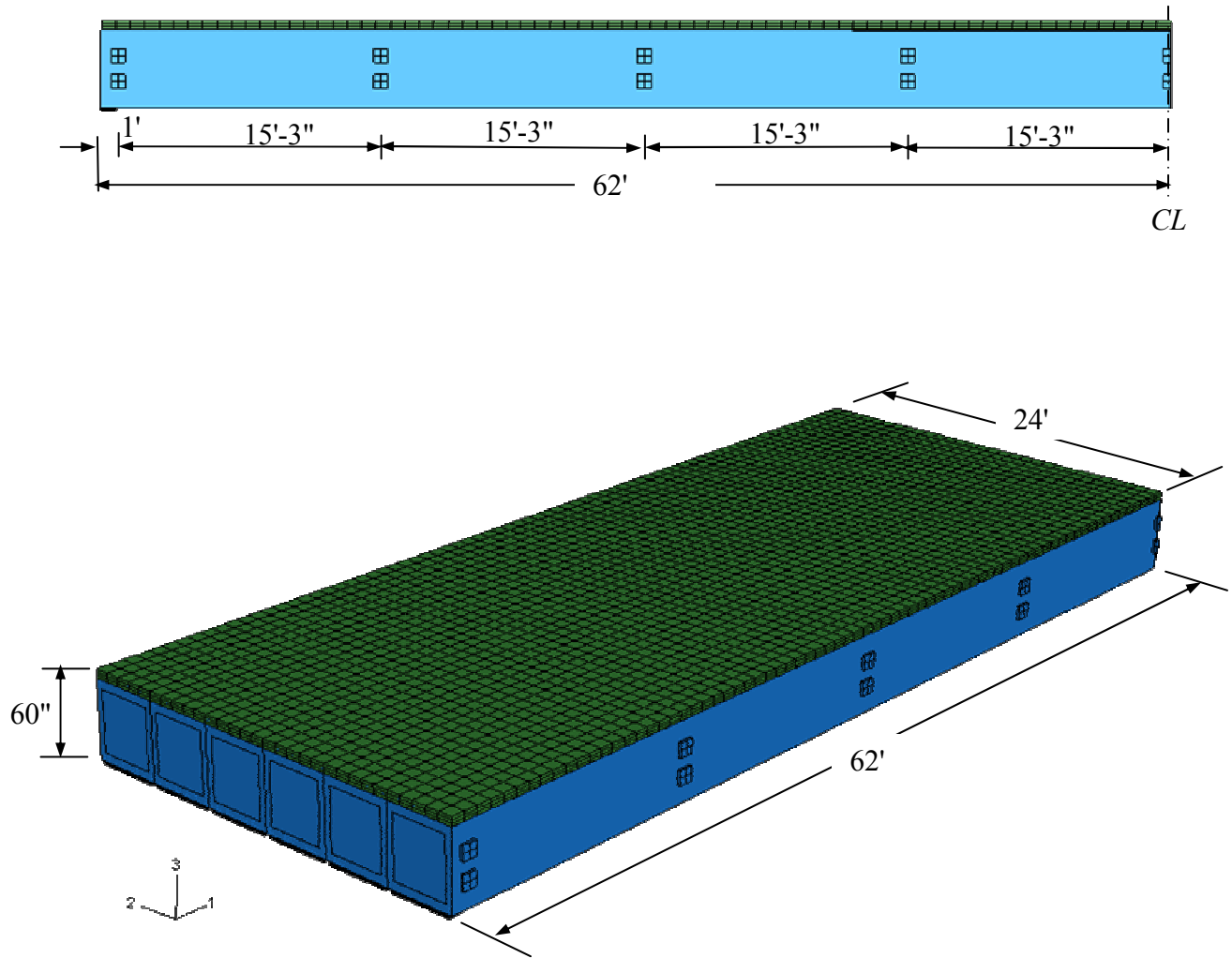


Figure 4.2-28 Modified assembly of 124 ft span bridge model.

Table 4.2-4 Maximum principal stresses in the deck slab of 124 ft span bridge model under service loads.

Model	No. of Diaphragms	TPT Force lb/diaphragm	MP Positive Gradient (psi)	MP LL+ IM (psi)	
				HS-25 truck	HL-93 load
Span = 124 ft Width = 24 ft	7	104,000	285	N/A (cracks)	N/A (cracks)
	7	150,000	277	N/A (cracks)	N/A (cracks)
	7	200,000	271	N/A (cracks)	N/A (cracks)
	9	100,000	270	N/A (cracks)	N/A (cracks)
	9	150,000	260	351	350

- MP: Maximum principal stresses
- LL: Live load
- IM: Impact allowances
- N/A: Not available

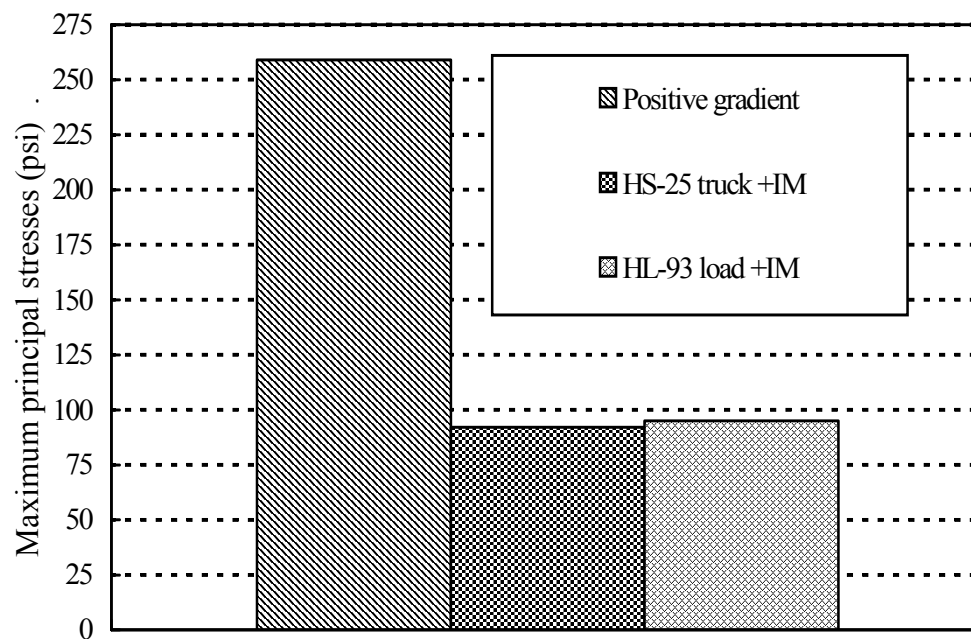


Figure 4.2-29 Service loads contribution in deck slab principal stresses (Case of seven diaphragms, TPT = 150,000 lb/diaphragm).

4.2.4.5 Effect of Deck Slab Concrete Strength on the TPT Arrangement

The previous analysis was performed assuming some deterioration in the concrete material in the deck slab and the concrete strength was reduced to 3,000 psi. However, the models were reanalyzed for concrete strength of 4,000 and 5,000 psi to establish the TPT arrangement for the cases of recently-constructed and special-quality deck slabs, respectively. The analysis revealed that the effect of the strength of the concrete in the deck slab on the adequate number of diaphragms is insignificant. On the other hand, the level of the TPT force can be reduced if higher concrete strength is reached in the deck slab. In summary, regardless of the span length:

- In case of using concrete of strength of 4,000 psi in the deck slab, the TPT force would be adjusted downward from 150,000 lb/diaphragm to 120,000 lb/diaphragm.
- In case of using concrete of strength of 5,000 psi in the deck slab, the TPT force would be adjusted downward to 100,000 lb/diaphragm.

The analysis and loading steps were the same as what was discussed earlier in this chapter; therefore, a detailed discussion is not provided, but the maximum principal stresses due to service loads in the deck slab are provided in Table 4.2-5. The detailed results for this case of analysis are provided in Bebawy (2007).

It should be noted that the analysis could have been performed with a reduced number of diaphragms rather than a reduced TPT force level to take into account the higher concrete strength in the deck slab. However, reducing the number of diaphragms resulted in developing some longitudinal deck cracks in some of the bridge models.

Table 4.2-5 Maximum principal stresses in the deck slab for bridge models with different deck slab concrete strengths.

Span (ft)	No.of Diaphragms	TPT Force lb/diaphragm	MP +ve TG (psi)	MP LL+ IM (psi)	
				HS-25 truck	HL-93 load
Concrete properties: $f'_c = 4,000$ psi, $f_r = 460$ psi, $E = 3.83 \times 10^6$ psi					
50	5	120,000	343	423	411
62	6	120,000	360	445	440
100	7	120,000	365	449	456
124	9	120,000	370	451	459
Concrete properties: $f'_c = 5,000$ psi, $f_r = 514$ psi, $E = 4.30 \times 10^6$ psi					
50	5	100,000	407	501	493
62	6	100,000	431	508	506
100	7	100,000	437	510	509
124	9	100,000	440	513	515

- MP: Maximum principal stresses
- LL: Live load
- IM: Impact allowances

4.2.5 Bridge Models Constructed Using 36 in. Wide Box-Beams

Using 36 in. wide box-beams, another set of FE models were generated for bridges of spans of 50, 62, and 100 ft and width of 24 ft. The fourth span, of 124 ft, could not be generated using 36 in. wide box-beams because spans greater than 100 ft require deep box-beams, which are not available in a width of 36 in. Eight box-beams were used to generate a bridge of a width of 24 ft, as shown in Figure 4.2-30. In addition, the concrete in the deck slab was assumed to have a strength of 4,000 psi, representative of a recently-constructed deck slab. As changing the box-beam width from 48 to 36 in. shall have the same influence on the analysis regardless of the strength of the concrete in the deck slab, the cases of deteriorated deck slab and special-quality deck slab were not simulated.

The analysis herein was performed by first generating FE bridge models with a number of diaphragms and TPT force similar to that recommended for bridges composed of 48 in. wide box-beams. Then, the number of diaphragms was readjusted without changing the TPT force for the models that experienced cracks in the deck slab.

4.2.5.1 50 ft Span Bridge Model

This model experienced no cracks in the deck slab under service loads when providing five diaphragms with each diaphragm post-tensioned with TPT force of 120,000 lb (Figure 4.2-30). The maximum principal stresses reached 358 psi after applying 100% of positive temperature gradient. The stresses then increased to 415 psi after applying AASHTO HL-93 load. Figure 4.2-31 shows the crack map in the deck slab bottom surface after applying AASHTO HL-93 load. Furthermore, Figure 4.2-32 shows the cracks expected if the bridge is overloaded by applying 120% of the load.

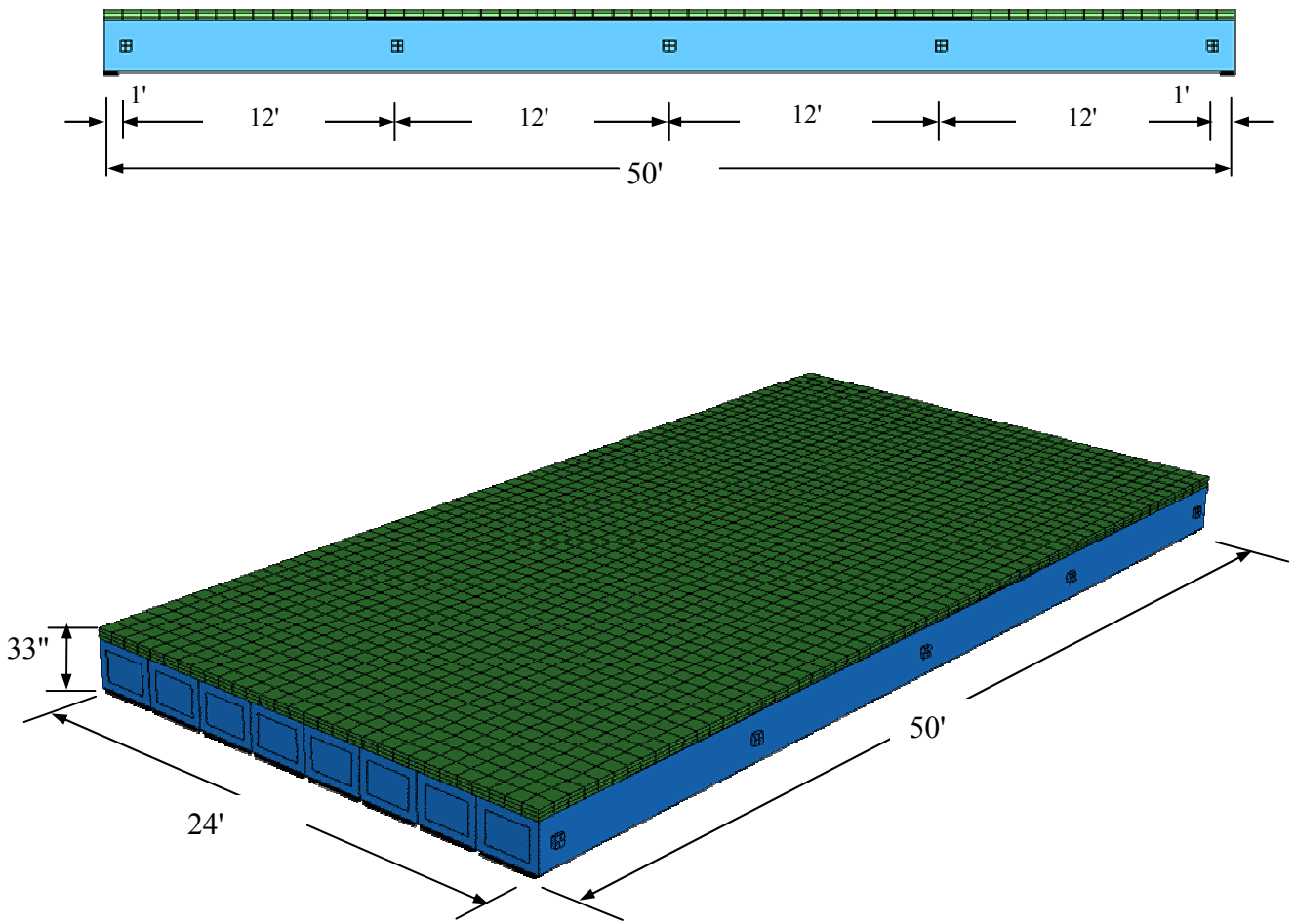


Figure 4.2-30 50 ft span bridge model constructed using 36 in. wide box-beams.

Diaphragms arrangement:

1 @ each end of beam
3 equally spaced in-between

TPT= 120,000 lb/diaphragm

TPT= 120,000 lb/diaphragm

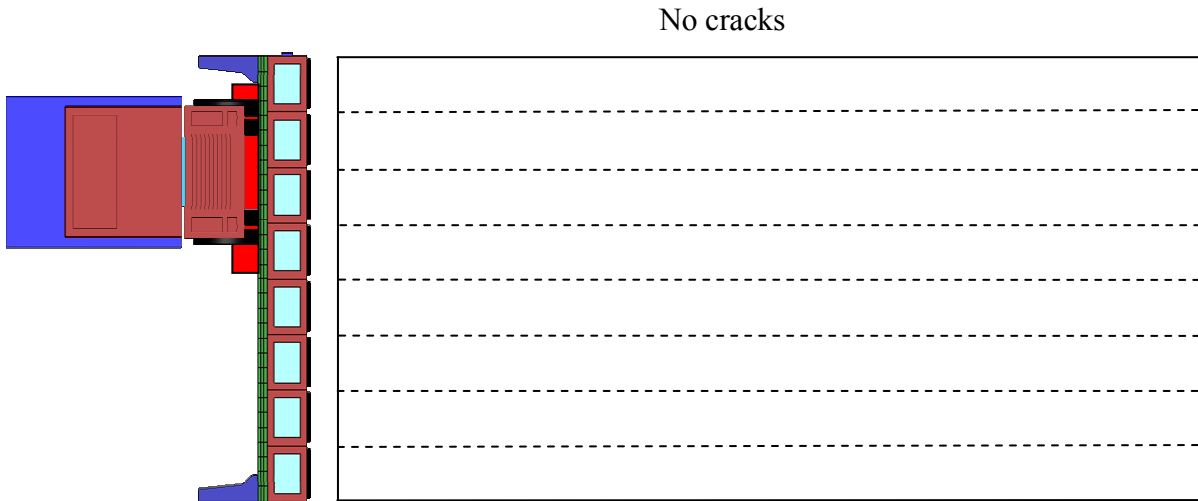


Figure 4.2-31 Crack development in the slab bottom surface after applying AASHTO HL-93 load.

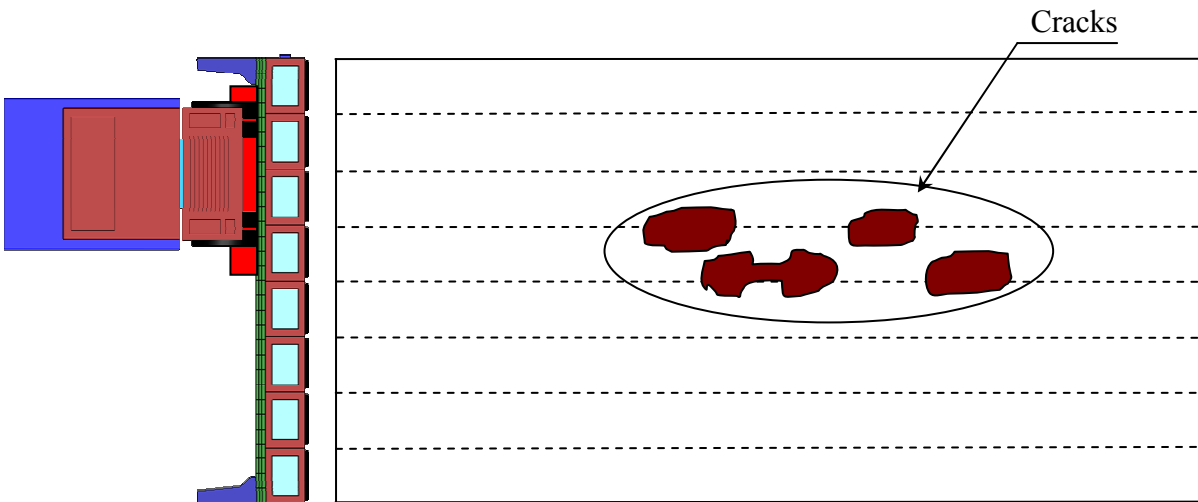


Figure 4.2-32 Crack development in the slab bottom surface after applying 120% of AASHTO HL-93 load.

4.2.5.2 62 ft Span Bridge Model

This bridge model was provided with six diaphragms with each diaphragm post-tensioned with TPT force of 120,000 lb (Figure 4.2-33). The deck slab did not experience any cracks after applying positive temperature gradient and AASHTO HL-93 load (Figure 4.2-34). The maximum principal stresses reached 410 psi when applying 100% of positive temperature gradient and 452 psi when applying AASHTO HL-93 load. However, when increasing the live load by 20% of the load, the deck slab experienced some cracks initiated from its bottom surface, as shown in Figure 4.2-35.

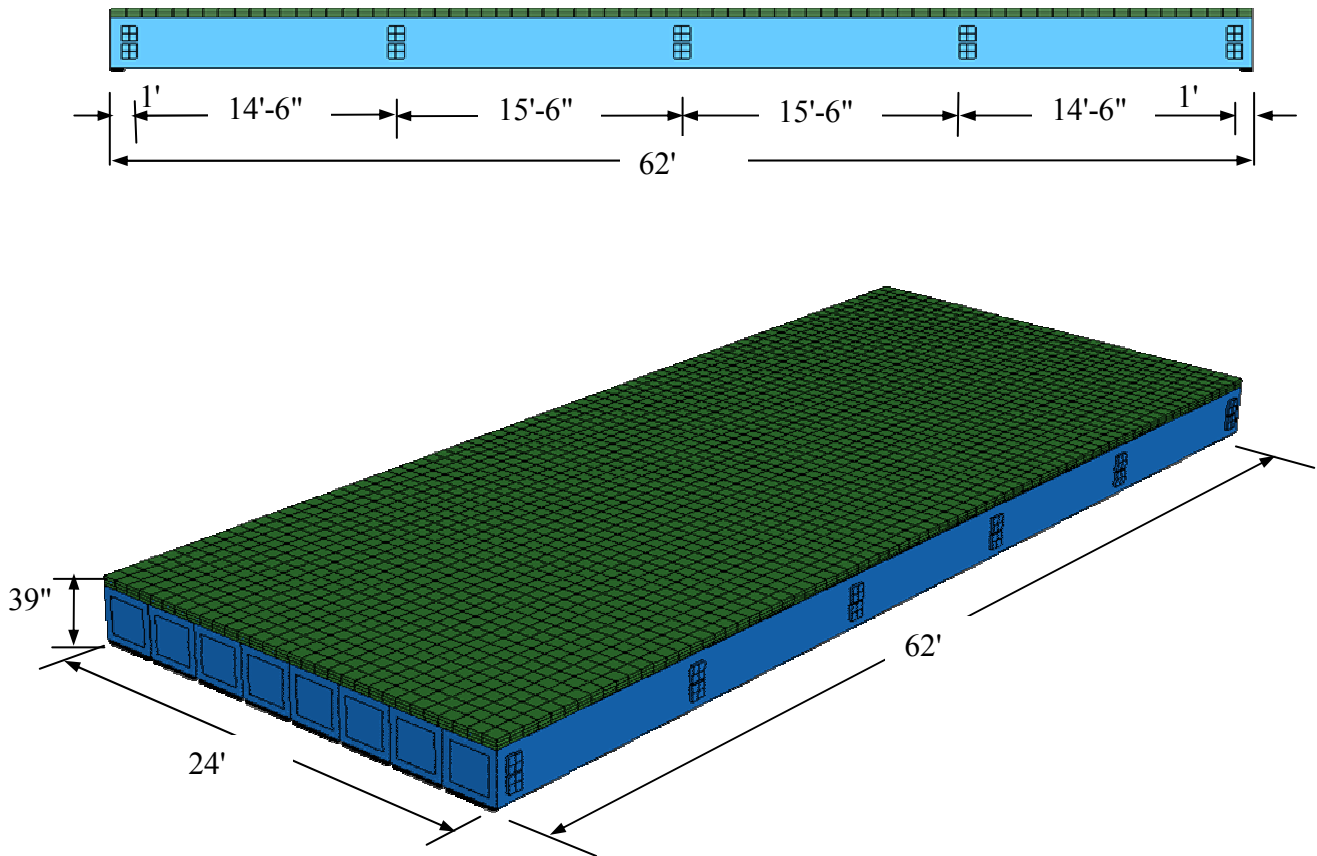


Figure 4.2-33 Assembly of 62 ft span bridge model constructed using 36 in. wide box-beams.

Diaphragms arrangement:

1 @ each end of beam
4 equally spaced in-between

TPT= 120,000 lb/diaphragm

TPT= 120,000 lb/diaphragm

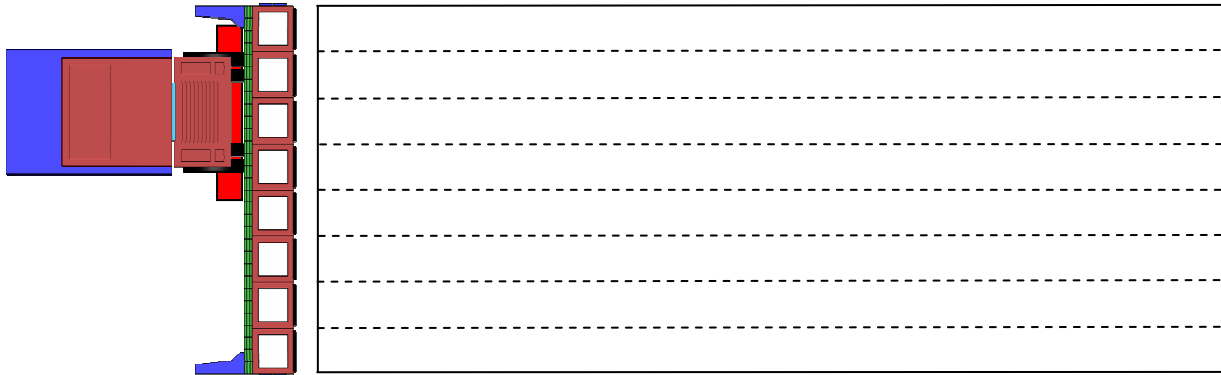


Figure 4.2-34 Crack development in the slab bottom surface after applying AASHTO HL-93 load.

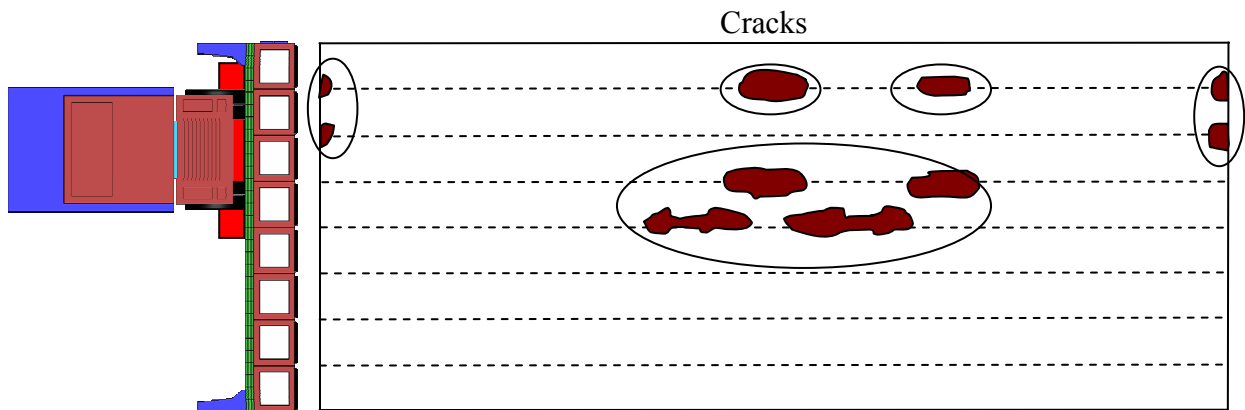


Figure 4.2-35 Crack development in the slab bottom surface after applying 120% of AASHTO HL-93 load.

4.2.5.3 100 ft Span Bridge Model

The analysis of 100 ft span bridge models constructed using 48 in. wide box-beams showed that this span required at least seven diaphragms. Therefore, the analysis herein was also conducted by providing seven diaphragms to the FE model (Figure 4.2-36). Each diaphragm was post-tensioned with a TPT force of 120,000 lb. After applying 100% of positive temperature gradient, the deck slab experienced tensile stresses up to 375 psi. However, the slab experienced longitudinal cracks over the shear-key locations, as shown in Figure 4.2-37 when adding the equivalent AASHTO HL-93 load. The bridge model, therefore, was provided with an additional diaphragm (Figure 4.2-38), and reanalyzed under the same loads. After applying 100% of positive temperature gradient, some areas in the deck slab bottom surface experienced tensile stresses of 355 psi. The stresses increased to 427 psi after applying AASHTO HL-93 load; the maximum stresses did not exceed the cracking strength of the concrete (460 psi); thus, the deck slab did not experience cracks, as shown in Figure 4.2-39. However, with additional 20% of the load, the slab would experience longitudinal cracks, as shown in Figure 4.2-40.

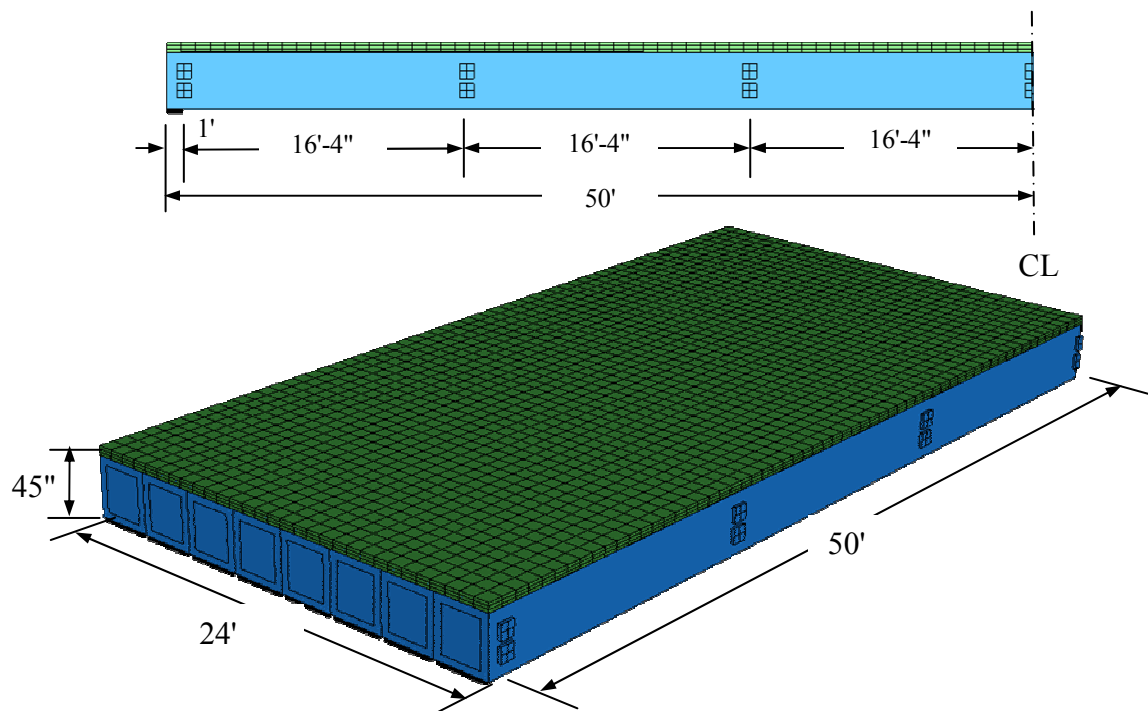


Figure 4.2-36 Assembly of 100 ft span bridge model constructed using 36 in. wide box-beams.

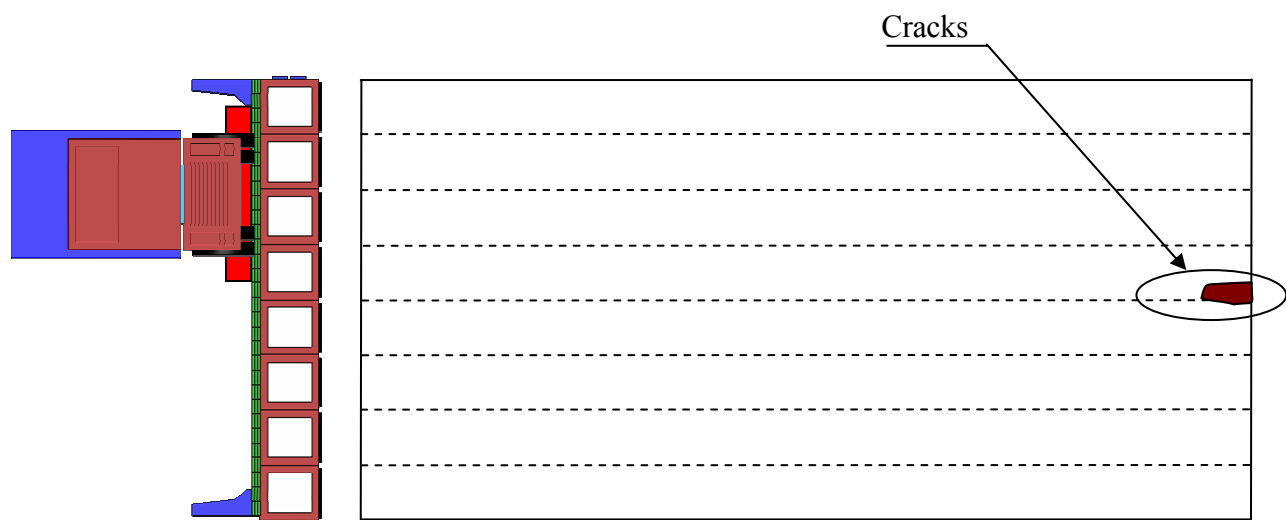


Figure 4.2-37 Crack development in the slab bottom surface after applying AASHTO HL-93 load.

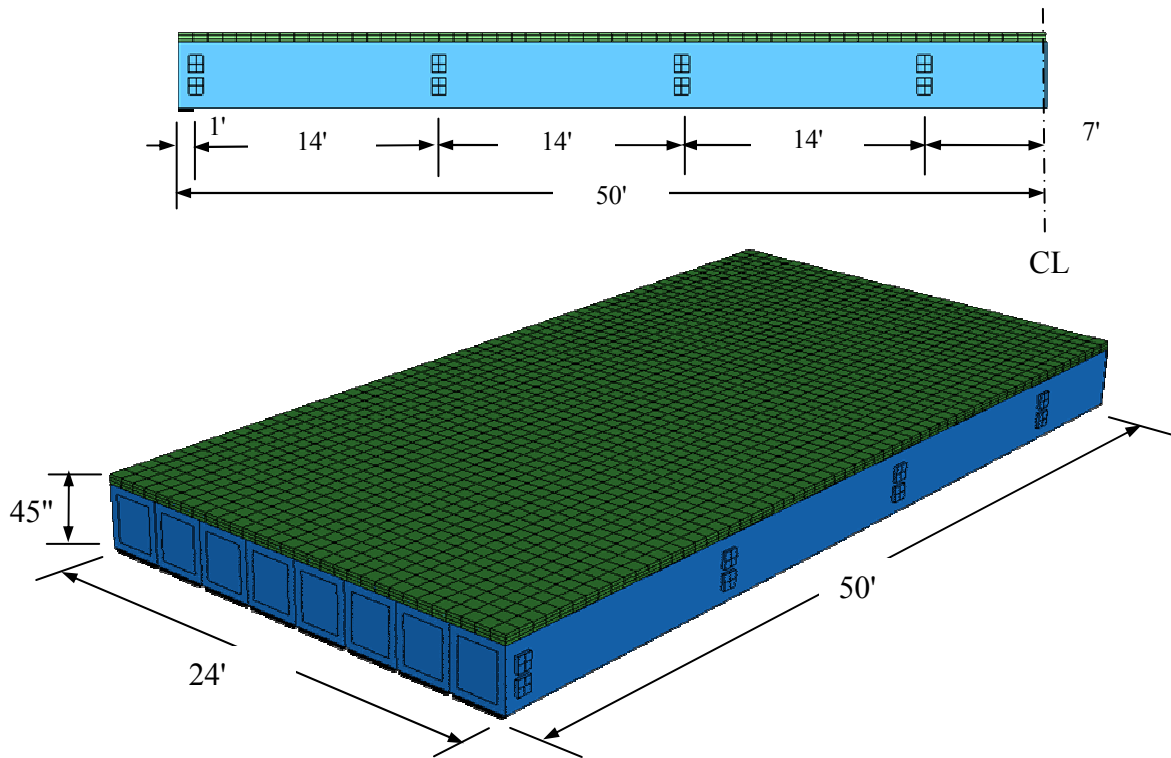


Figure 4.2-38 Modified assembly of 100 ft span bridge model constructed using 36 in. wide box-beams.

Diaphragms arrangement:

1 @ each end of beam
6 equally spaced in-between

TPT= 120,000 lb/diaphragm

TPT= 120,000 lb/diaphragm

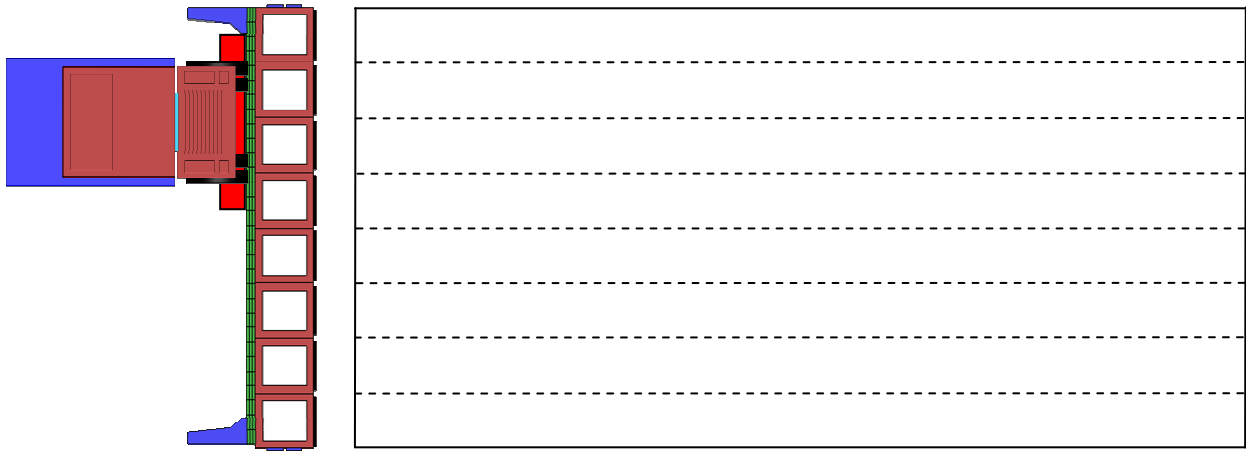


Figure 4.2-39 Crack development in the slab bottom surface after applying equivalent AASHTO HL-93 load.

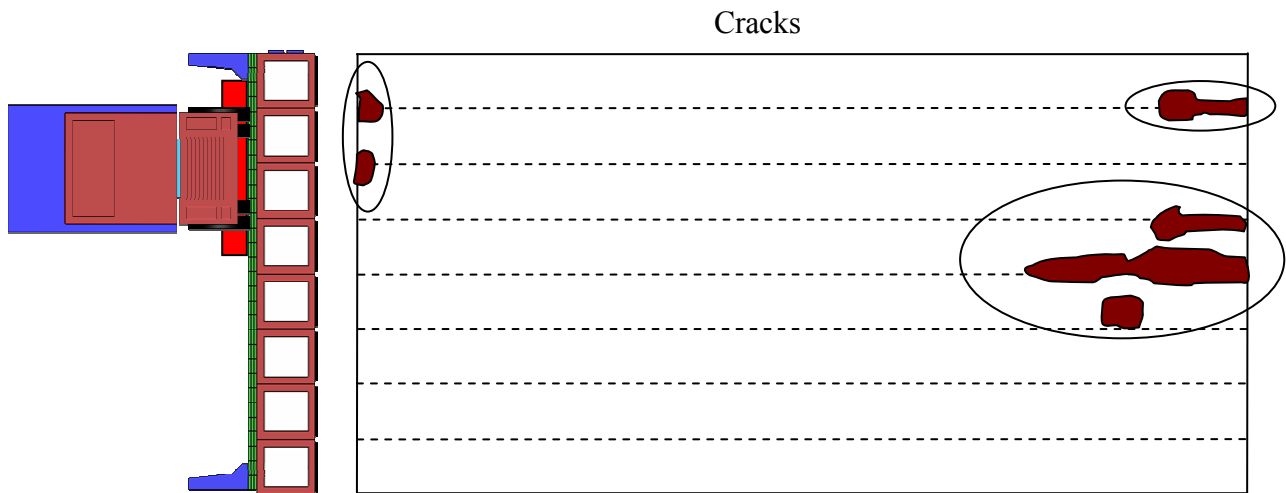


Figure 4.2-40 Crack development in the slab bottom surface after applying 120% of equivalent AASHTO HL-93 load.

4.2.6 Discussion of the Results

Based on the analysis of FE models for 24 ft wide side-by-side box-beam bridges with spans of 50, 62, 100, and 124 ft, using box-beams of widths of 36 and 48 in., the following findings were established:

1. The longitudinal deck cracks are expected to develop in side-by-side box-beam bridges when the current MDOT Specifications (2006) for TPT arrangement are followed.
2. In order to delay the development of the longitudinal deck slab cracks in bridges constructed using 48 in. wide side-by-side box-beams, the recommended number of diaphragms should be provided based on the bridge span, as shown in Figure 4.2-41. The Figure presents the minimum number of diaphragms required to prevent the longitudinal cracks. The diaphragms should be equally spaced along the entire bridge span.
3. The minimum number of diaphragms was selected to merely avoid the crack development in the deck slab; and the stresses in the deck slab in all cases of analysis were slightly less than the cracking strength of the concrete. Therefore, it may be beneficial to add more diaphragms over the minimum number as a safety factor to account for any unpredictable loads or concrete deterioration.
4. In case of 36 in. wide side-by-side box-beam bridges, the number of diaphragms should be provided according to Figure 4.2-42. This Figure presents the minimum number of diaphragms required to prevent longitudinal cracks along with the recommend number of diaphragms.
5. The number of diaphragms obtained from Figure 4.2-41 or Figure 4.2-42 is applicable for all bridges having the corresponding span regardless of their widths. However, the recommended TPT force per diaphragm depends on the concrete strength in the deck slab and the bridge width as well; the TPT force should be adjusted to counteract the effect of increasing the bridge width as presented in the following section. Finally, for 24 ft wide bridges, a TPT force of:
 - 150,000 lb/diaphragm should be applied in the case of deteriorated slabs.

- 120,000 lb/diaphragm should be applied in the case of recently-constructed slabs.
- 100,000 lb/ diaphragm should be applied in the case of special-quality slabs.

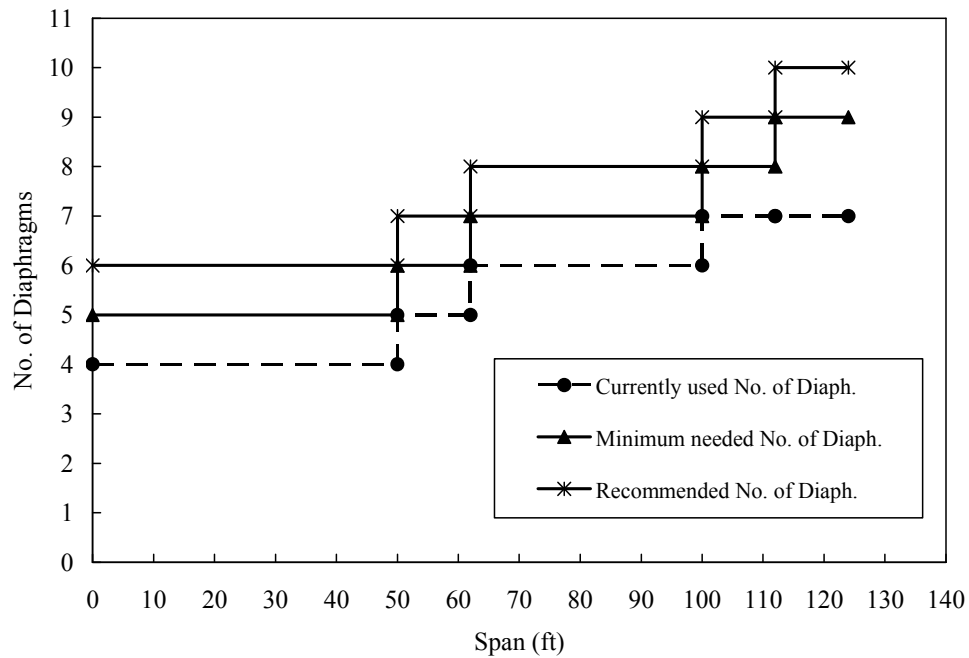


Figure 4.2-41 Adequate number of diaphragms for bridges constructed using 48 in. wide beams.

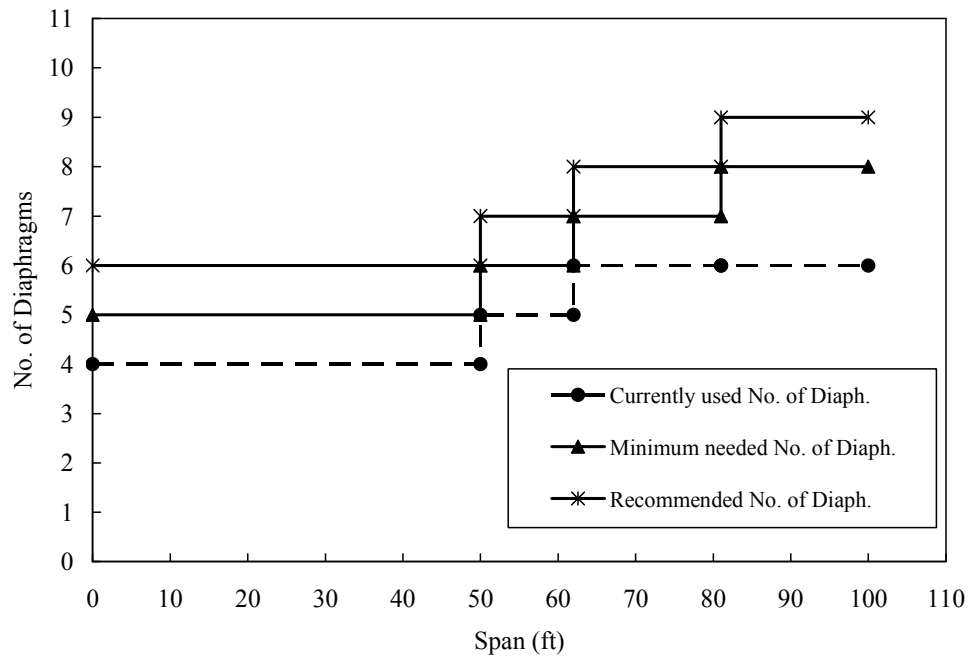


Figure 4.2-42 Adequate number of diaphragms for bridges constructed using 36 in. wide beams.

4.3 Appropriate Transverse Post-Tensioning Force

In the preceding section, the relationship between the bridge span and the adequate number of diaphragms was established for 24 ft wide bridge models. The transverse post-tensioning force per diaphragm was adjusted to 150,000 lb/diaphragm in the case of a deteriorated deck slab (concrete of strength of 3,000 psi) and to 120,000 and 100,000 lb/diaphragm for concrete of strength of 4,000 and 5,000 psi, respectively. In this section, the analysis is extended to establish the appropriate TPT force for wider bridges (Figure 4.3-1). The FE models for bridges of widths of 45, 58, 70, and 78 ft were generated, as shown in Figure 4.3-2 and provided with the minimum number of diaphragms as recommended from the previous section.

The models were subjected to the same analysis and loading steps discussed in the previous section; the service load included applying 100% of positive temperature gradient and then applying the vehicular load along with the presence and impact allowances. In the case of wide bridge models, the vehicular loads were applied at three different locations, as shown in Figure 4.3-3 and Figure 4.3-4. The load locations can be demonstrated as following:

1. One truck over one shoulder denoted as Location I.
2. Two trucks over both shoulders; one truck per shoulder -case of maximum transverse negative moment, denoted as Location II.
3. Two trucks adjacent to each other at the mid-width of the bridge model -case of maximum transverse positive moment, denoted as Location III.

In the longitudinal direction, the trucks were positioned to create the largest positive bending moment in simply supported spans. The spans of 50, 62, and 100 ft were investigated for the aforementioned bridge widths though changing span length does not affect the appropriate TPT force. Furthermore, the analysis was performed using AASHTO HS-25 truck load as well as AASHTO HL-93 load (placed at the same locations as AASHTO HS-25 truck) as vehicular loads although no significant difference was observed in the model response under both loads.

The analysis revealed that the appropriate TPT force should be increased when increasing the bridge width in order to delay the onset of cracking. Nevertheless, the required TPT force slightly decreases with increasing the strength of the concrete in the deck slab. The following subsection presents and discusses the results of the analysis.

4.3.1 Models Geometry

Two sets of models were generated, as shown in Figure 4.3-1; the first set of models was generated using 48 in. wide box-beams and the second set was generated using 36 in. wide box-beams. The geometry of the models in both sets is described below.

4.3.2 Bridge Models Generated Using 48 in. Wide Box-Beams

FE bridge models of spans of 50 and 100 ft and widths of 24, 45, 58, 70, and 78 ft were generated using 48 in. wide box-beams, as shown in Figure 4.3-2.

1. Six box-beams were used to form bridge models with a width of 24 ft; these models have been analyzed and discussed in the previous chapter.
2. Eleven box-beams were used to form bridge models with a width of 45 ft. Each bridge model accommodated two 12 ft wide traffic lanes, 8.5 and 9.75 ft wide shoulders, and two 1.5 ft wide barriers. The cross-section dimensions and reinforcement details of the beams were similar to those of the previous models.
3. Fourteen box-beams were used to form bridge models with a width of 58 ft. Each bridge model accommodated three 12 ft wide traffic lanes, 8.5 and 10.13 ft wide shoulders, and two 1.5 ft wide barriers.
4. Seventeen box-beams were used to form bridge models with a width of 70 ft. Each bridge model accommodated four 12 ft wide traffic lanes, two 9.5 ft wide shoulders, and two 1.5 ft wide barriers.
5. Nineteen box-beams were used to form bridge models with a width of 78 ft. Each bridge model accommodated five 12 ft wide traffic lanes, two 7.5 ft wide shoulders, and two 1.5 ft wide barriers. However, only half of the 78 ft wide bridge was modeled due to model size limitation.

Similar to the previous models, this set of models was analysed with deteriorated, recently constructed, and special-quality deck slabs (concrete of strength 3,000, 4,000, and 5,000 psi, respectively). Section 4.3.4 presents detailed results for the models constructed using 48 in. wide box-beams with a deteriorated deck slab (concrete of strength 3,000 psi, modulus of rupture 350 psi, and modulus of elasticity 3×10^6 psi). The results of analyzing models

constructed using concrete of strength of 4,000 or 5,000 psi are presented as a summary at the end of this section.

4.3.3 Bridge Models Generated Using 36 in. Wide Box-Beams

After analyzing the aforementioned bridge models and establishing the appropriate TPT force for each bridge width, the other set of models was generated using 36 in. wide box-beams. The models had spans of 50, 62, and 100 ft and widths of 24, 47, 59, 72, and 84 ft (Figure 4.3-1):

1. Eight box-beams were used to form bridge models with a width of 24 ft.
2. Fifteen box-beams were used to form bridge models with a width of 47 ft. Each bridge model accommodated two 12 ft wide traffic lanes, two 10 ft wide shoulders, and two 1.5 ft wide barriers. The cross-section dimensions and reinforcement details of the beams were similar to those of the previous models.
3. Nineteen box-beams were used to form bridge models with a width of 59.25 ft. Each bridge model accommodated three 12 ft wide traffic lanes, 10.0 and 10.25 ft wide shoulders, and two 1.5 ft wide barriers.
4. Twenty three box-beams were used to form bridge models with a width of 71.75 ft. Each bridge model accommodated four 12 ft wide traffic lanes, 10 ft and 10.75 ft wide shoulders, and two 1.5 ft wide barriers. Only half of the 72 ft wide bridge was modeled.
5. Twenty seven box-beams were used to form bridge models with a width of 84.25 ft. Each bridge model accommodated five 12 ft wide traffic lanes, 10 ft and 11.25 ft wide shoulders, and two 1.5 ft wide barriers. Only half of the 84 ft wide bridge was modeled.

The models were initially provided with TPT forces similar to those recommended for bridges constructed using 48 in. wide box-beams. The deck slab was considered recently constructed with concrete of strength of 4,000 psi, modulus of rupture of 460 psi, and modulus of elasticity of 3.83×10^6 psi. The results of analyzing models constructed using 36 in. wide box-beams are presented as a summary at the end of this section.

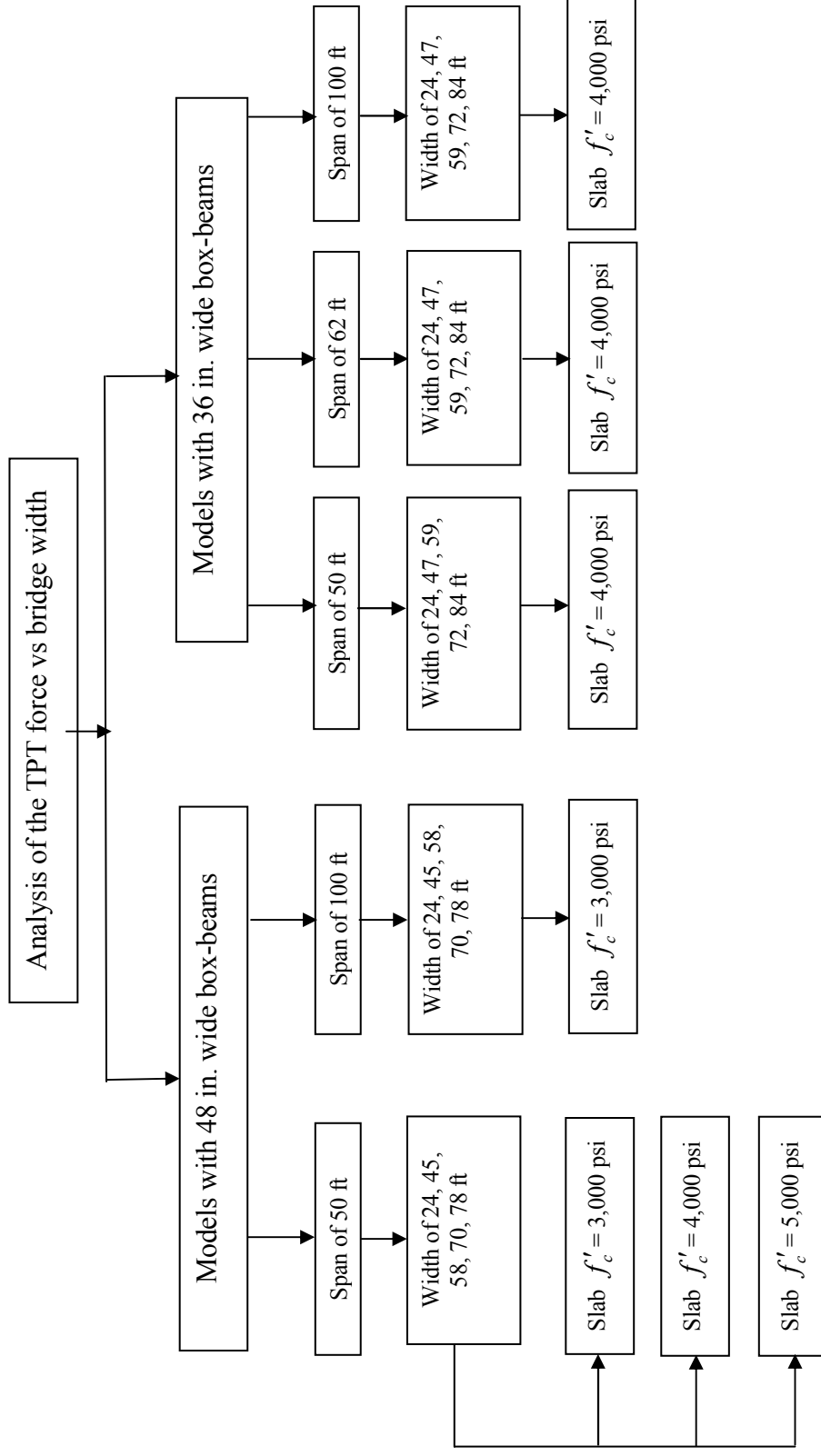


Figure 4.3-1 FE models to establish the appropriate TPT force.

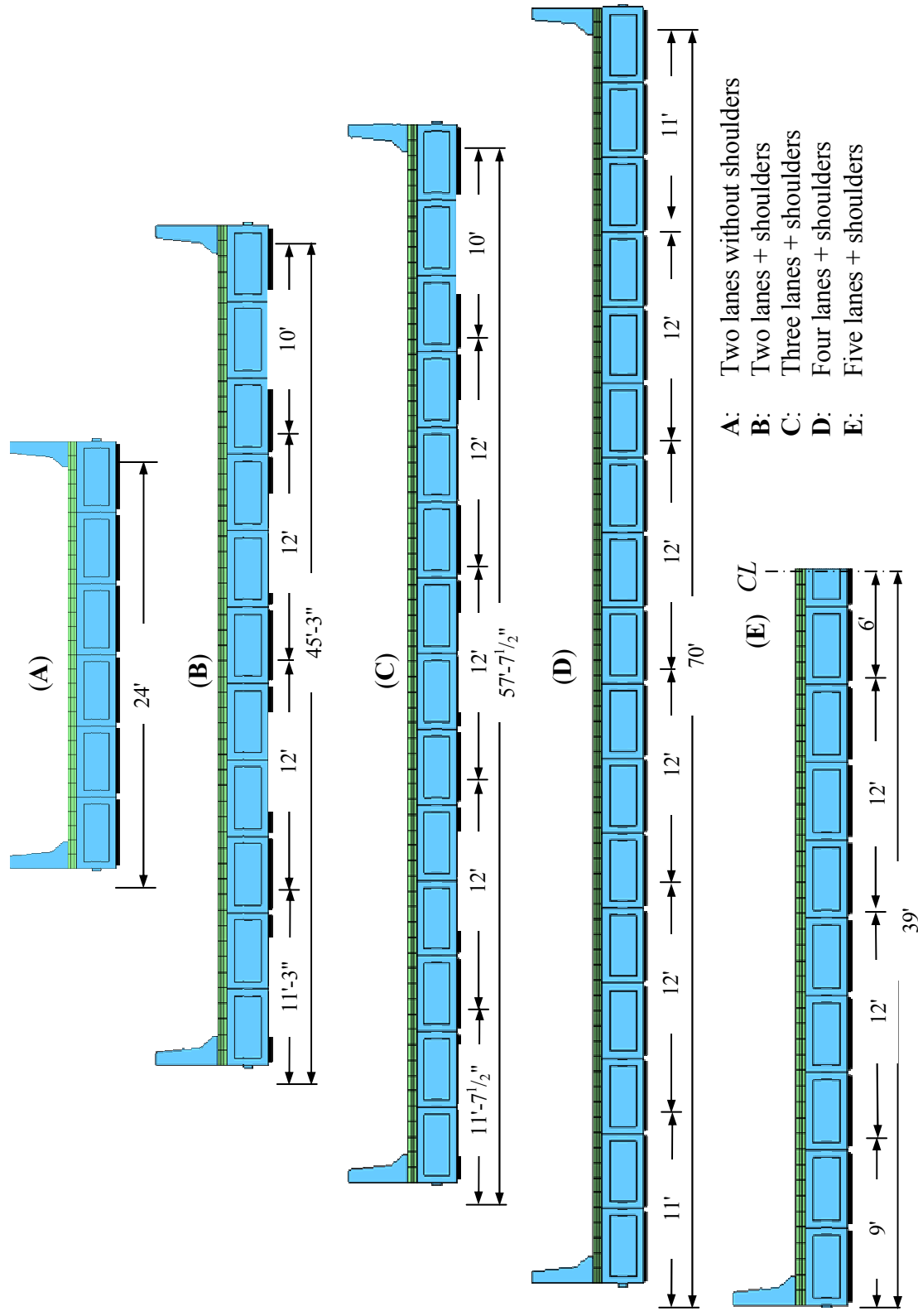


Figure 4.3-2 Bridge widths examined under different loading cases.

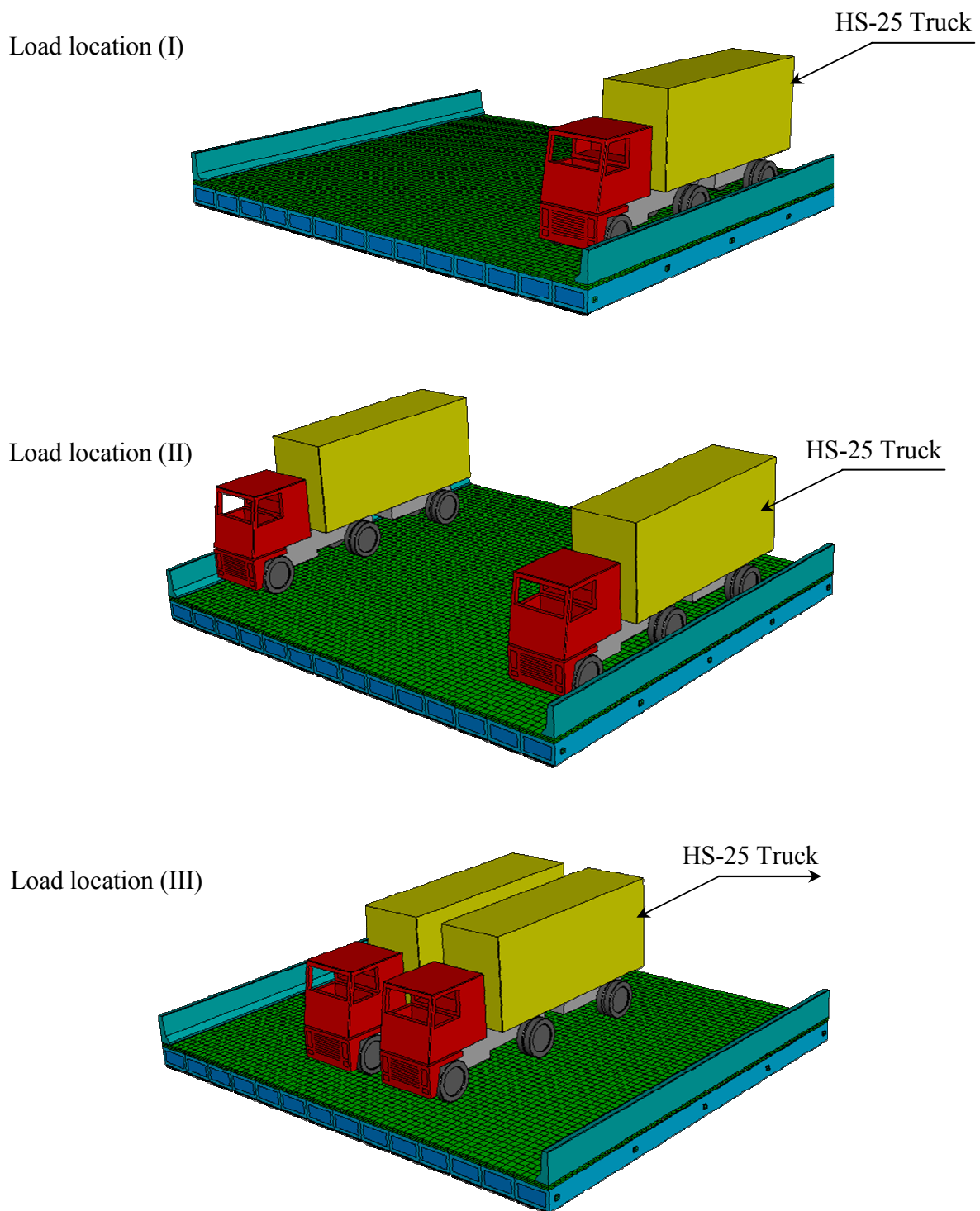


Figure 4.3-3 Load locations for live loads (3-lane model, isometric view).

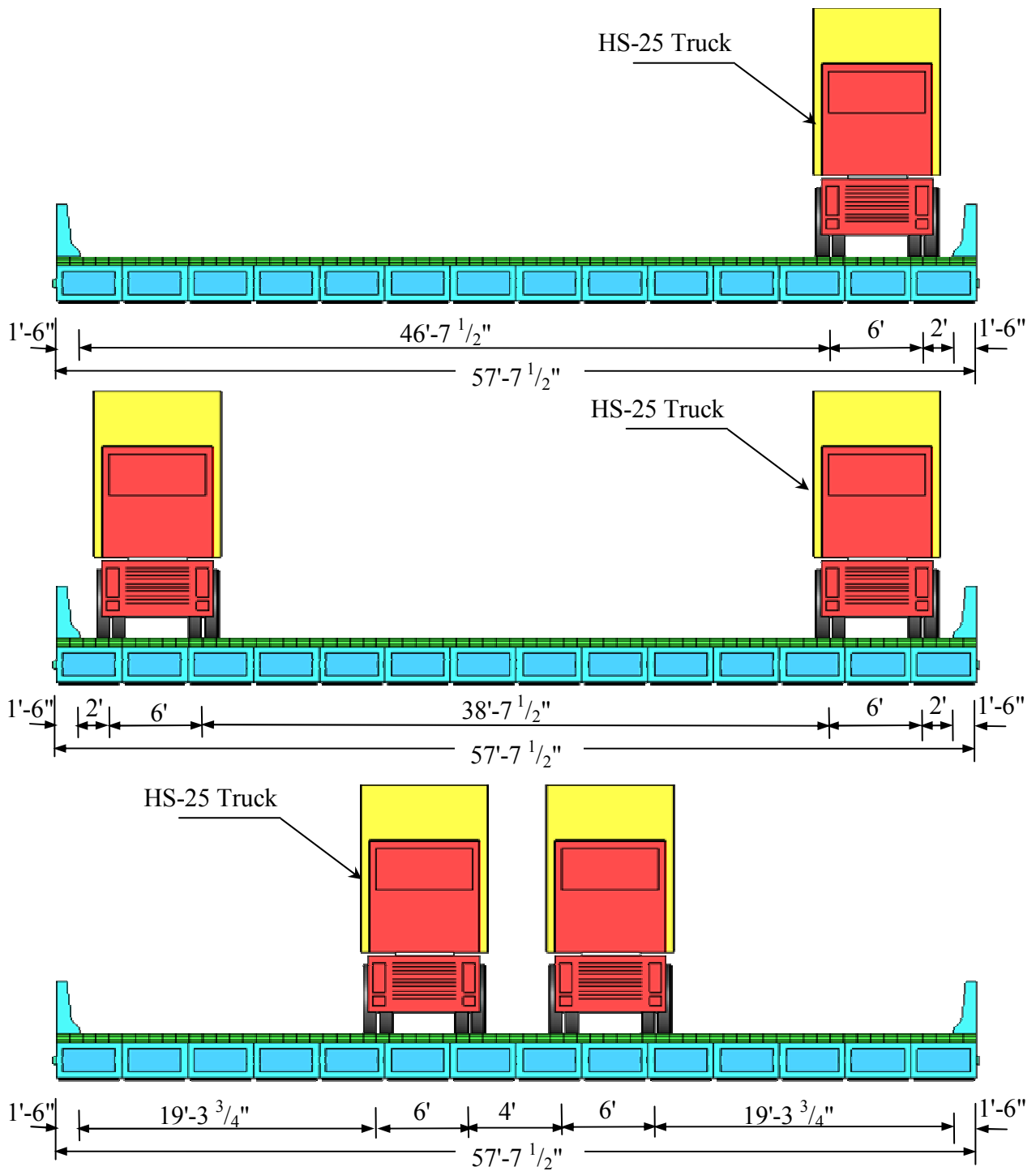


Figure 4.3-4 Load locations for live loads (3-lane model, front view).

4.3.4 Bridge Models Generated Using 48 in. Wide Box-Beams

4.3.4.1 Two-Lane Bridge Model (Span = 50 ft, Width = 45 ft)

The 45 ft wide bridge model was composed of eleven side-by-side box-beams of a depth of 27 in. and a width of 48 in. each. The reinforcement of the box-beams and the deck slab was similar to that described in the chapter 3 for 50 ft span bridge models. Five diaphragms were used to tie the beams together and the TPT force was set first to 125,000 lb/diaphragm. The force was applied through one strand at the beams mid-depth.

The construction stages before casting the deck slab were the same as what have been discussed in the previous section; thus, detailed discussion for the results from these stages is not presented. Most of the results in this section address the stresses developed after casting the deck slab.

Stress progressions in the deck slab ($f'_c = 3,000$ psi)

1. The stresses in the deck slab in both the longitudinal and transverse direction were negligible before applying the second stage of TPT force. However, after applying the second stage of TPT force (100,000 lb/diaphragm after casting deck slab), the stress distribution in the slab changed; the transverse stresses reached compressive stress level up to 182 psi at the slab ends. Conversely, the majority of the slab experienced compressive stresses in the range between 23 and 59 psi. In the longitudinal direction, the slab experienced negligible compressive and tensile stresses.
2. After deducting the time dependent losses and applying the superimposed dead loads, the slab experienced additional longitudinal compressive stresses. Some tensile stresses of value less than 66 psi developed at the slab ends near the outer shear-keys location at the fascia beams, most likely because of the barriers weight.
3. When applying positive temperature gradient, the slab bottom surface experienced maximum principal tensile stresses up to 272 psi concentrated at the shear-keys location.
4. **Live load Location I:** subsequent to applying the positive temperature gradient, applying one AASHTO HS-25 truck load over one of the shoulders (2 ft away from the barrier edge) increased the longitudinal stresses in the deck slab top surface up to 935

- psi (compression). At the same time, additional tensile stresses developed in the transverse direction (220 psi), and caused the principal stresses to reach 348 psi. The slab did not experience any cracks under the applied load, as shown in Figure 4.3-5.. Furthermore, when the loads exceed the AASHTO HS-25 load by 20%, the cracks would be developed, as shown in Figure 4.3-6.
5. **Live load Location II:** subsequent to applying the positive temperature gradient, applying two AASHTO HS-25 trucks over both shoulders simultaneously after applying the temperature gradient (one AASHTO HS-25 truck per shoulder) increased the longitudinal stresses in the top surface to 971 psi (compression) and developed additional tensile stresses in the transverse direction (224 psi). The principal stresses increased to 344 psi. However, the slab did not yet experience cracks under the applied loads, as shown in Figure 4.3-7. If the loads exceed the AASHTO HS-25 truck by 20%, the cracks would be developed, as shown in Figure 4.3-8.
 6. **Live load Location III:** subsequent to applying the positive temperature gradient, applying two AASHTO HS-25 trucks over the mid-width of the model after applying the temperature gradient caused the principal stresses to exceed the cracking strength of the concrete and the deck slab experienced cracks, as shown in Figure 4.3-9. By increasing the TPT level from 125,000 to 150,000 lb/diaphragm, the principal stresses reached a maximum of 351 psi and the slab did not experience any cracks, as shown in Figure 4.3-10.
 7. With a TPT force of 150,000 lb/diaphragm and applying the positive temperature gradient in addition to AASHTO HL-93 load in locations I, II, and III, the deck slab experienced maximum principal stresses of 338, 297, and 306 psi, respectively. No cracks developed in the deck slab under any of the combined thermal and truck load conditions.

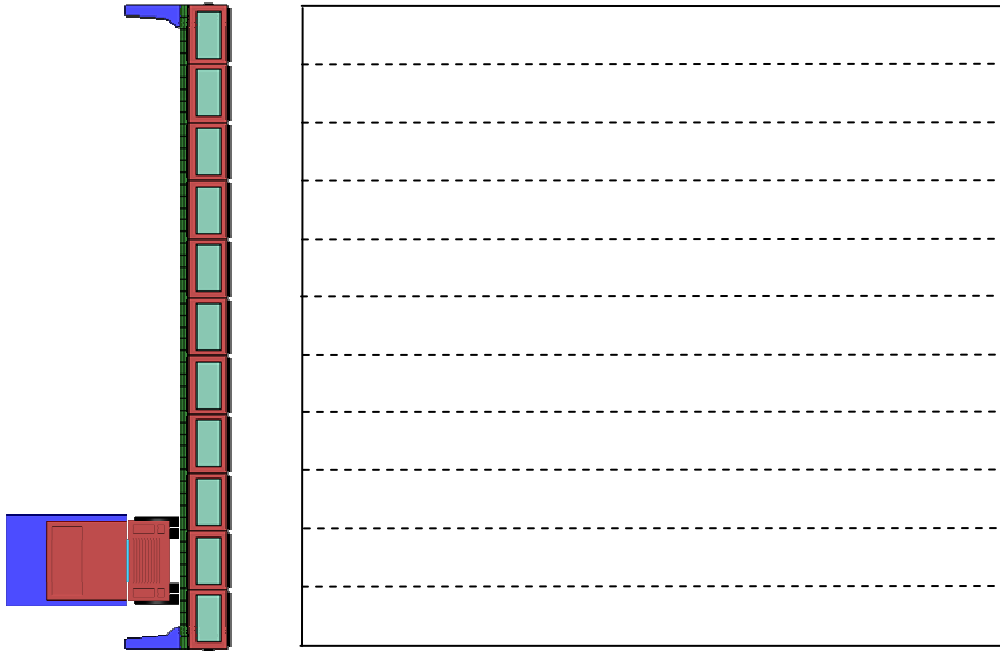


Figure 4.3-5 Crack development in the slab bottom surface after applying AASHTO HS-25 truck (Location I, TPT = 125,000 lb/diaphragm).

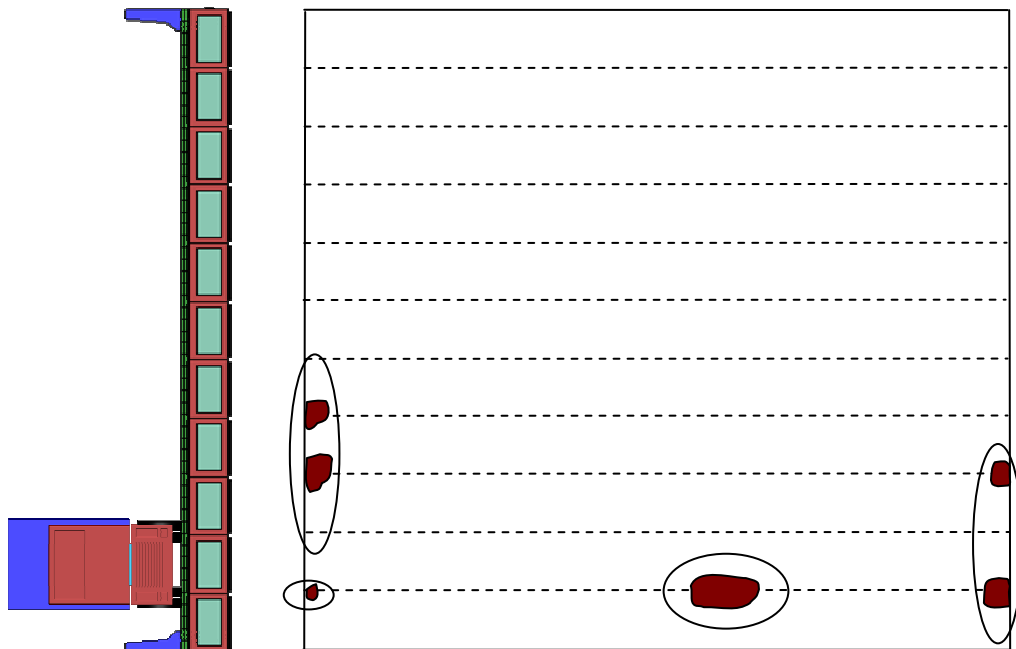


Figure 4.3-6 Crack development in the slab bottom surface after applying 120% of AASHTO HS-25 truck (Location I, TPT = 125,000 lb/diaphragm).

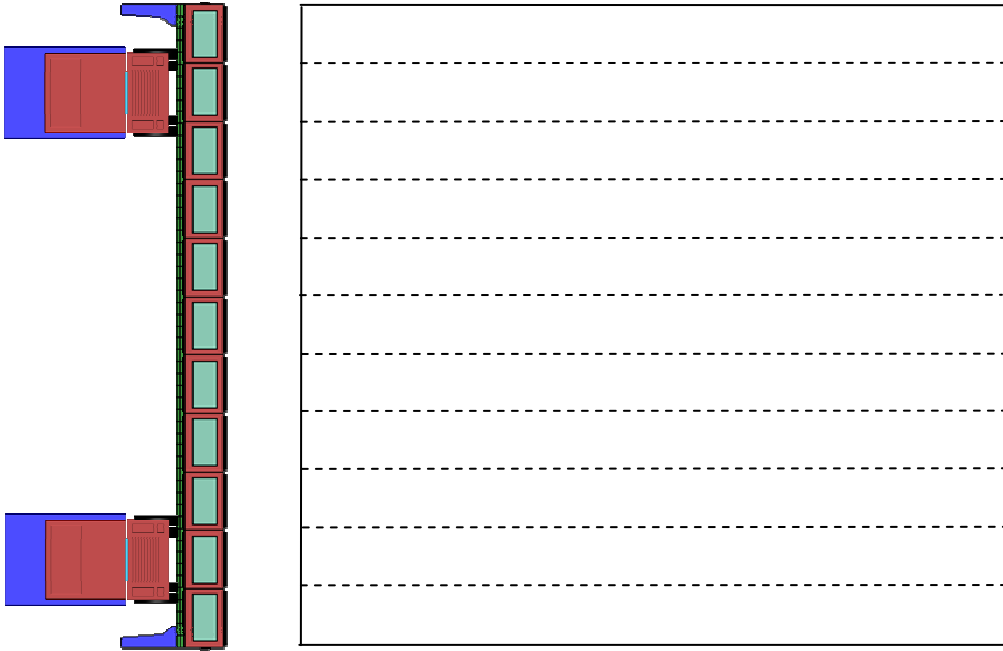


Figure 4.3-7 Crack development in the slab bottom surface after applying AASHTO HS-25 truck (Location II, TPT = 125,000 lb/diaphragm).

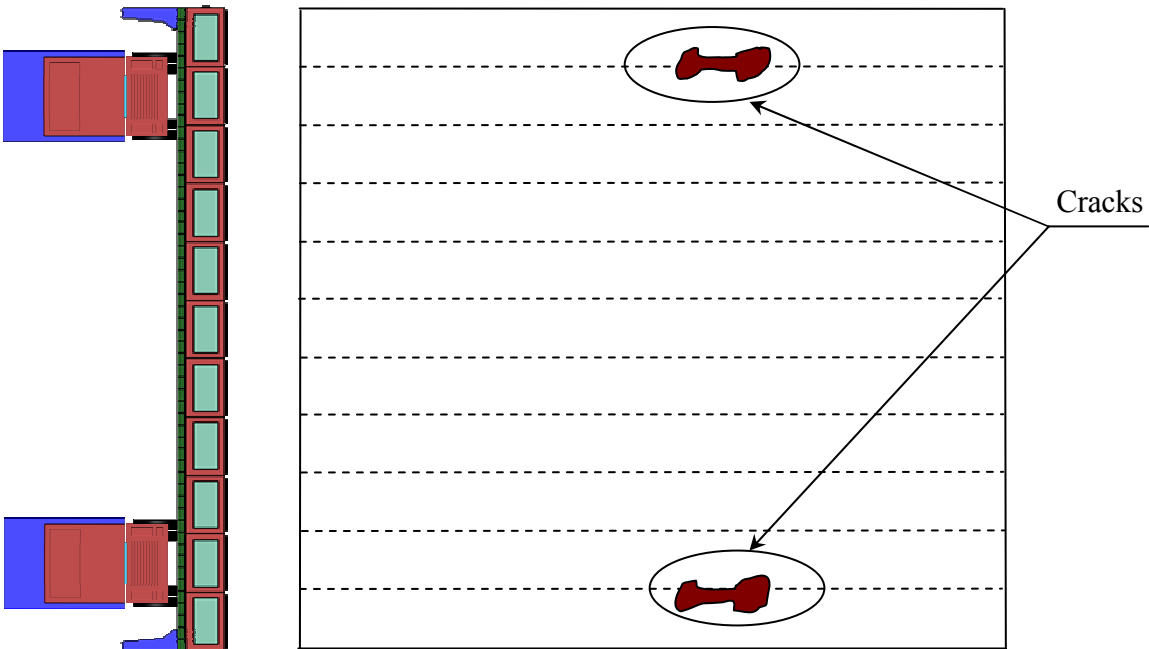


Figure 4.3-8 Crack development in the slab bottom surface after applying 120% of AASHTO HS-25 truck (Location II, TPT = 125,000 lb/diaphragm).

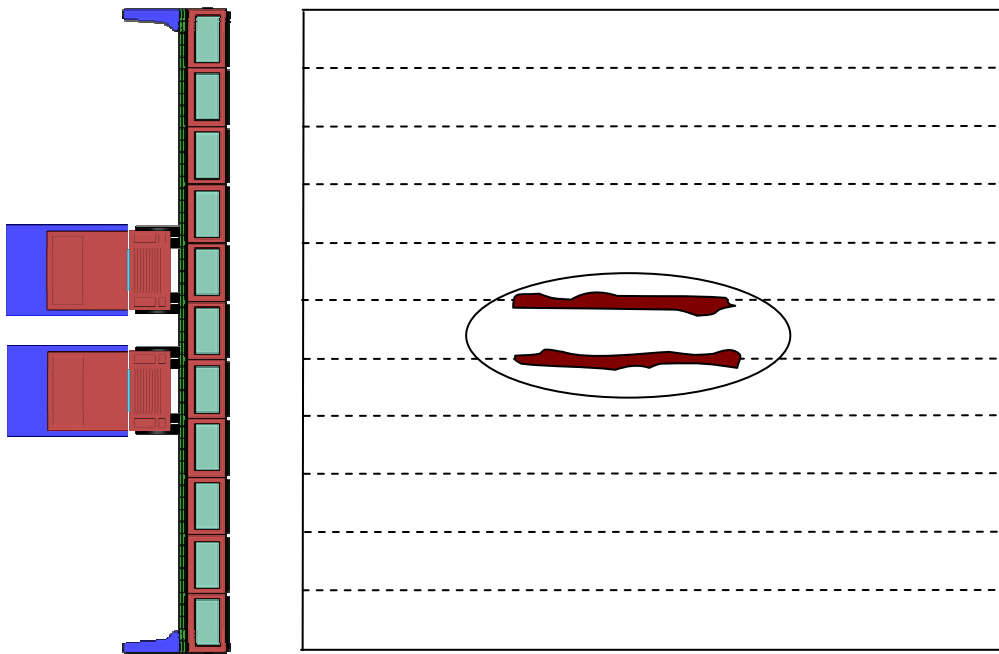


Figure 4.3-9 Crack development in the slab bottom surface after applying AASHTO HS-25 truck (Location III, TPT = 125,000 lb/diaphragm).

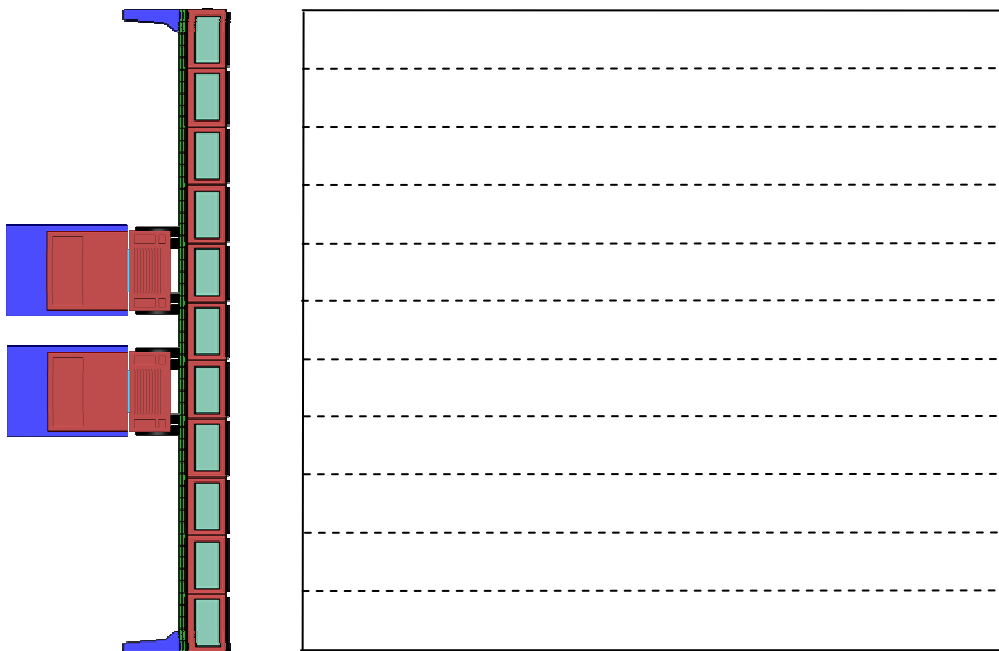


Figure 4.3-10 Crack development in the slab bottom surface after applying AASHTO HS-25 truck (Location III, TPT = 150,000 lb/diaphragm).

4.3.4.2 Three-Lane Bridge Model (Span = 50 ft, Width = 58 ft)

The 58 ft wide bridge model was composed of fourteen side-by-side box-beams of a width of 48 in. each. The initial TPT force was set to 150,000 lb/diaphragm applied through 5 diaphragms based on the final results for 45 ft wide bridge model.

Stresses and crack development in the deck slab ($f'_c = 3,000$ psi)

1. Both the longitudinal and transverse stresses in the deck slab were negligible before applying the second stage of TPT force.
2. After applying the second stage of TPT force (125,000 lb/diaphragm after casting the deck slab), the transverse compressive stresses reached 182 psi at the slab ends. Conversely, the majority of the slab experienced compressive stresses in the range of 23 to 59 psi. In the longitudinal direction, the slab experienced small stress values either in compression or in tension ranging from -20 to +98 psi. The stress on interior sides of the box-beam reached 471 psi at the diaphragms only.
3. When applying the positive temperature gradient, the slab bottom surface experienced localized tensile stresses up to 273 psi at the shear-key locations.
4. **Live load Location I:** subsequent to applying positive temperature gradient, applying one AASHTO HS-25 truck load over one of the shoulders (2 ft away from the barrier edge) increased the maximum principal stresses up to 351 psi. The slab experienced no cracks; however, the TPT force was considered just enough to prevent the cracks because if the load increases by 20% of the load, the cracks would develop.
5. **Live load Location II:** subsequent to applying positive temperature gradient, applying two AASHTO HS-25 trucks over the shoulders simultaneously (one truck per shoulder, 2 ft away from the barrier edge) increased the maximum principal stresses up to 341 psi. The slab did not experience cracks under the applied load.
6. **Live load Location III:** subsequent to applying positive temperature gradient, applying two AASHTO HS-25 trucks simultaneously over the mid-width of the model (4 ft apart from each other) caused maximum principal stresses to reach 185 psi at the slab bottom surface. The slab did not experience cracks under two AASHTO trucks, but when

applying 20% more than AASHTO HS-25 trucks, it experienced longitudinal cracks at the mid-width. In this particular loading case, the maximum principal stresses decreased with the application of the live loads because the response of the live load counteracted the response of the positive temperature gradient; the highest value of the principal stresses was reached at the slab edges when applying temperature gradient only and at the mid-width after the live loads were added.

7. By using TPT force of 150,000 lb/diaphragm, the deck slab experienced maximum principal stresses of 353, 330, and 186 psi when applying AASHTO HL-93 load in locations I, II, and III, respectively subsequent to applying positive temperature gradient. No cracks were developed in the deck slab under any of the load cases.

4.3.4.3 Four-Lane Bridge Model (Span = 50 ft, Width = 70 ft)

The 70 ft wide bridge model was composed of seventeen side-by-side box-beams of a width of 48 in. each. The initial TPT force level was 150,000 lb/diaphragm applied through five diaphragms.

Stress and crack development in the deck slab ($f'_c = 3,000$ psi)

1. After applying second stage of TPT force (125,000 lb/diaphragm after casting the deck slab), the transverse stress distribution reached compressive stresses of 220 psi at the slab ends. The majority of the slab experienced compressive stresses in the range of 49 to 92 psi. In the longitudinal direction, the slab experienced small stress values either in compression or in tension ranging between -19 and +83 psi.
2. After deducting time dependent losses and applying superimposed dead loads SDL, the tensile stresses reached a value of 102 psi at the slab ends.
3. When applying positive temperature gradient, the slab bottom surface experienced tensile stresses of 269 psi. These high tensile stresses were found at the shear-key locations near the supports of the fascia beams.
4. **Live load Location I:** subsequent to applying the positive temperature gradient, applying one AASHTO HS-25 truck over one of the shoulders (2 ft away from the

barrier edge) increased the maximum principal stresses to 353 psi and the slab experienced small cracks.

5. **Live load Location II:** subsequent to applying the positive temperature gradient, when applying two AASHTO HS-25 trucks over the shoulders simultaneously (one truck per shoulder, 2 ft away from the barrier edge), the slab experienced small cracks mainly at the locations of the shear-keys near the supports of the fascia beams.
6. **Live load Location III:** subsequent to applying the positive temperature gradient, when applying two AASHTO HS-25 trucks simultaneously over the mid-width of the model (4 ft apart from each other), the slab experienced cracking. The crack development implied that the applied TPT force was insufficient to eliminate the deck slab cracking in the four-lane bridge.
7. The TPT level was increased to 175,000 lb/diaphragm and the bridge model was reanalyzed. Increasing TPT level eliminated the crack development. However, the mid-region at the slab bottom surface remained the most likely region to develop cracks. By using a TPT force of 175,000 lb/diaphragm, the deck slab experienced maximum principal stresses up to 342, 327, and 267 psi when applying the positive temperature gradient with AASHTO HL-93 load in locations I, II, and III, respectively. No cracks were developed in the deck slab under these load cases.

4.3.4.4 Five-Lane Bridge Model (Span = 50 ft, Width = 78 ft)

The 78 ft wide bridge model was composed of nineteen side-by-side box-beams of a width of 48 in. each (total width of 78 ft). The entire bridge could not be modeled because of the required extensive FE elements. Instead, half of the width was modeled and symmetry conditions were provided along the longitudinal centerline. After a few trials, the TPT force was set to 180,000 lb/diaphragm applied through five diaphragms in order to eliminate the deck slab cracks.

Stresses and crack development in the deck slab ($f'_c = 3,000$ psi)

1. After applying the second stage of TPT force (155,000 lb/diaphragm after casting the deck slab), the transverse compressive stresses reached 265 psi at the slab ends. At the

- same time, the majority of the slab experienced compressive stresses in the range of 61 to 112 psi.
2. After deducting time dependent losses and applying SDL, localized tensile stresses reached a value of 131 psi near the end supports.
 3. When applying positive temperature gradient, the slab bottom surface experienced tensile stresses up to 262 psi. Again, the high tensile stresses were mainly observed above the outer shear-keys near the supports.
 4. **Live load Location I:** as a result of modeling only half of the width of the bridge model, it was not possible to load one side only of the model with a truck; therefore, the first load case was not performed for the five-lane model.
 5. **Live load Location II:** subsequent to applying the positive temperature gradient, applying two AASHTO HS-25 trucks over the shoulders simultaneously (one truck load per shoulder) increased the maximum principal stresses to 349 psi. The slab did not experience cracks under the applied load, but with an additional 20% of the loads applied, the slab experienced small cracks at the far ends.
 6. **Live load Location III:** by applying two AASHTO HS-25 trucks simultaneously over the mid-width of the model after applying the positive temperature gradient, the maximum principal stresses increased to 324 psi. The slab did not experience cracks under the AASHTO HS-25 trucks. However, when applying an additional 20% of the load, the slab experienced cracks.
 7. By using TPT force of 180,000 lb/diaphragm, the deck slab experienced maximum principal stresses up to 342 and 305 psi when applying the positive temperature gradient with AASHTO HL-93 loading in Location II and III, respectively. No cracks were developed in the deck slab under any of the load locations.

4.3.4.5 Two-Lane Bridge Model (Span = 100 ft, Width = 45 ft)

This bridge model was composed of eleven side-by-side box-beams of a width of 48 in. each (total width of 45 ft) and depth of 39 in. as specified earlier for bridge models with 100 ft span.

The TPT force was set to 150,000 lb/diaphragm, applied through two strands at the third points of the beam depth.

Only half of the span was modeled and symmetry conditions were applied at the mid-span section. Furthermore, because of the span symmetry, the response due to AASHTO HS-25 truck could not be replicated. Instead, AASHTO equivalent lane load was applied with a transformation ratio as explained earlier in Section 2.2.4.3. Also, AASHTO HL-93 load was applied as lane load and tandem load multiplied by the transformation ratio instead of the truck load.

Stress and crack development in the deck slab ($f'_c = 3,000$ psi)

1. After applying the second stage of TPT force (125,000 lb/diaphragm after casting deck slab), the transverse compressive stresses reached 223 psi at the slab ends. At the same time, the majority of the slab experienced compressive stresses in the range of 12 to 36 psi.
2. After deducting time dependent losses and applying SDL, the slab experienced additional compressive stresses. Some tensile stresses of about 86 psi developed at the slab ends near first and last shear-keys.
3. When applying positive temperature gradient, the slab bottom surface experienced localized tensile stresses of about 308 psi, mainly above the shear-keys.
4. **Live load Location I (after positive temperature gradient):** subsequent to applying the positive temperature gradient, applying the equivalent AASHTO HS-25 truck load over one shoulder (2 ft away from the barrier edge) increased the maximum principal stresses to 340 psi. The slab did not experience cracks under the applied load.
5. **Live load Location II (after positive temperature gradient):** subsequent to applying the positive temperature gradient, by applying load of two equivalent AASHTO HS-25 trucks over both the shoulders simultaneously (one truck per shoulder), the principal stresses reached 342 psi. The slab did not experience cracks under the applied load.
6. **Live load Location III (after positive temperature gradient):** subsequent to applying the positive temperature gradient, by applying two equivalent AASHTO HS-25 trucks

- at the mid-width of the model after applying the positive temperature gradient, the maximum principal stresses increased to 303 psi. The slab did not experience cracks. However the slab experienced cracks when the load exceeded the load by 20%.
7. By providing a TPT force of 150,000 lb/diaphragm and applying positive temperature gradient then equivalent AASHTO HL-93 loading in Location I, II, and III, the deck slab experienced maximum principal stresses up to 342, 323, and 311 psi, respectively. No cracks were developed in the deck slab under any of these load cases.

4.3.4.6 Three-Lane Bridge Model (Span = 100 ft, Width = 58 ft)

This bridge model was composed of fourteen side-by-side box-beams of a width of 48 in. each. The initial TPT force was set to 150,000 lb/diaphragm, applied through seven diaphragms.

Stress and crack development in the deck slab ($f'_c = 3,000$ psi)

1. After applying the second stage of TPT force (125,000 lb/diaphragm after casting the deck slab), the transverse compressive stresses reached 275 psi at the slab ends. At the same time, the majority of the slab experienced compressive stresses on the order of 16 to 45 psi.
2. When deducting the time dependent losses and applying SDL, the slab experienced some localized tensile stresses of about 107 psi near the supports.
3. When applying positive temperature gradient, the slab bottom surface experienced tensile stresses up to 291 psi at the shear-key locations.
4. **Live load Location I:** subsequent to applying the positive temperature gradient, applying the equivalent AASHTO HS-25 truck over one of the shoulders increased the maximum principal stresses to 352 psi. The slab experienced no cracks under the applied loads. However, the TPT force can be considered just enough to prevent the cracks because the maximum tensile stresses were very close to the concrete cracking strength. If the load exceeds the load by 20%, the cracks would develop.
5. **Live load Location II:** when applying two equivalent AASHTO HS-25 trucks over both the shoulders simultaneously after applying the positive temperature gradient, the

maximum principal stresses reached 319 psi. This load case did not result in longitudinal cracking in the deck slab.

6. **Live load Location III:** when applying two equivalent AASHTO HS-25 trucks simultaneously over the mid-width of the model after applying the positive temperature gradient, the maximum principal stresses in the deck slab bottom surface reached 316 psi; the slab experienced no cracks. However, the cracks developed at the mid-width under the trucks location when applying 120% of the load.
7. By providing TPT force of 150,000 lb/diaphragm and applying the positive temperature gradient then equivalent AASHTO HL-93 loading in locations I, II, and III, the deck slab experienced maximum principal stresses up to 351, 328, and 315 psi, respectively. No cracks were developed in the deck slab under any of the load cases.

4.3.4.7 Four-Lane Bridge Model (Span = 100 ft, Width = 70 ft)

The 70 ft wide bridge model was composed of seventeen side-by-side box-beams of a width of 48 in. each. The TPT force was set to 150,000 lb/diaphragm applied through seven diaphragms.

Stress and crack development in the deck slab ($f'_c = 3,000$ psi)

1. After applying the second stage of TPT force (125,000 lb/diaphragm after casting the deck slab), the transverse compressive stresses increased to 269 psi at the slab ends. At the same time, the majority of the slab experienced compressive stresses not exceeding 70 psi.
2. After deducting the time dependent losses and applying SDL, some tensile stresses of a value of about 131 psi developed locally in the slab bottom surface near the ends.
3. When applying positive temperature gradient, the slab bottom surface experienced tensile stresses up to 287 psi over the shear-keys of the fascia beams near the supports.
4. **Live load Location I:** when applying equivalent AASHTO HS-25 truck over one of the shoulders after applying the positive temperature gradient, the principal stresses in the deck slab bottom surface reached 350 psi; the slab experienced small cracks;

however, the TPT force can be considered just enough to prevent the cracks. The cracks propagated when increasing the load.

5. **Live load Location II:** subsequent to applying the positive temperature gradient, applying two equivalent AASHTO HS-25 trucks over both shoulders simultaneously (one truck per shoulder) increased the maximum principal stresses in the slab bottom surface to 352 psi. Small cracks developed near the edges and propagated when increasing the loads by 20%.
6. **Live load Location III:** when applying two equivalent AASHTO HS-25 trucks simultaneously over the mid-width of the model after applying the positive temperature gradient, the slab experienced longitudinal cracks. The crack sizes and propagation implied that the applied TPT force was not adequate for the four-lane bridge; therefore, a TPT force level of 175,000 lb/diaphragm was applied to the model.
7. Increasing the TPT level eliminated the development of the deck cracks. However, when applying an additional 20% of the load, the slab experienced longitudinal cracks.
8. By providing TPT force of 175,000 lb/diaphragm and applying the positive temperature gradient with equivalent AASHTO HL-93 load in Locations I, II, and III, the deck slab experienced maximum principal stresses of 310, 342, and 311 psi, respectively. No cracks were developed in the deck slab under any of these load cases.

4.3.4.8 Five-Lane Bridge Model (Span = 100 ft, Width = 78 ft)

This 78 ft wide bridge model was composed of nineteen side-by-side box-beams of a width of 48 in. each; however, it was not possible to model the entire bridge width. Instead, only one quarter of the bridge was modeled; symmetry conditions were applied through the mid-width section and the mid-span section. Considering the finding from the previous five-lane bridge model, a TPT force of 180,000 lb/diaphragm was applied through seven diaphragms.

Stress and crack development in the deck slab ($f'_c = 3,000$ psi)

1. After applying the second stage of TPT force (155,000 lb/diaphragm after casting the deck slab), the transverse compressive stresses increased to 309 psi at the slab ends. At

- the same time, the majority of the slab experienced compressive stresses ranging between 17 and 82 psi.
2. Tensile stresses of about 152 psi developed locally at the slab ends after deducting the time dependent losses and applying SDL.
 3. When applying the positive temperature gradient, the slab bottom surface experienced tensile stresses up to 282 psi at the outer shear-keys near the supports.
 4. **Live load Location I:** the live load was not applied in Location I for the five-lane bridge model.
 5. **Live load Location II:** when applying two equivalent AASHTO HS-25 trucks over the shoulders simultaneously after applying the positive temperature gradient, the maximum principal stresses increased to 352 psi in the slab bottom surface. The slab did not experience cracks under the applied load. With an extra 20% of the load, the slab experienced small cracks at the far ends.
 6. **Live load Location III:** when applying two equivalent AASHTO HS-25 trucks simultaneously over the mid-width of the model after applying the positive temperature gradient, the maximum principal stresses increased to 325 psi, and the slab experienced no cracks under the loads. However, when applying additional 20% of the load, some longitudinal cracks developed near the mid-width.
 7. By providing a TPT force of 180,000 lb/diaphragm, the deck slab experienced maximum principal stresses up to 349 and 344 psi when applying the positive temperature gradient and an equivalent AASHTO HL-93 loading in Locations II and III, respectively. No cracks were developed in the deck slab under any of the load cases.

Table 4.3-1 Stress development in the deck slab due to surface loads in FE bridge models generated using 48 in. wide box-beams.

Span (ft)	Width (ft)	No. of Diaph.	TPT Force lb/diaph.	Transverse Stresses* (psi)	MP +ve TG (psi)	MP Live load (HL-93 load) IM = 75% (psi)		
						Location I <i>m</i> = 1.14	Location II <i>m</i> = 0.95	Location III <i>m</i> = 0.95
Concrete properties: f'_c = 3,000 psi, f_r = 350 psi, $E = 3 \times 10^6$ psi								
50	24	5	150,000	11-54	229	286	N/A	N/A
50	45	5	150,000	29-59	259	338	375	306
50	58	5	150,000	23-59	273	353	383	186
50	70	5	175,500	36-112	259	342	379	267
50	78	5	180,000	61-112	262	N/A	386	305
100	24	7	150,000	15-72	234	351	N/A	N/A
100	45	7	150,000	12-36	308	342	323	311
100	58	7	150,000	16-45	291	351	328	315
100	70	7	175,500	15-81	285	310	342	311
100	78	7	180,000	17-82	282	N/A	349	344
Concrete properties: f'_c = 4,000 psi, f_r = 460 psi, $E = 3.83 \times 10^6$ psi								
50	24	5	120,000	5-80	343	411	N/A	N/A
50	45	5	140,000	29-95	366	434	426	450
50	58	5	140,000	28-93	367	427	421	436
50	70	5	160,000	30-106	346	441	424	448
50	78	5	165,000	32-110	348	N/A	441	447
Concrete properties: f'_c = 5,000 psi, f_r = 514 psi, $E = 4.3 \times 10^6$ psi								
50	24	5	100,000	3-66	407	493	N/A	N/A
50	45	5	130,000	28-97	423	491	480	511
50	58	5	130,000	29-98	420	476	482	510
50	70	5	150,000	29-105	397	511	501	513
50	78	5	155,000	29-107	399	N/A	510	511

* = Range of compressive transverse stresses developed in the deck slab due to TPT force

MP = Maximum principal stresses in the deck slab (tension)

TG = Temperature gradient

IM = Impact allowances

m = Presence factor

N/A = Not available

4.3.5 Bridge Models Generated Using 36 in. Wide Box-Beams

The previous models simulated bridges constructed using 48 in. wide box-beams. The results in terms of adequate TPT force were also verified for bridges constructed using the 36 in. wide box-beams. FE models for bridges with spans of 50, 62, and 100 ft (Figure 4.3-11) and widths of 24, 47, 59, 72, and 84 ft Figure 4.3-12 were generated using 36 in. wide box-beams. The same technique of analysis was employed, and the results were compared with those of the previous models. The analysis revealed that adequate TPT force level to prevent the deck slab cracking is independent of the box-beams width.

The entire analysis in this section was performed assuming recently constructed deck slab with concrete ultimate compressive strength of 4,000 psi, modulus of rupture of 460 psi, and modulus of elasticity of 3.83×10^6 psi. No analysis was performed for the cases of deteriorated and special-quality deck slabs since the influence of the concrete strength on the adequate TPT force shall be similar to what was observed in the case of 48 in. wide box-beams. Table 4.3-2 shows the stress values that were achieved in the deck slab after applying service loads. Except for the stress values due to applying the TPT force, all the presented stresses are tensile and compared with a value of 460 psi (the cracking strength of the concrete in the deck slab).

Table 4.3-2 Stress development in the deck slab due to surface loads in FE bridge models generated using 36 in. wide box-beams.

Span (ft)	Width (ft)	No. of Diaph.	TPT Force lb/Diaph.	Transverse Stresses* (psi)	MP +ve TG (psi)	MP Live load (HL-93 load) IM = 75% (psi)		
						Location I <i>m</i> = 1.14	Location II <i>m</i> = 0.95	Location III <i>m</i> = 0.95
50	24	5	120,000	16-71	358	415	N/A	N/A
50	47	5	140,000	49-111	328	400	375	427
50	59	5	140,000	36-109	334	434	383	396
50	72	5	161,500	44-111	323	N/A	379	398
50	84	5	169,000	49-121	317	N/A	386	376
62	24	6	120,000	3-52	410	452	N/A	N/A
62	47	6	140,000	21-74	383	462	406	413
62	59	6	140,000	40-94	379	447	414	430
62	72	6	161,500	41-101	368	N/A	446	447
62	84	6	169,000	46-107	361	N/A	451	433
100	24	8	120,000	18-56	355	427	N/A	N/A
100	47	8	140,000	21-66	384	459	451	391
100	59	8	140,000	21-66	426	460	457	404
100	72	8	161,500	26-104	419	N/A	458	433
100	84	8	169,000	27-108	417	N/A	459	444

* = Range of compressive transverse stresses developed in the Deck slab due to TPT force

MP = Maximum principal stresses in the deck slab (tension)

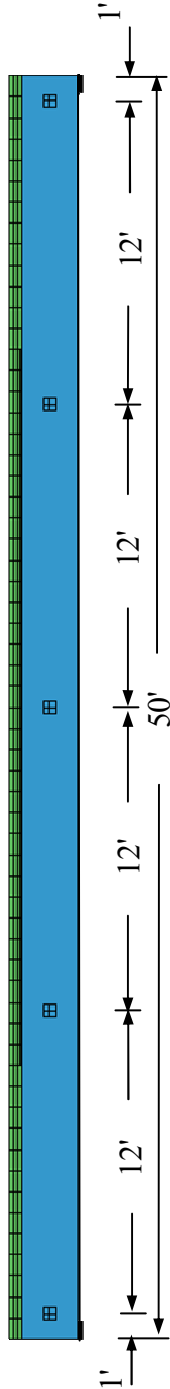
TG = Temperature gradient

IM = Impact allowances

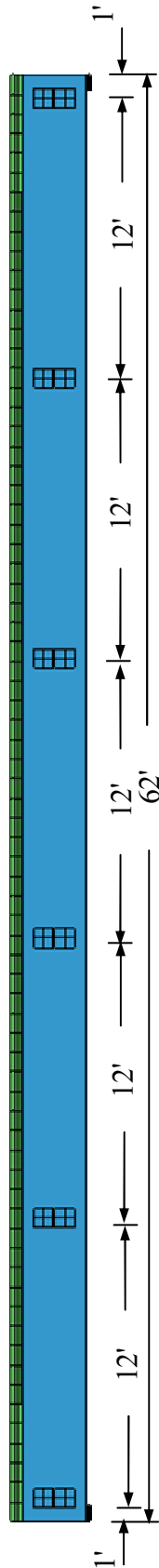
m = presence factor

N/A= Not available

50 ft span bridge model (8, 15, 19, 23, 27 box-beams)



62 ft span bridge model (8, 15, 19, 23, 27 box-beams)



100 ft span bridge model (8, 15, 19, 23, 27 box-beams)

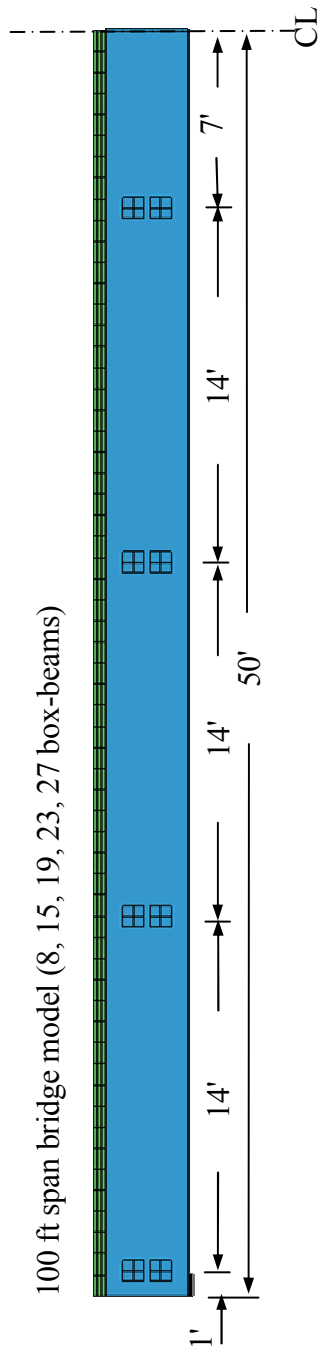


Figure 4.3-11 Bridge models generated using 36 in. wide box-beams (spans).

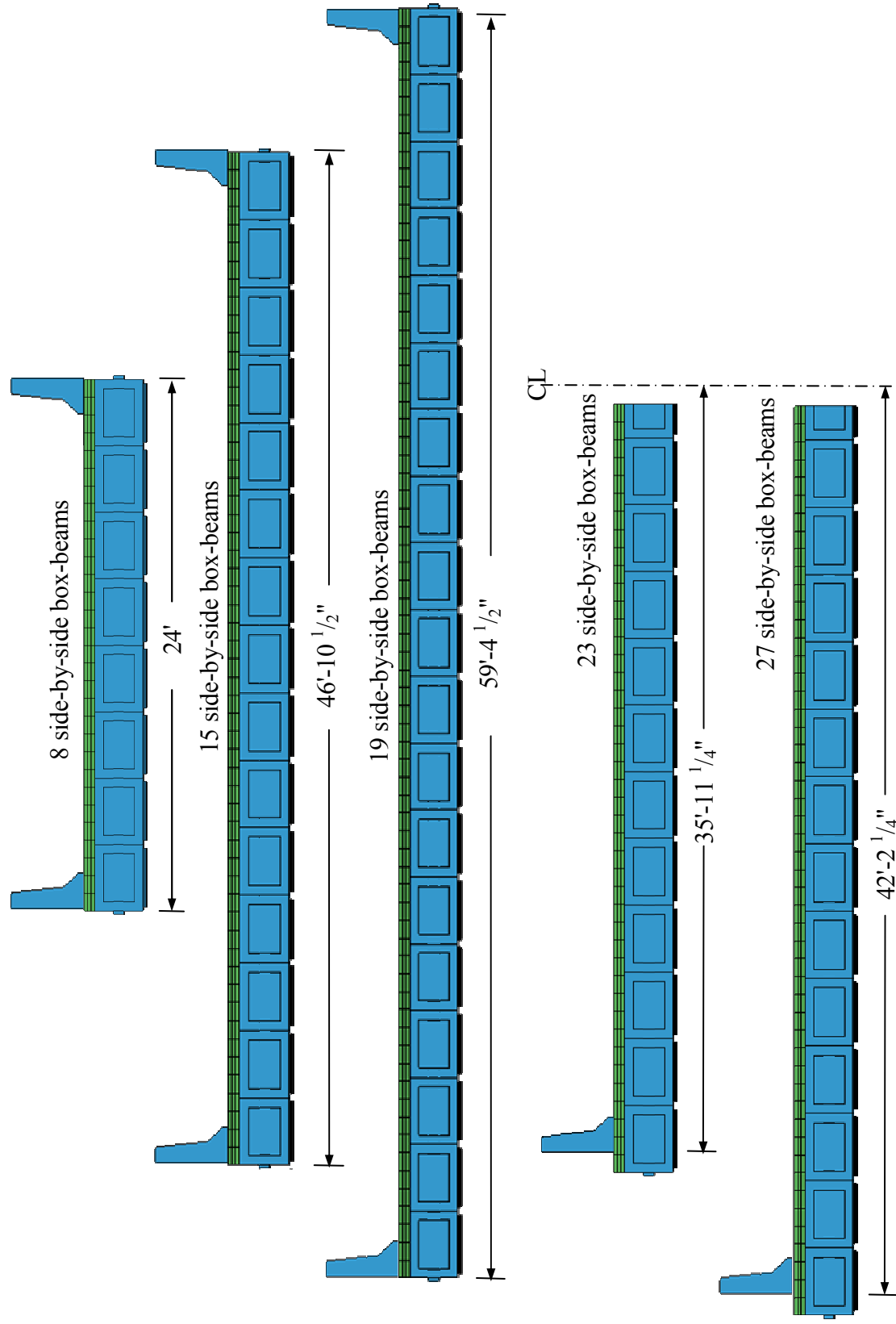


Figure 4.3-12 Bridge models generated using 36 in. wide box-beams (widths).

4.3.6 Discussion of the Results

Based on the analysis presented in this section for wide bridge models, the following findings were obtained:

1. The current TPT force recommended in the MDOT Bridge Design Guide (2006) is not adequate in preventing the development of longitudinal deck slab cracking in side-by-side box-beam bridges.
2. The AASHTO LRFD (2004) limit of 250 psi as a minimum uniform prestress in the longitudinal joints between the box-beams is not achievable regardless of the applied TPT force.
3. The adequate number of diaphragms was established for various bridge spans while keeping the TPT force level as close as possible to current recommended levels. Therefore, the TPT force required per diaphragm was independent of bridge span.
4. The analysis of the models generated using 48 in. wide box-beams and those generated using 36 in. wide box-beams yielded the same results for the adequate level of the TPT force to prevent longitudinal deck cracking. In other words, the required TPT force level for a given bridge width is independent of the width of the individual box-beams.
5. The appropriate level of the TPT force increases with increasing the bridge width and slightly decreases with increasing the concrete strength of the deck slab, as shown in Figure 4.3-13.
6. It is recommended to consider future slab deterioration when applying TPT force during construction to reduce any future repair labor.

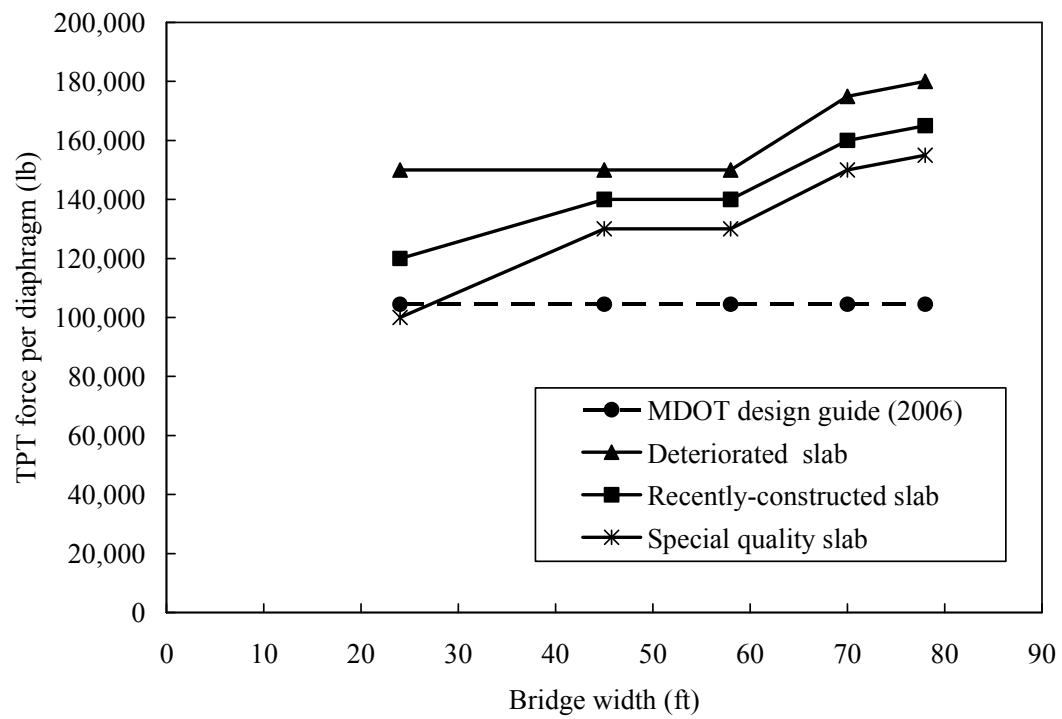


Figure 4.3-13 Appropriate TPT force vs. bridge width (valid for bridges constructed using 36 or 48 in wide box-beams).

CHAPTER 5: EXPERIMENTAL INVESTIGATION

5.1 Introduction

A 30° skewed precast prestressed box-beam bridge model was constructed to study its behavior in the transverse direction. The bridge model consisted of four adjacent precast prestressed concrete box-beams with a total span of 31 ft, as shown in Figure 5.1-1. The four box-beams were designated as B-1, B-2, B-3, and B-4.



Figure 5.1-1 General view of precast prestressed box-beam bridge model.

The construction of the formwork of the box-beams and the steel cages was completed in the casting yard located in the Center for Innovative Materials Research (CIMR) at the Lawrence Technological University (LTU). The precast prestressed concrete box-beams were pre-tensioned using seven-wire steel strands and constructed from high strength concrete. When the beams had gained adequate strength, the prestressing forces were released and subsequently, the beams were transported to the Structural Testing Center (STC) at the LTU. The bridge model was assembled using the four box-beams, steel reinforced deck slab, shear-

keys, and unbonded transverse post-tensioning (TPT) strands using carbon fiber composite cables (CFCC).

After the bridge deck slab had gained adequate strength, the experimental investigation was launched to study the transverse behavior of the bridge model under three different service life conditions. The first condition (uncracked deck slab) simulated a highway bridge, which was newly constructed and has not experienced any major cracks on the bridge deck. The second condition (cracked deck slab) simulated a highway bridge, which had experienced longitudinal deck cracking over the shear-key locations. The third condition (beam replacement stage), where an individual box-beam of the bridge was assumed damaged and replaced.

The bridge model behavior under these three conditions was evaluated using the strain and the load distribution tests. The purpose of the strain distribution test was to monitor the transverse strains developed in the deck slab due to the application of different levels of TPT force with different number of diaphragms. The purpose of the load distribution test was to investigate the deflection behavior of the individual box-beams and the deflection based load distribution when applying eccentric loads. In addition, the ultimate load test was conducted on the bridge model to study the efficiency of the TPT system and to determine the ultimate load-carrying capacity.

The chapter is divided into two major sections:

1. Construction program of the bridge model containing the description of all the materials used and a detailed description of the formwork and the steel cage construction.
2. Test program including the instrumentation of the bridge model and a detailed description of all the tests conducted in the study.

5.2 Bridge Model Construction Phase

5.2.1 Materials

The bridge model consisted of box-beams, shear-keys, deck slab, and TPT strands. These components were constructed from high strength concrete, steel reinforcements, non-shrink grout, and CFCC. Details of these materials are provided in the following sections.

5.2.1.1 Concrete

The precast prestressed concrete box-beams were made of high strength concrete, with steel prestressing strands and non-prestressing steel rebars as flexural reinforcements. Steel stirrups were also provided as shear reinforcement. The box-beams were constructed from a high strength concrete mix. The concrete mix design and the quantities as delivered are shown in Table 5.2-1. In order to ensure that the concrete mix had the appropriate workability before casting the beams, two slump tests were conducted. The designed slump was 8 in., which was close to the measured slump. Electrical vibrators as well as mechanical rods were used during the casting of the beams to ensure a uniform compaction of the concrete. The uniaxial compressive strength was determined according to the American Society for Testing and Materials (ASTM) C39 at 7, 21, and 28 days. The average 28 day compressive strength was 6,268 psi, as shown in Figure 5.2-1. The uniaxial compression test apparatus is shown in Figure 5.2-2. The mechanical properties of concrete mix are tabulated in Table 5.2-2.

Table 5.2-1 Concrete mix proportions for beams.

Material	Design Quantity per Cubic Yard, lb	Total Quantity, lb
Fine aggregates	1,287	7,915
Coarse aggregates	1,760	10,560
Cement (Type 1)	534	3,204
Cementitious material	288	1,728
Water reducing admixture	2.05	12.33
High range water-reducer	6.17	37
Water	265	1,590

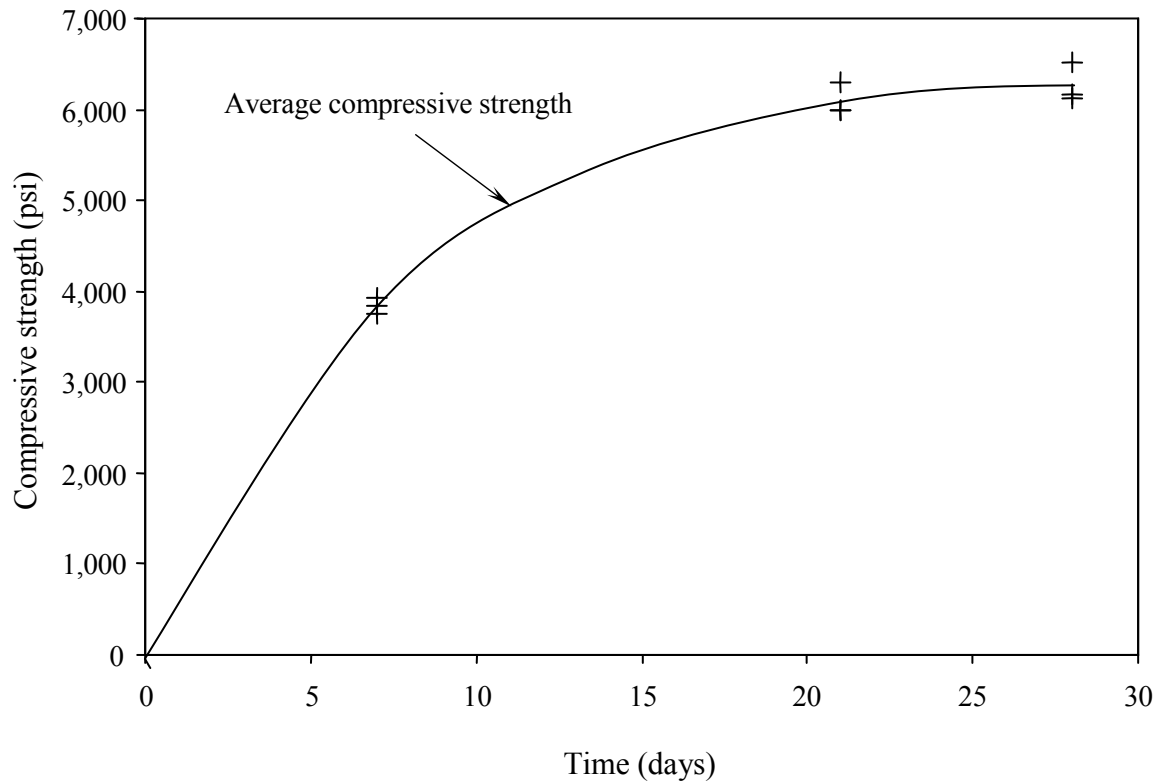


Figure 5.2-1 Compressive strength of concrete with time.

Table 5.2-2 Mechanical properties of the concrete mix.

Time, Days	Compressive Strength, psi	Average Compressive Strength, psi	Modulus of Elasticity, ksi
7	3,749	3,837	N/A *
	3,836		
	3,926		
21	6,287	6,086	N/A
	5,990		
	5,981		
28	6,130	6,268	4,450
	6,510		
	6,164		

N/A*: Not Applicable



(a) Concrete cylinder being tested



(b) Failure of concrete cylinder

Figure 5.2-2 Typical uniaxial compression test setup for concrete cylinders.

5.2.1.2 Steel Reinforcement

The box-beams were constructed from steel reinforcement cages as mentioned earlier. The flexural reinforcement consisted of non-prestressing rebars and seven-wire prestressing strands. Details of the various reinforcements are presented in the following sections.

Prestressing strands

The longitudinal prestressing reinforcement used was 0.5 in. high strength low-relaxation seven-wire steel strands of Grade 270 supplied by the Victory Re-Steel, Inc. Three strands were provided in each box-beam at the bottom level resulting in an eccentricity of 5 in. from the centroid of the cross-section of the box-beam. Typical mechanical properties of the steel strands used are shown in Table 5.2-3 (Nawy, 2003).

Non-prestressing bars

Conventional normal-strength #4 steel bars of Grade 60 were used as the longitudinal non-prestressing reinforcements. Typical characteristics and mechanical properties of the #4 bars are shown in Table 5.4 (Macgregor and Wight, 2004). Each box-beam consisted of four bottom and four top non-prestressing reinforcements.

Shear reinforcements

The shear reinforcements were stirrups made of conventional #3 steel bars of Grade 60, and its characteristics and mechanical properties are shown in Table 5.2-4 (Macgregor and Wight, 2004). The non-prestressing reinforcements were tied to the stirrups using commercially available Weather Resistant Nylon Wire Ties (plastic zip-ties) supplied by the Industrial Products, Inc.

Table 5.2-3 Characteristics and mechanical properties of a typical seven-wire steel strand.

Property of Strand	Seven-Wire Prestressing Steel Strands
Grade	270
Nominal diameter, in.	0.5
Nominal weight, lb/ft	0.52
Cross-sectional area, in ²	0.153
Perimeter, in.	1.571
Min. breaking strength, lb	41,300
Specified minimum yield strength, ksi	229.5
Minimum tensile strength, ksi	250
Modulus of elasticity, ksi	27,000
Minimum load at 1% extension, lb	35,100
Yield strain, %	1

5.2.1.3 Carbon Fiber Reinforced Polymers (CFRP) Reinforcement

Conventional steel strands used as TPT system for side-by-side box-beam bridges are usually vulnerable to corrosion when exposed to harsh environmental conditions and deicing salt. The detrimental effect of this phenomenon is the reduction of the strength of the steel strands, which leads to a reduction in the load-carrying capacity of the bridge. To avoid this problem, the concept of using CFRP strands was introduced as an alternative material. The CFRP used for this project was CFCC manufactured by the Tokyo Rope Mfg. Co., Ltd., Japan. A total of

ten 1×7 0.67 in. diameter CFCC were used during the test program to apply the TPT forces at the transverse diaphragms. Table 5.2-.5 and Figure 5.2-3 show the mechanical properties and dimensions of the CFCC, respectively.

Table 5.2-4 Mechanical properties of the non-pretressing bars and stirrups.

Property of Reinforcements	Non-Prestressing Bars	Stirrups
Designation	#4 bars	#3 bars
Grade	60	60
Diameter, in.	0.5	0.375
Weight, lb/ft	0.668	0.376
Cross-sectional area, in ²	0.20	0.11
Perimeter, in.	1.571	1.178
Yield load, kip	12	6.6
Minimum yield strength, psi	60,000	60,000
Breaking strength, kip	18	9.9
Minimum tensile strength, psi	90,000	90,000
Modulus of elasticity, ksi	29,000	29,000
Minimum elongation, %	9	9

Table 5.2-5 CFCC Quality Report (Tokyo Rope Mfg. Co., Ltd., 2007).

Item	Specifications		Test Results				
	Nominal	Tolerance					
Lot No.	–	–		N346	–	–	–
Diameter, in.	0.67		Ave.	0.68	–	–	–
Effective cross-sectional area, in ²	0.23		–	–	–	–	–
Pitch, in.	–		Ave.	9.53	–	–	–
Linear density, lb/in.	16.2		Ave.	15.98	–	–	–
Breaking load, kip	78.4	78.4 or above	Ave.	92.29 95.42 84.90	–	–	–
Tensile strength, ksi	0.34	0.34 or above	Ave.	0.39	–	–	–
Tensile rigidity, kip	–	–	Ave.	5,279.7	–	–	–
Tensile modulus, ksi	22,330	–	Ave.	22,620	–	–	–
Elongation at break, %	1.5	–	Ave.	1.8	–	–	–

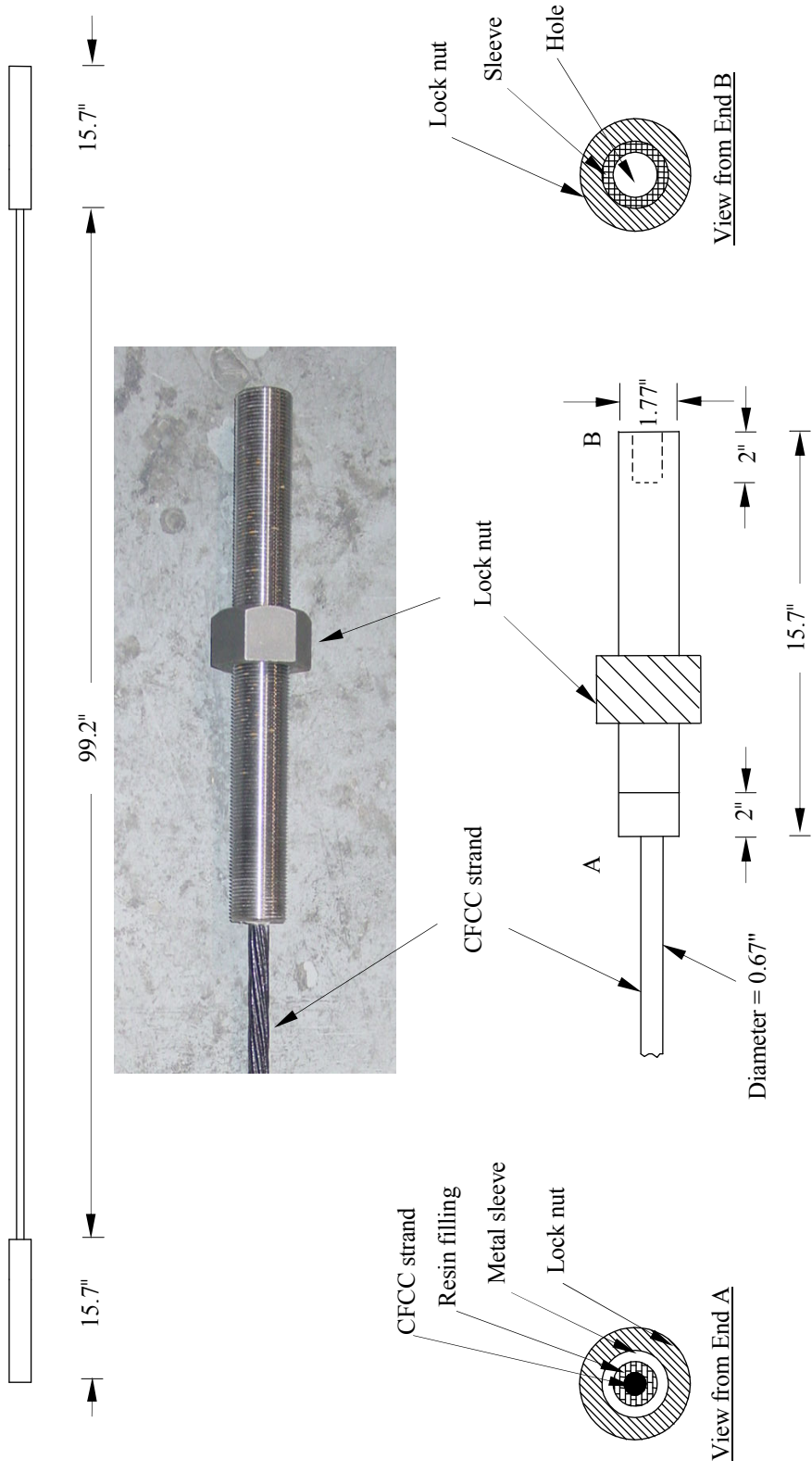


Figure 5.2-3 Dimensions of 1x7, 0.67 in. diameter CFCC for TPT.

5.2.2 Formwork

The formwork was designed to facilitate easy construction and disassembling. The formwork, constructed mainly from plywood, consisted of chairs, base plates, center plate and side plates. The formwork was supported on chairs with two vertical stiffeners at a spacing of 3 ft beneath the base plates to prevent the base plate from sagging when subjected to the weight of the concrete. Horizontal and vertical stiffeners were also provided to support the side plates and to ensure straight alignment of the edges of the box-beams. The cross-sections of the formwork for the interior and exterior beams are shown in Figure 5.2-4.

The formwork of the two exterior beams (B-1 and B-4) was constructed next to each other, likewise the two interior beams (B-2 and B-3). The major difference between the exterior box-beams and the interior box-beams was the presence of the protruded steel notches provided at the transverse diaphragm locations of the exterior beams, as shown in Figure 5.2-5. Steel plates of 0.08 in. thick were used as metal forms for the exterior beams notches. The inner faces of the exterior box-beams and both the inner and the outer faces of interior box-beams were designed geometrically to form full-depth keyways when placed side-by-side. Steel tie rods of 0.5 in. diameter were also provided to hold the center plate and the side plates in place, which ensured that the designed width of the box-beams was maintained while the concrete cured. More details of the formwork are shown in Figures 5.2-6 through Figure 5.2-1.

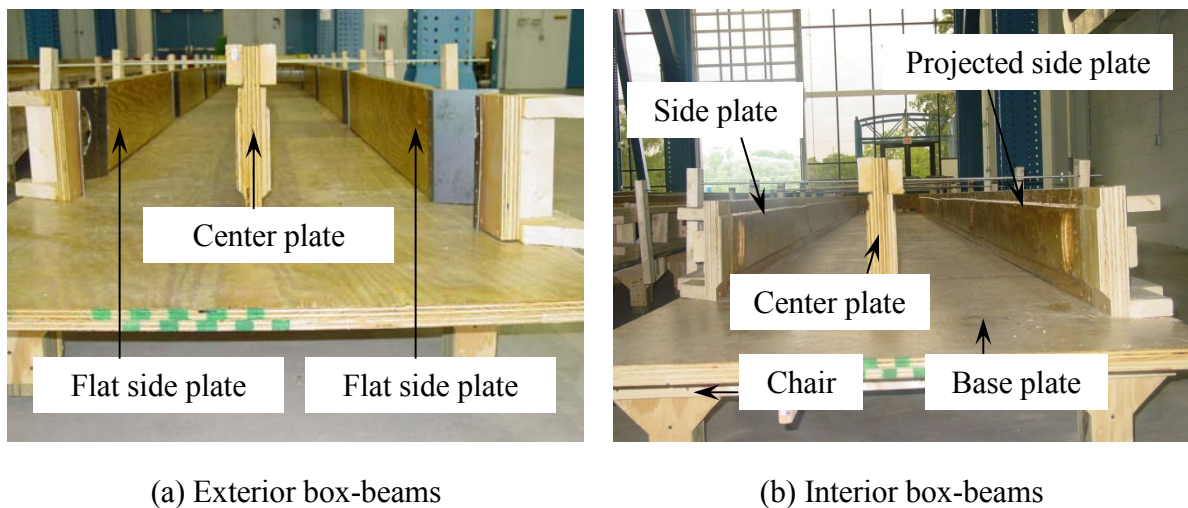
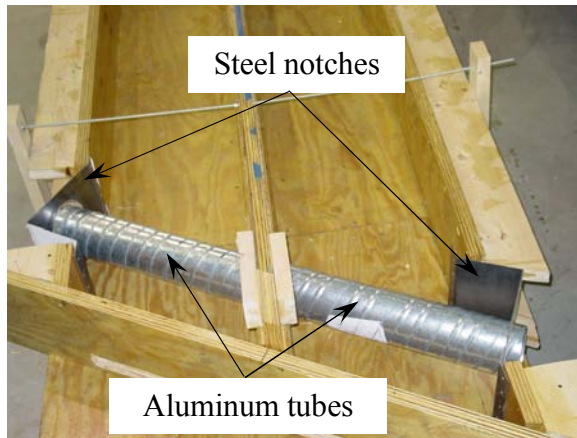


Figure 5.2-4 Cross-section of formwork.



(a) Plan view for steel notches

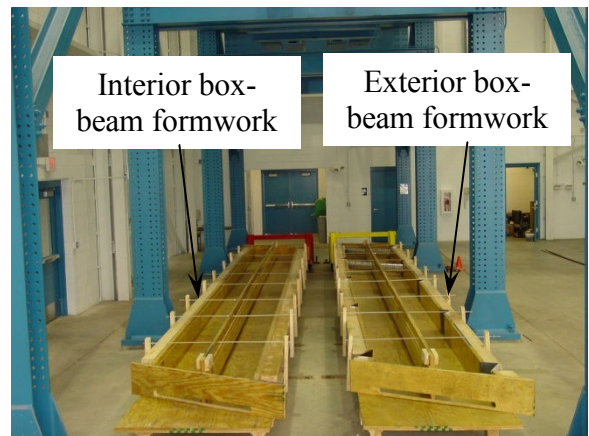


(b) Side view for steel notches

Figure 5.2-5 Details of the steel notches.



(a) Side view of formwork



(b) General view of formwork

Figure 5.2-6 Formwork prepared for box-beams.

In order to accommodate the TPT strands and to avoid potential misalignment problems due to differential camber, oval-shape ducts were created by inserting aluminum tubes at the appropriate transverse diaphragm locations, as shown in Figure 5.2-5(a). The major vertical axis and the minor horizontal axis of the tube were 5.75 in. and 4.5 in., respectively.

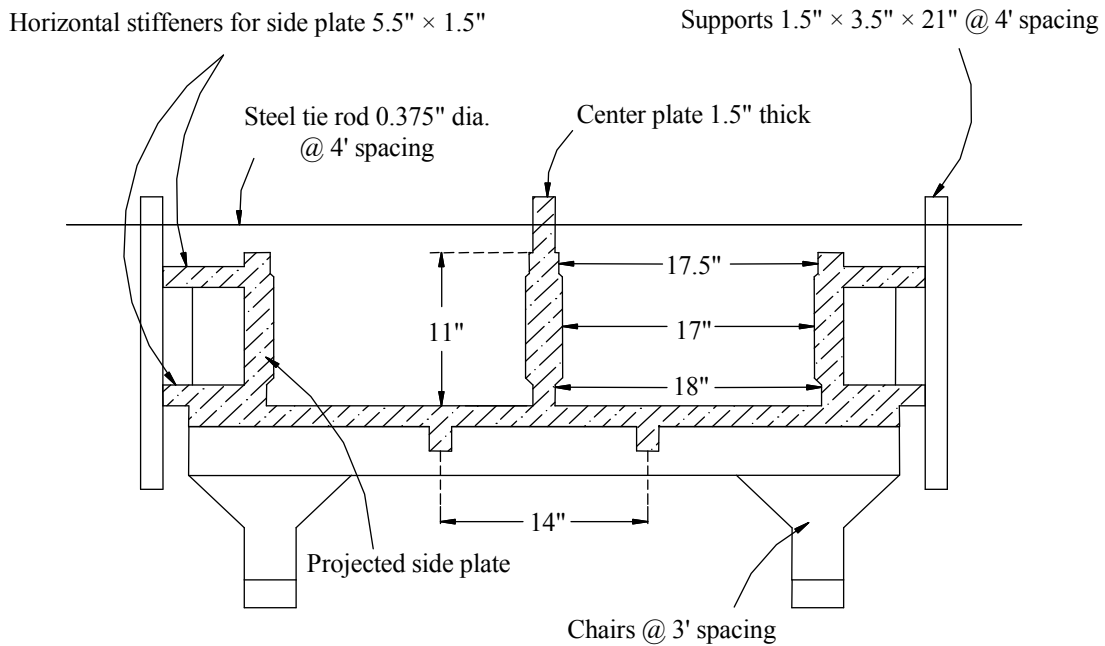


Figure 5.2-7 Cross-section of the formwork for the interior box-beams.

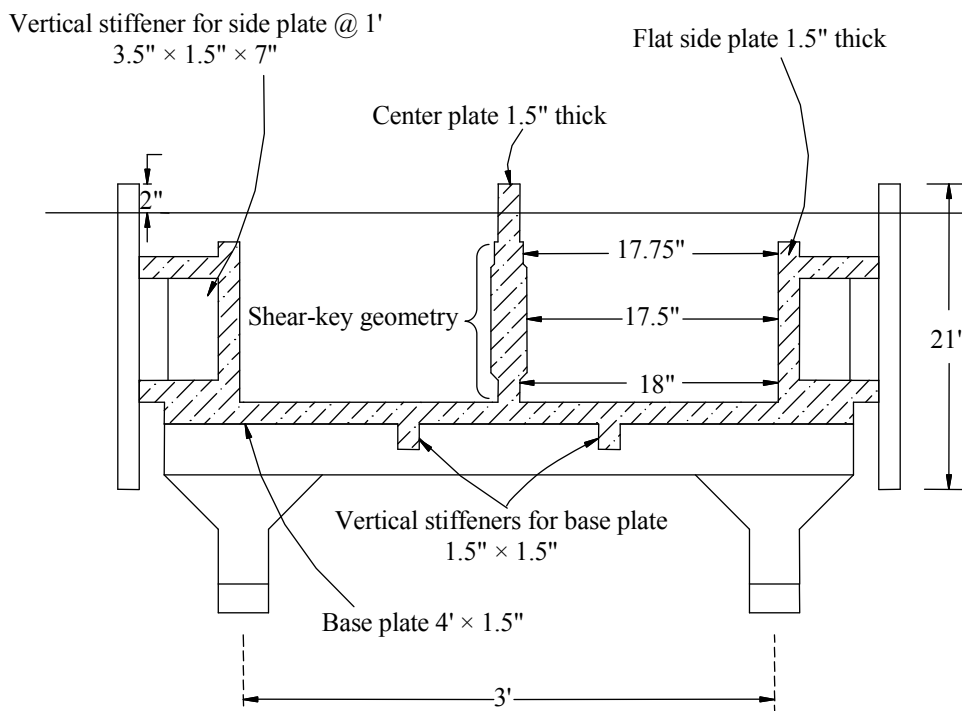


Figure 5.2-8 Cross-section of the formwork for the exterior box-beams.

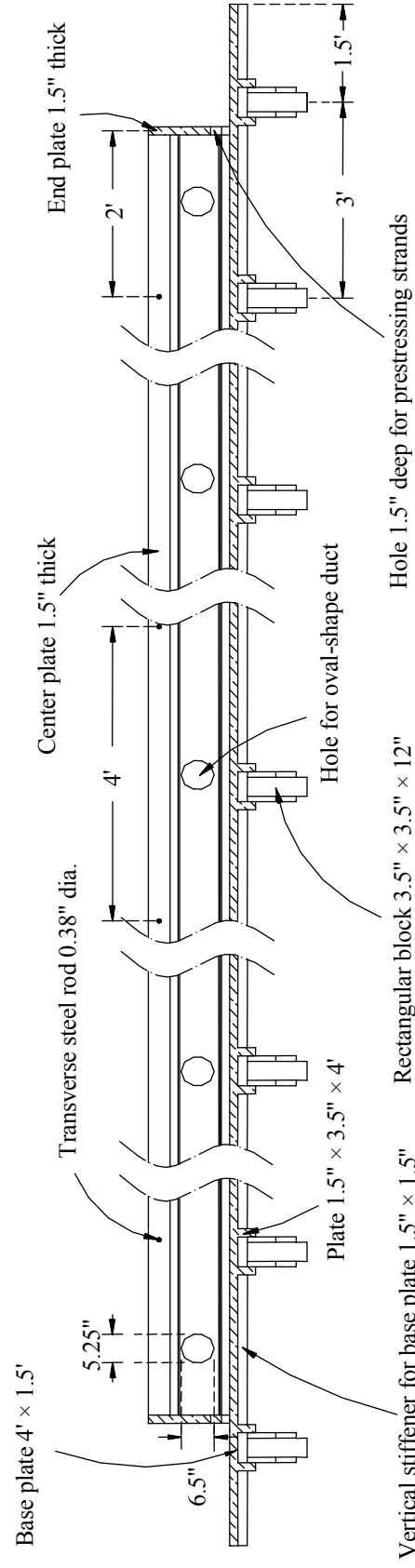


Figure 5.2-9 Longitudinal section of the formwork.

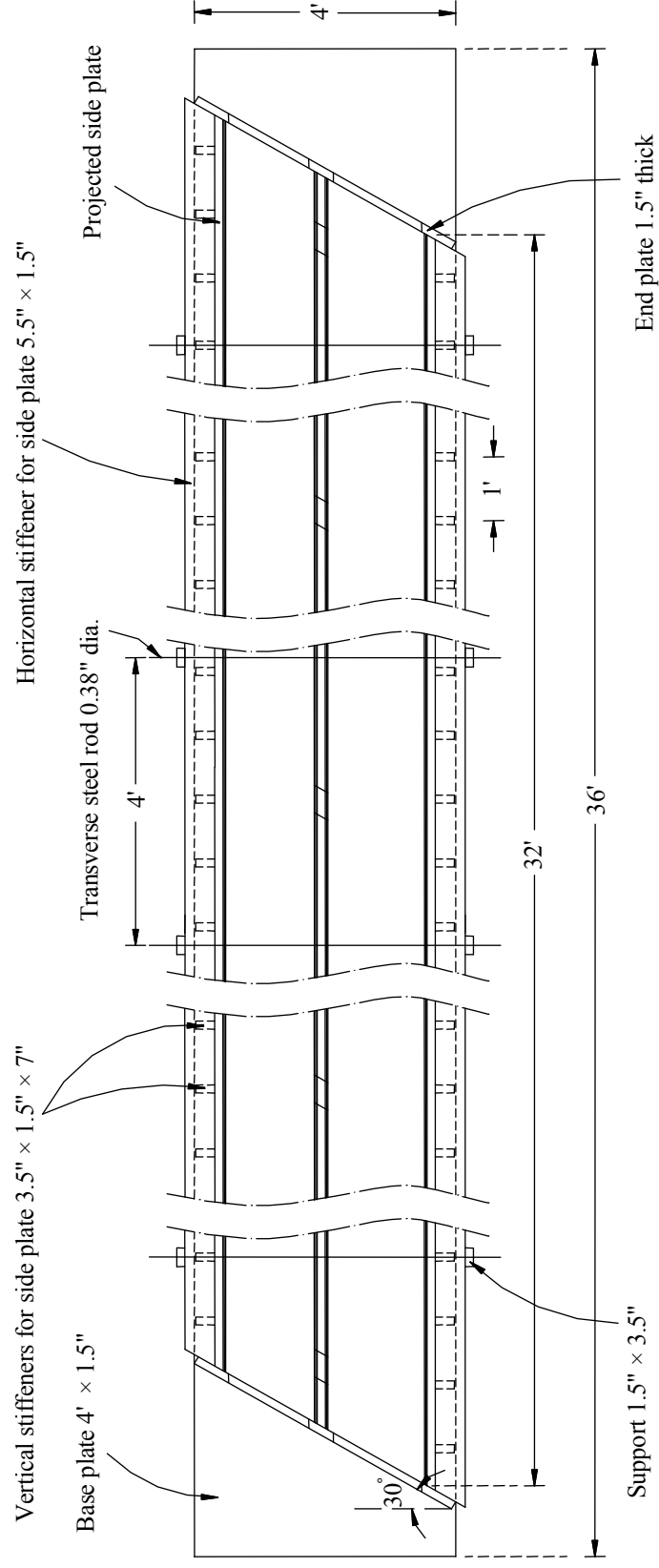


Figure 5.2-10 Plan view of the formwork for box-beams.

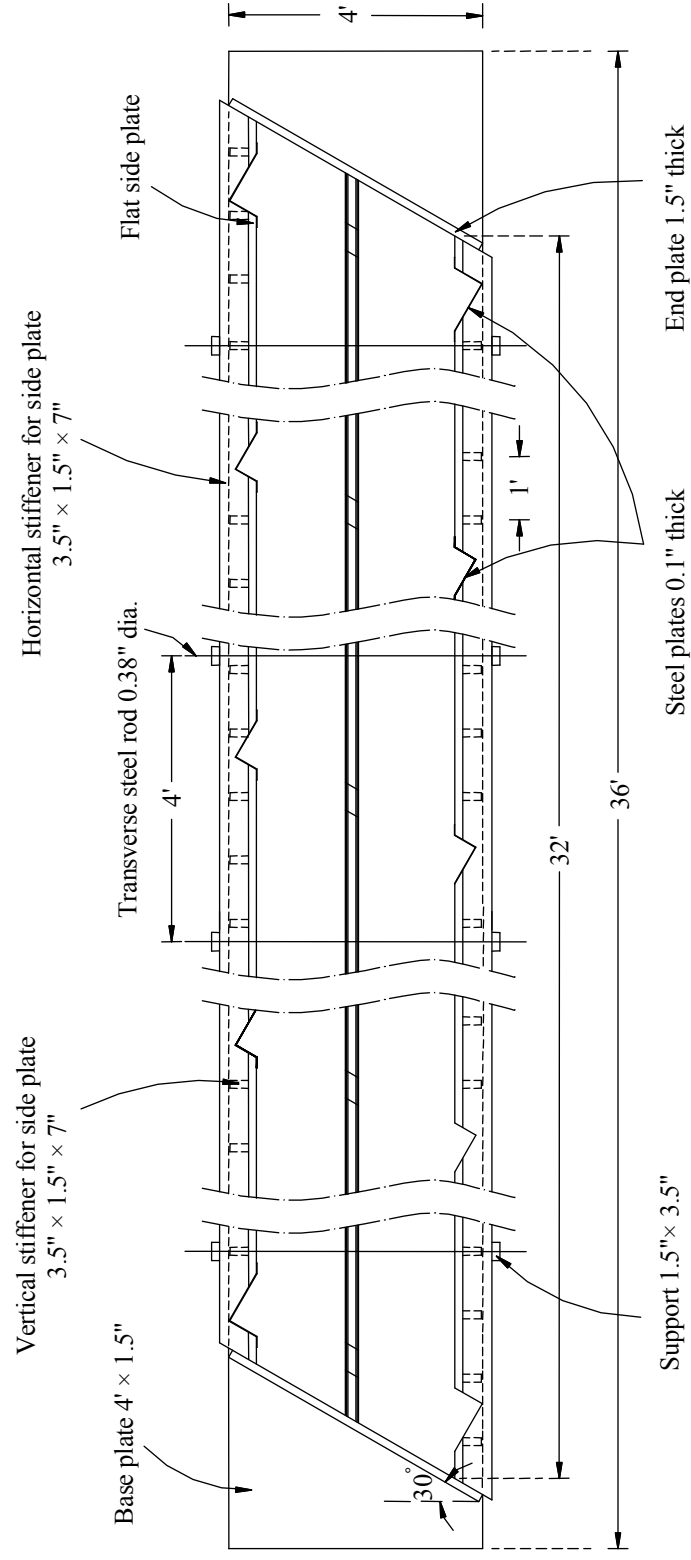


Figure 5.2-11 Plan view of the formwork for box-beams with projected side plates.

5.2.3 Reinforcement Cages

As mentioned earlier, each box-beam consisted of four #4 non-prestressing bars provided as top and bottom reinforcements. In addition, three 0.5 in. seven-wire steel strands were provided as prestressing strands and were located 2 in. from the bottom surface of the box-beams. The top reinforcements were located at 1.5 in. from the top surface of the box-beams and were held in position using #4 hanger bars placed at successive spacing of 4 ft. The stirrups were 11 in. deep and 15 in. wide from center-to-center and were placed at equal spacing of 5 in. The stirrups protruded 1.5 in. from the top surface of beams to achieve composite action between the box-beams and deck slab. Styrofoam of depth 5 in. and width of 10 in. was used to create the hollow portion within the cross-section of the box-beams and was placed at the mid-height of the box-beam cross-section. The box-beam cross-section is shown in Figure 5.2-12. The cross-section of the box-beams at the locations of the transverse diaphragms was modified to accommodate the Styrofoam gasket in order to ensure continuity of the aluminum tube in each beam and to also facilitate grouting of the shear-keys. The modified box-beam cross-section at diaphragm locations is shown in Figure 5.2-13.

Galvanized aircraft lifting cables were attached to the reinforcement cages at five equally spaced locations along the span to facilitate transportation and handling of the box-beams from the casting yard in the CIMR to the STC. The cables were made out of high strength strands with diameter of 0.25 in. and axial ultimate capacity of 7 kip as specified by the supplier, National Tool Grinding, Inc. Figure 5.2-14 and Figure 5.2-15 show the longitudinal section of the box-beam and steel reinforcement cages, respectively.

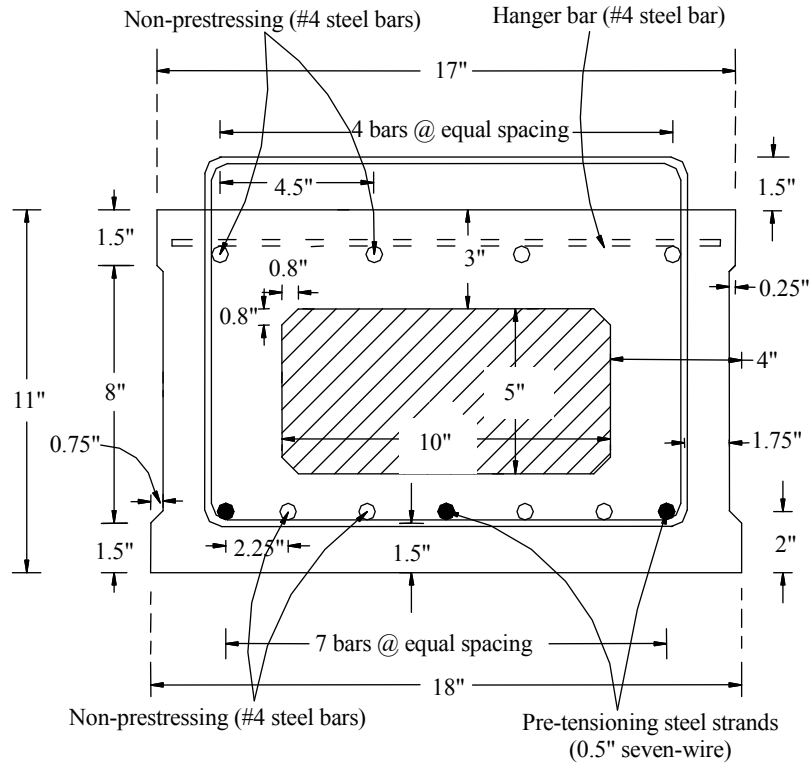


Figure 5.2-12 Cross-sectional details of the box-beams.

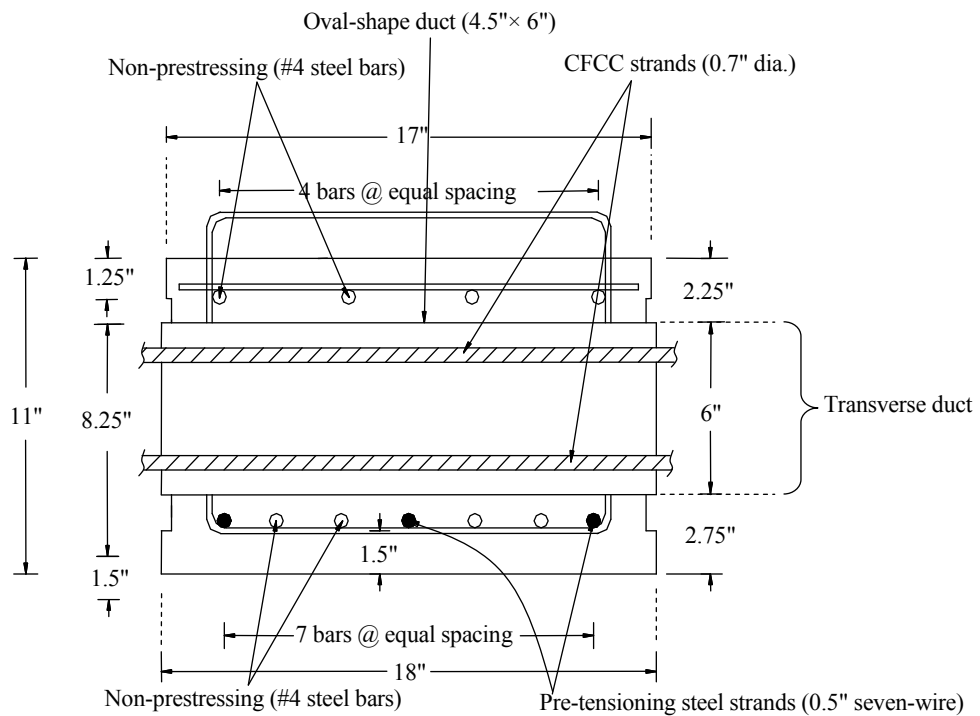
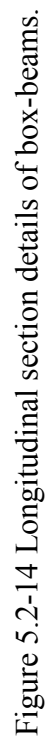


Figure 5.2-13 Cross-sectional details of the box-beams at diaphragms.





(a) Reinforcement cages for the box-beams



(b) Diaphragm reinforcement details

Figure 5.2-15 Steel reinforcement cages containing Styrofoam within.

5.2.4 End-Blocks

The end-blocks were designed to accommodate the localized stresses due to the pre-tensioning forces applied to the box-beams. Different levels of pre-tensioning forces were applied in order to develop the differential camber between the adjacent box-beams such as observed in the field. The reduced spacing between the stirrups at the end-blocks were employed to provide confinement for the concrete in order to resist the localized stresses that would be developed due to the pre-tensioning forces. The strength of the concrete was designed to resist the developed localized stresses at the end-blocks. The arrangements of the stirrups provided at the end-blocks and the end diaphragms are shown in Figures 5.2-16 through 5.2-18.

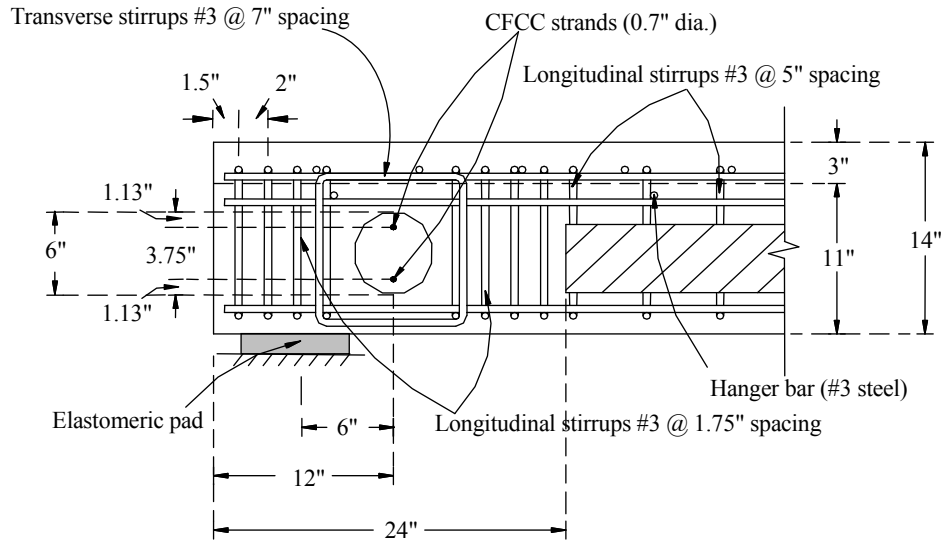


Figure 5.2-16 Cross-sectional details of the end diaphragm.

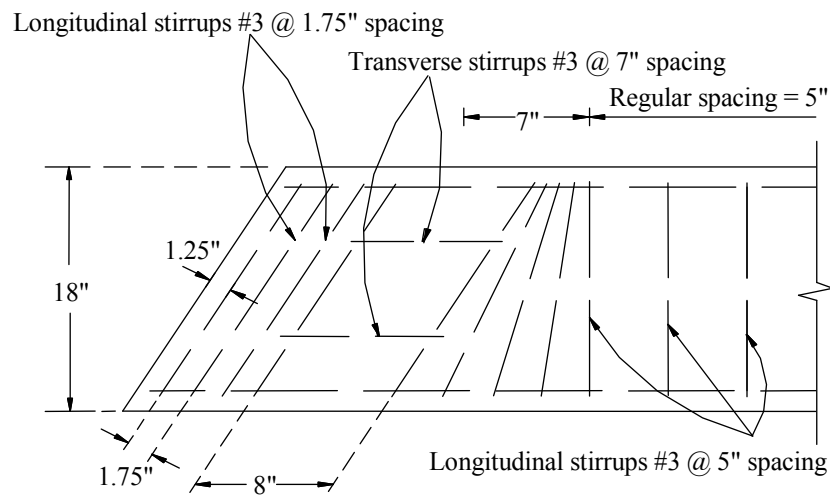


Figure 5.2-17 Reinforcement of interior box-beams at the end diaphragm.

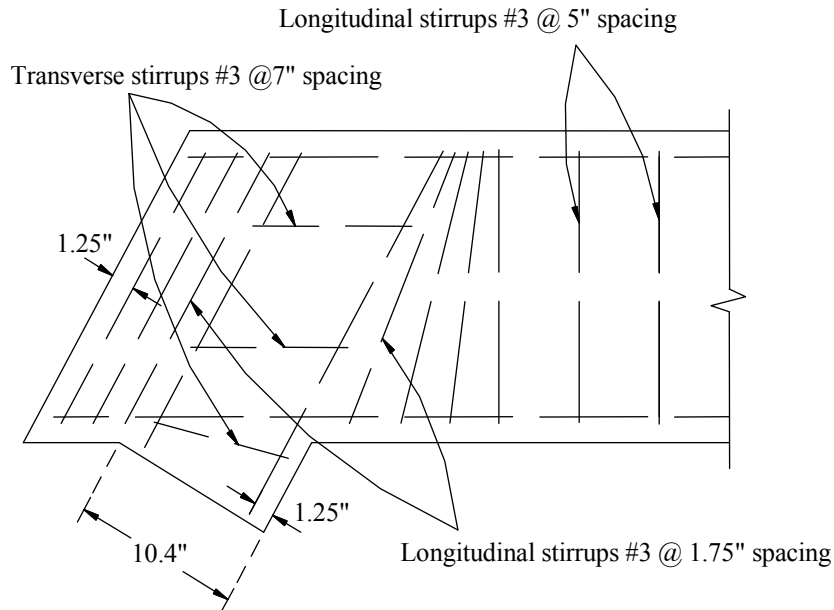


Figure 5.2-18 Reinforcement of exterior box-beams at the end diaphragm.

5.2.5 Transverse Diaphragms

As mentioned earlier, each box-beam contained five transverse diaphragms located at the ends, quarter-span, and the mid-span locations. The width of the intermediate diaphragms was 8 in. while that of the end/support diaphragms was 10.4 in. Because the bridge model had 30° skewed alignment, the centerlines of the diaphragms were made parallel to the support lines (i.e. making an angle of 60° with the longitudinal axis of the bridge model). The stirrups provided between the locations of the diaphragms were placed perpendicular to the longitudinal axes of the box-beams. However, the stirrups near the diaphragms locations were placed at gradually varying angles to ensure uniformity with the alignment of the transverse diaphragm. In addition, transverse stirrups were also provided within the diaphragms and placed at 7 in. spacing in order to resist localized stresses developed due to TPT forces as stipulated in the (MDOT Bridge Design Guide 6.65.12 and 6.65.13). The reinforcements provided in the transverse intermediate diaphragms for the interior and exterior box-beams are shown in Figure 5.2-19 through Figure 5.2-21. The details of the steel cages and the transverse ducts located at the transverse diaphragms locations are also shown in Figure 5.2-22.

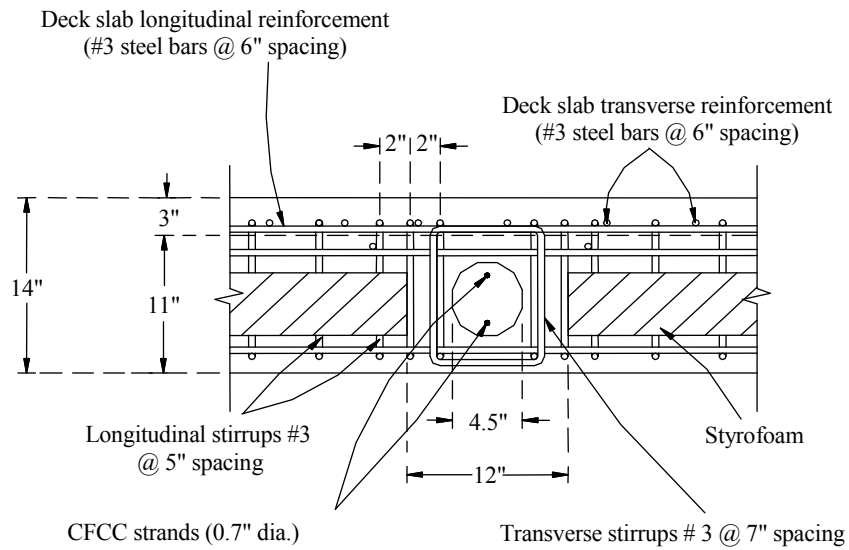


Figure 5.2-19 Cross-sectional details of intermediate diaphragm.

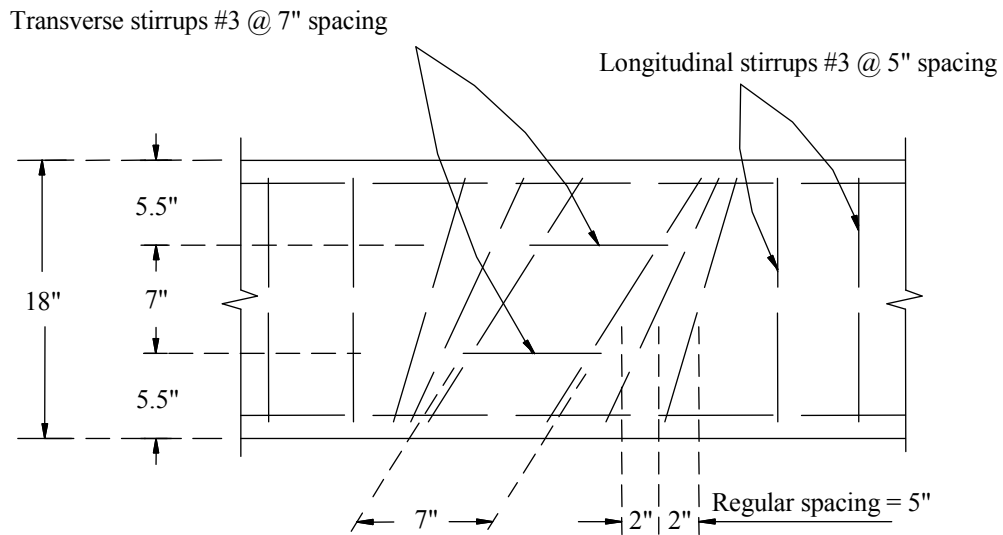


Figure 5.2-20 Reinforcement of interior box-beams at the intermediate diaphragm.

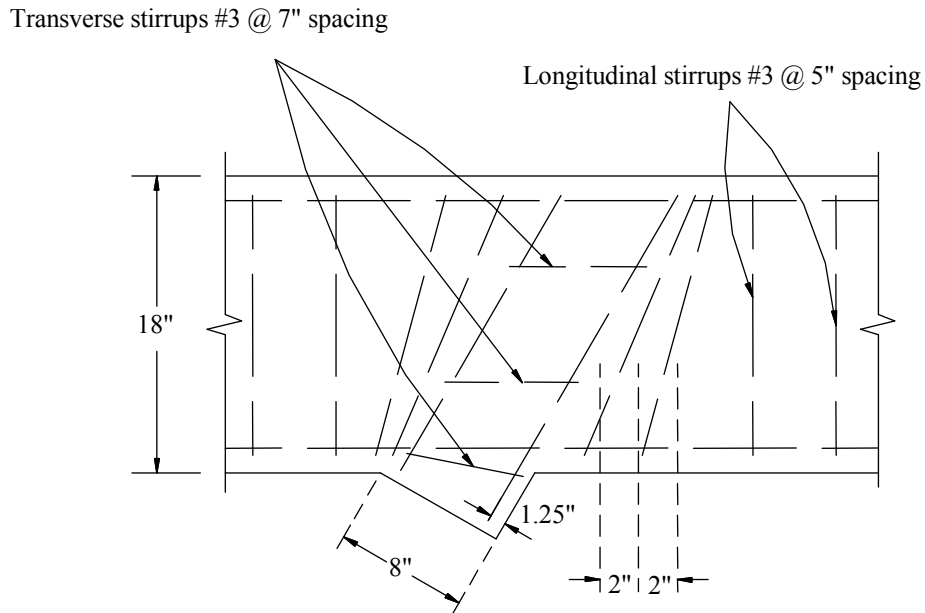
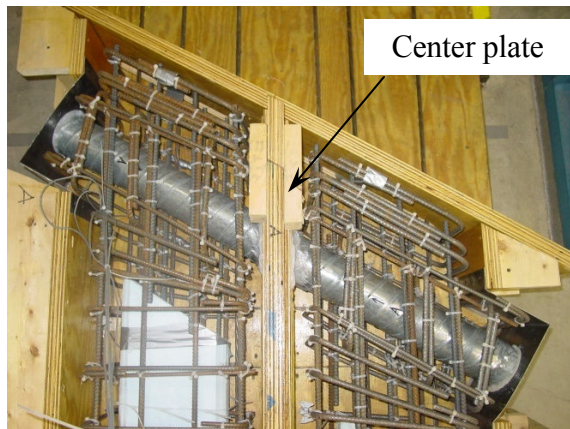


Figure 5.2-21 Reinforcement of exterior box-beams at the intermediate diaphragm.

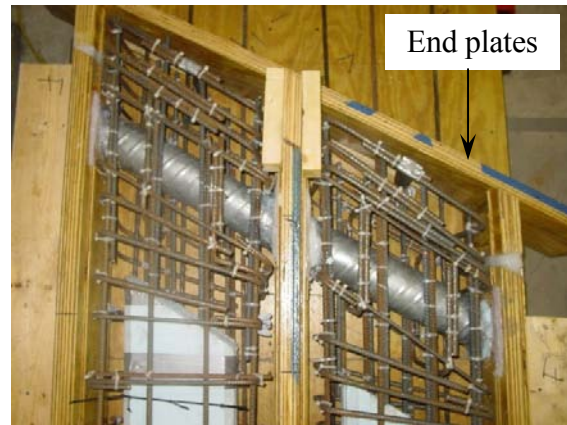
5.2.6 Prestressing of Steel Strands

After the construction of the steel cages and the formwork were completed, the steel cages were placed inside the formwork. Plastic chairs with effective height of 1.25 in. were attached to the underside cages to create the bottom concrete cover, subsequently, another set of chairs with effective height of 0.75 in. were also attached to either side of the cages to create the concrete cover along the sides.

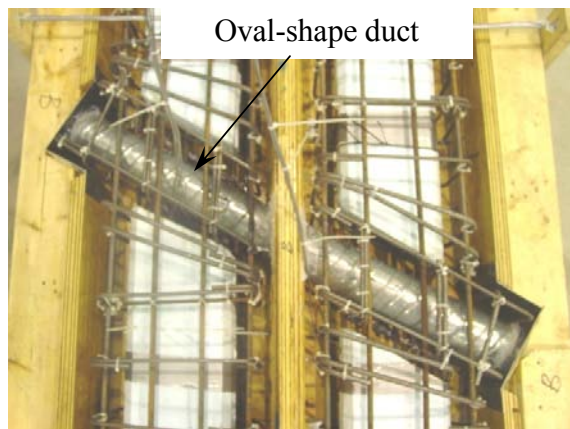
Bulkheads, needed for prestressing, were placed at both ends of the formwork, one set for the interior beams and one set for the exterior beams. Each bulkhead was anchored to the ground with six 1 in. diameter high strength bolts in order to transfer the pre-tensioning forces of the steel strands to the foundation. The steel strands were inserted through the holes of bulkheads along the length of box-beams. Conventional steel chucks were used as anchorage systems for the steel strands and attached at both the live and the dead-ends of the steel strands, as shown in Figure 5.2-23.



(a) End diaphragm for exterior beams



(b) End diaphragm for interior beams



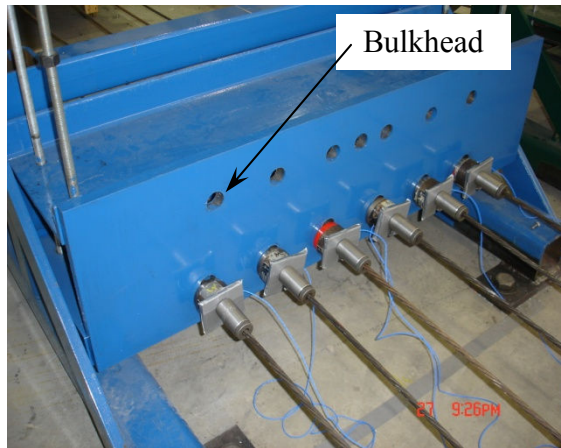
(c) Intermediate diaphragm for exterior beams



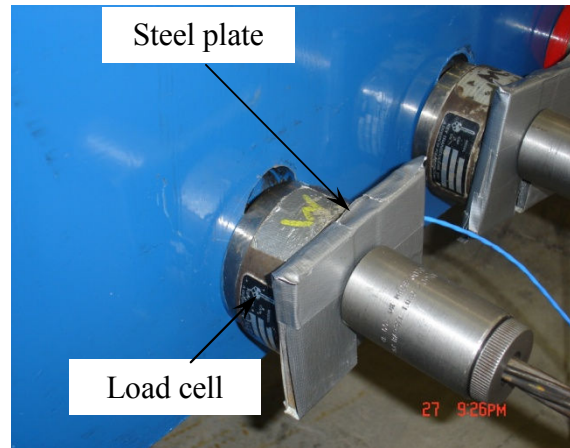
(d) Intermediate diaphragm for interior beams

Figure 5.2-22 Reinforcements and oval-shape ducts at the transverse diaphragms locations.

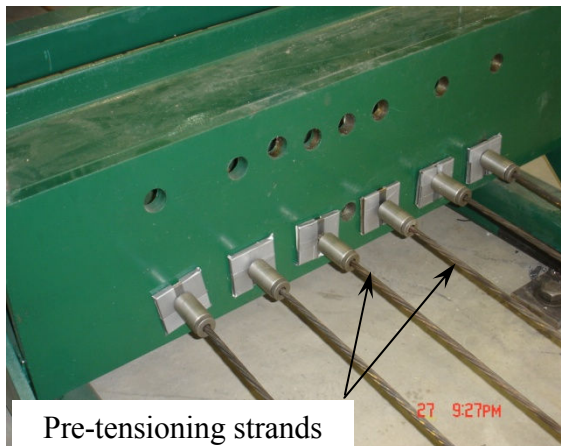
The live-end is the end of the box-beam where the strands are pulled while the other end is the dead-end. Center-hole load cell was attached to the dead-end of each strand to monitor the pre-tensioning forces applied to the steel strands during the pre-tensioning operation, as shown in Figure 5.2-23. The pre-tensioning sequence was designed to prevent the rotation of the bulkheads due to a possible eccentric reaction of the pre-tensioning force applied in the strands. Elongations of the steel strands were also measured to confirm the stresses developed due to pre-tensioning, as presented in Table 5.2-6. The pre-tensioning of the steel strands is shown in Figure 5.2-24.



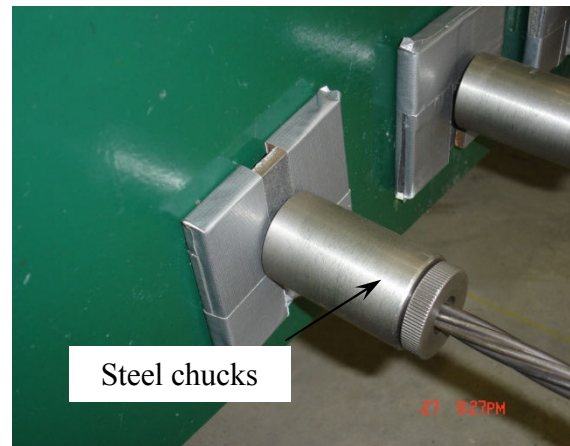
(a) Bulkhead placed at the dead-end



(b) Details of the dead-end for steel strands



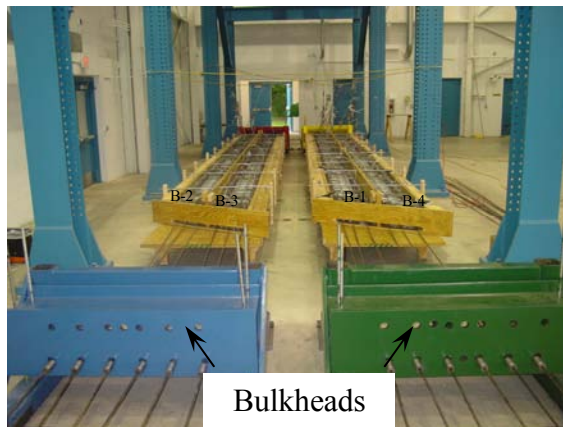
(c) Bulkhead placed at the live-end



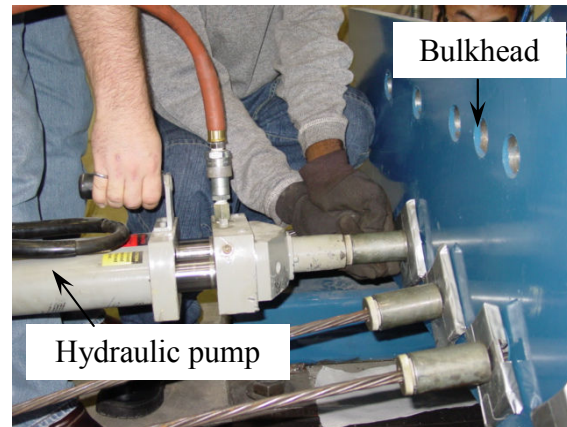
(b) Details of the live-end for steel strands

Figure 5.2-23 Instrumentation of the pre-tensioning steel strands.

In order to simulate differential camber observed in the field, the two exterior beams were prestressed with an average force of 20 kip/strand, i.e. 60 kip/box-beam, while the interior beams were prestressed with an average force of 25 kip/strand, i.e. 75 kip/box-beam. As a result, different levels of cambers were anticipated to occur at the mid-span of the exterior and the interior box-beams. The levels of prestressing measured during the casting of the concrete are shown in Table 5.2-6.



(a) Live-end for box-beams



(b) Prestressing of steel strands

Figure 5.2-24 Pre-tensioning operation at the live-end of the box-beam.

5.2.7 Concrete Placement

A ready-mix concrete was used to cast the four box-beams. As mentioned earlier, the concrete mix was designed to achieve the required strength and the proper workability. Two slump tests were conducted according to ASTM C143/C143 to confirm the required workability of the concrete during the casting process. One test was conducted just before casting of the box-beams and the other was conducted immediately after casting two box-beams. The designed slump was 8 in. The first measured slump was 9 in. and the second slump was 8 in.

In order to ensure uniform compaction, three electrical pencil vibrators were used, simultaneously. Moreover, mechanical rods were used around the diaphragm locations and the end-block locations where the steel reinforcements were closely spaced. The box-beams were cast in succession (one after the other) in order to avoid premature setting of a concrete. Twenty test cylinders, 6 in. diameter and 12 in. in height were cast. Ten of them were cast at the beginning of placing the concrete in the box-beams and the remaining ten were cast immediately after casting the first two box-beams. The total duration of the concrete placement was approximately two hours. Figure 5.2-25 shows slump test in progress and cylinders been formed. Figure 5.2-26 shows the casting and curing of the box-beams.

Table 5.2-6 Pre-tensioning forces and the corresponding elongations of steel strands.

Box-Beam	Strand	Pre-Tensioning Force, kip	Average Force per Strand, kip	Elongation, in.
B-1 (exterior)	1	21.79	20.90	3.52
	2	20.67		3.40
	3	20.25		3.75
B-2 (interior)	1	25.73	25.14	4.80
	2	24.6		4.63
	3	25.08		4.10
B-3 (interior)	1	24.83	24.87	4.85
	2	24.58		4.45
	3	25.20		4.30
B-4 (exterior)	1	19.19	20.3	3.25
	2	20.36		3.86
	3	21.40		3.38

The load cells were connected to the data acquisition system and the forces in the prestressing strands were monitored continuously for one week after casting the box-beams. The box-beams and test cylinders were cured using wet burlap covered with plastic sheets to prevent water from evaporation during the hydration process. The side plates of the box-beams were removed the following day to ensure proper curing by increasing the surface area exposed to moisture.



(a) Compaction of concrete during slump test



(b) Measuring of concrete slump



(c) Compaction of concrete cylinders



(b) Smoothing of concrete cylinders

Figure 5.2-25 Conducting concrete slump test and casting the cylinders.

5.2.8 Release of Pre-Tensioning Forces

The steel strands were cut from the bulkheads in order to transfer the compressive stresses to the concrete after it had attained adequate strength. As described earlier, compression tests were conducted on three test cylinders after 7, 21, and 28 days of casting of the box-beams to monitor the compressive strength of the concrete with time. Based on the results from the compressive strength test, it was determined that the concrete had gained the required strength after 21 days and hence the steel strands were cut. The sequence of cutting the strands followed the same as that of applying the pre-tensioning forces to avoid any rotation of the bulkheads. The steel pre-tensioning strands were cut using the standard shock de-tensioning method, in

which a hot, oxy-acetylene flame was used to melt the strands, as shown in Figure 5.2-27(a) and (b). The cutting operation was done simultaneously at both ends of the box-beam for each strand. No cracks were observed at the ends of the box-beams after cutting the prestressing strands.



(a) Vibration of concrete for exterior beam



(b) Casted box-beams



(c) Wetting of burlap for curing



(d) Covered box-beams

Figure 5.2-26 Placement of concrete and curing process.

One linear motion transducer was attached at the mid-span of each box-beam to measure the camber developed due to the release of pre-tensioning forces, as shown in Figure 5.2-27(c). The cambers recorded at this stage were 0.11 in. and 0.09 in. for the interior box-beams corresponding to the pre-tensioning force of 25 kip/strand. The cambers for the exterior box-beams were 0.02 in. and 0.05 in. corresponding to the pre-tensioning force of 20 kip/strand.

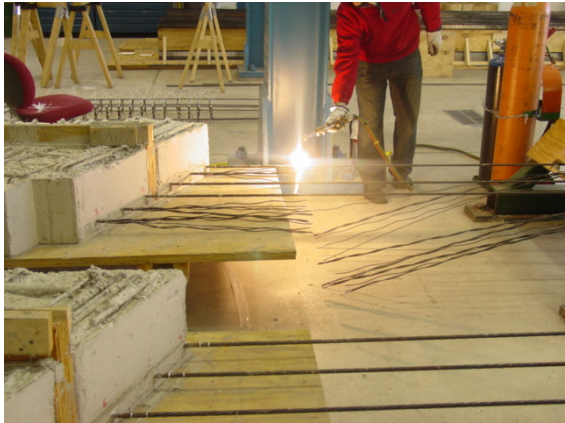
Demountable Mechanical (DEMEC) points were attached at both ends of the interior box-beams at the level of the prestressing strands to measure the compressive strains for the determination of the transfer length. The DEMEC points were not attached to the exterior beams because of presence of the protruded notches. Figure 5.27(d) shows the arrangement of the DEMEC points attached to the interior box-beams.

5.2.9 Transporting Precast Beams from Casting Yard to Test Frame

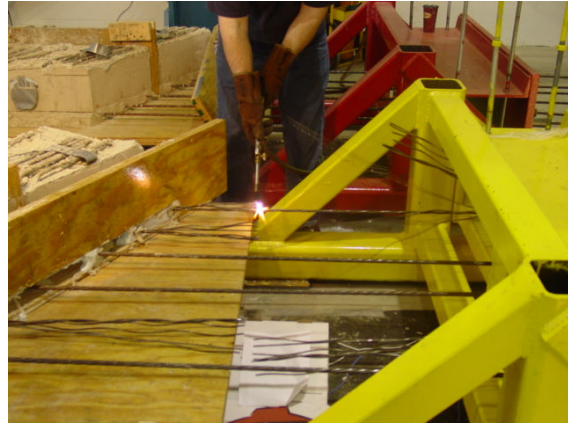
After cutting the steel strands, the four box-beams were removed from the formwork and transported from the casting yard at the CIMR to the STC, where they were tested. Each box-beam was lifted up from the four designed lifting points using crane which has a maximum capacity of 50 kip. At the STC, steel supports were arranged at 60° with respect to the longitudinal axis to simulate the skew angle of support lines of the bridge model. The steel supports were 14 in. wide, 54 in. long, and 30 in. high. Elastometric bearing pads, supplied by the Seismic Energy Products, L.P. Athens, Texas, with dimensions of 6 in. wide, 16 in. long and 1 in. thick, were placed between the box-beams and the steel supports. Figure 5.2-28 and Figure 5.2-29 show the transportation operation and alignment of the box-beams for the final arrangements of the bridge model.

5.2.10 Addition of Superimposed Dead Load

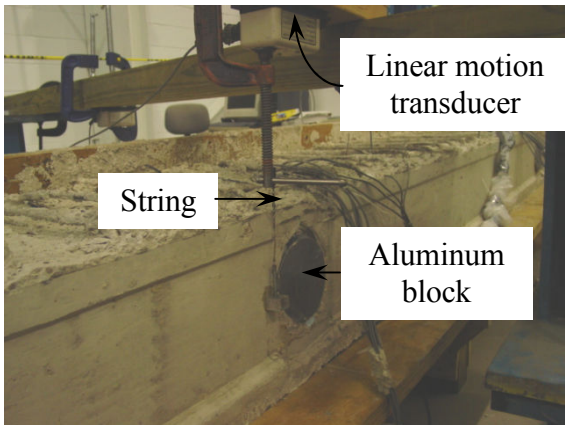
Figure 5.2-30 and Figure 5.2-31(a) show the box-beams aligned on the supports. In order to increase the differential camber developed between the interior and exterior box-beams, two superimposed dead loads each weighing 1,000 lb were placed on the exterior box-beams, as shown in Figure 5.2-31(b). The dead load was achieved by adding two tin containers, with diameter of 2 ft and depth of 3 ft, containing dry sand. The applied superimposed dead loads were placed at the mid-span of the box-beams in order to reduce the levels of camber of the exterior box-beam, and hence increase the differential camber between the interior and exterior box-beams to the order of 0.38 in. The superimposed dead loads were removed after a week. The cambers in all the four box-beams were continuously monitored for a period of three weeks and the results are discussed in the following chapter.



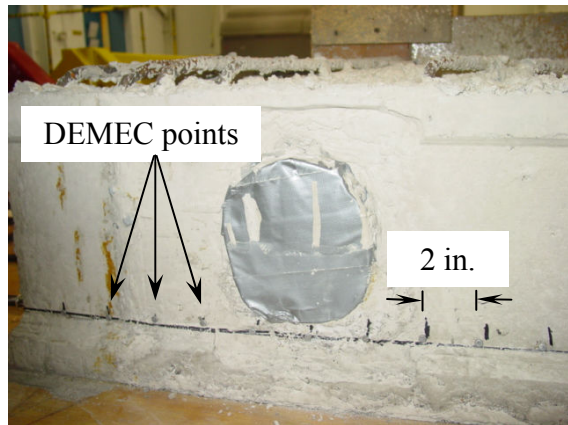
(a) Cutting of steel strands at live-end



(b) Cutting of steel strands at dead-end

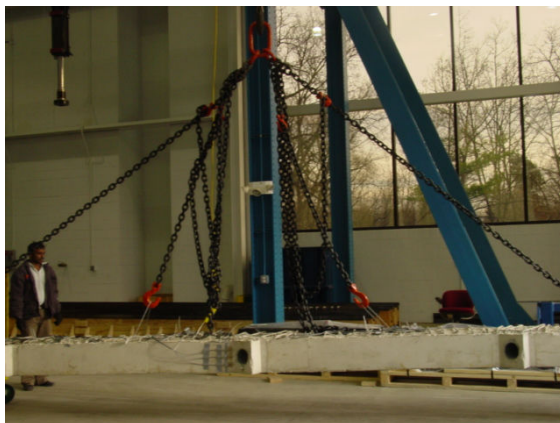


(c) Linear motion transducer at mid-span

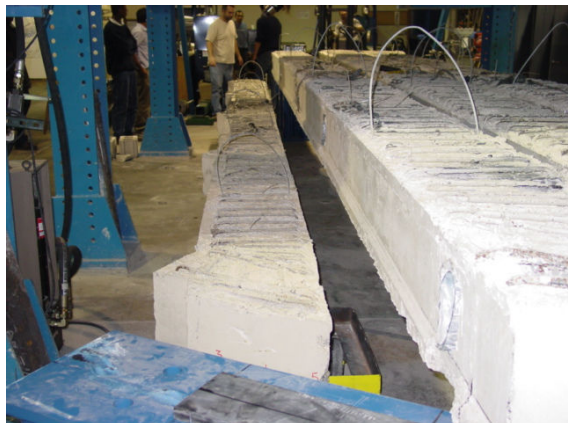


(d) DEMEC points at the end of box-beam

Figure 5.2-27 Instrumentation on box-beams and shock de-tensioning of steel strands.



(a) Box-beam lifted using crane



(b) Placing box-beam on supports

Figure 5.2-28 Transportation of precast box-beams to the STC.

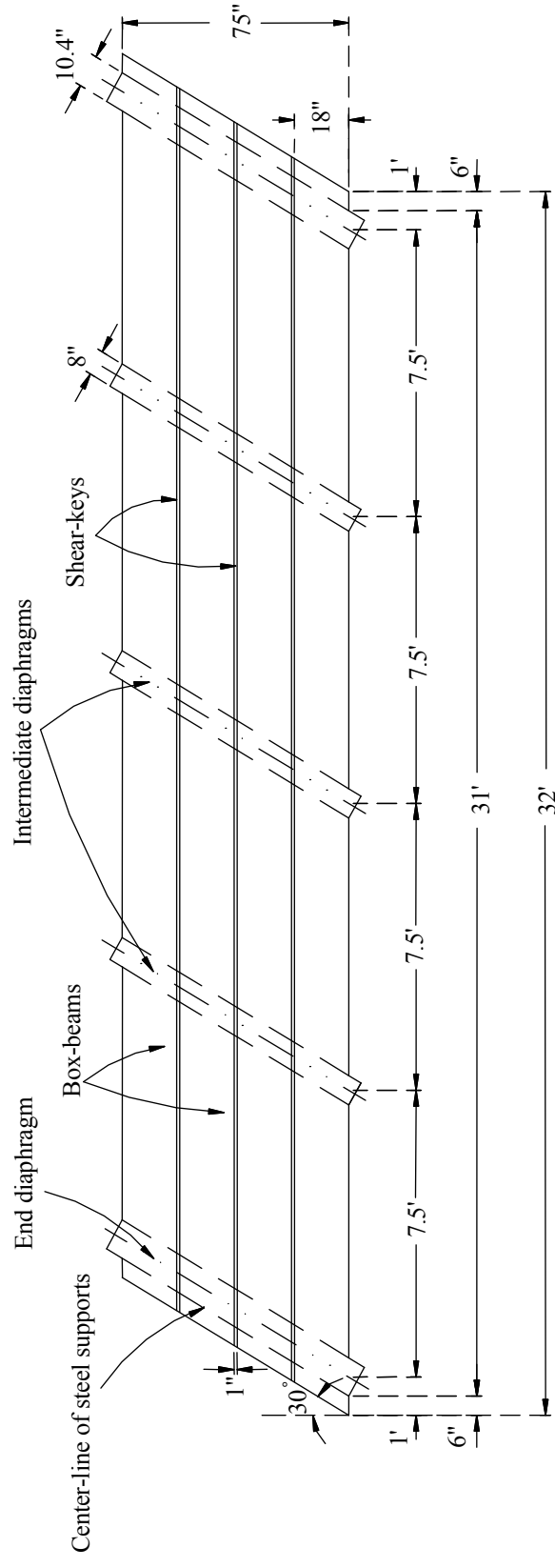
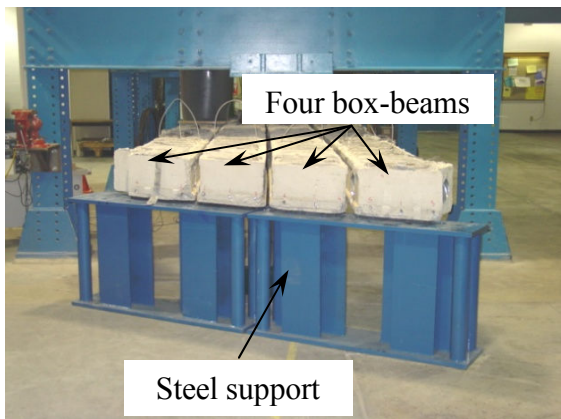


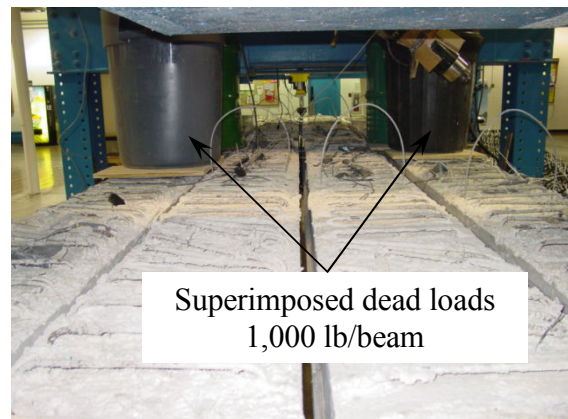
Figure 5.2-29 Plan view of the box-beams.



Figure 5.2-30 Aerial view of the four box-beams.



(a) Four box-beams on supports



(b) Dead loads placed on exterior beams

Figure 5.2-31 Box-beams placed side-by-side and adding superimposed dead loads.

5.2.11 Deck Slab Construction

5.2.11.1 Formwork Construction

After the superimposed dead loads were removed, the keyways were formed between the beams with top and bottom widths of 2 in. and 1 in., respectively. Styrofoam gaskets were attached at the ends of each transverse duct opening between adjacent beams, as shown in Figure 5.2-32, to avoid the possible leakage of the shear-key grout into the ducts and to ensure the continuity of the ducts.

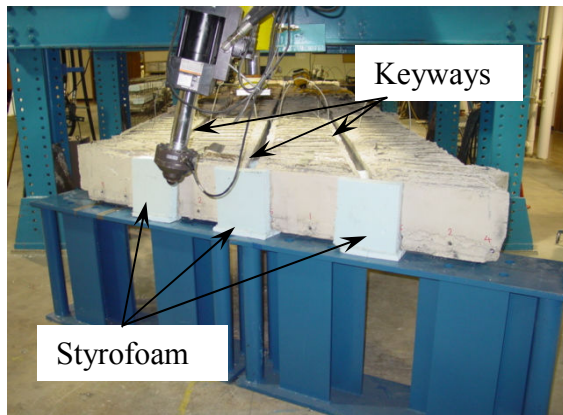
5.2.11.2 Shear-Key Casting

The shear-keys were constructed using Five Star Structural Concrete 300[®] (FSSC), manufactured by Five Stars Products Inc. The shear-keys were cured with wet burlap and plastic sheets. A bag of FSSC weighed 150 lb yielding 0.42 ft³ at maximum water content of 0.1 ft³. The construction and curing processes are shown in Figure 5.2-33. The properties of the FSSC as provided by the manufacturer are listed in the Table 5.2-7 and the gain of compressive strength of the shear-key grout is shown in Table 4.2-8.

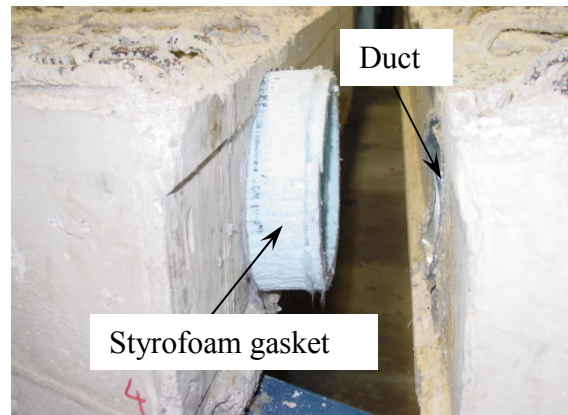
Table 5.2-7 Mechanical properties of FSSC.

Compressive strength, psi	7,000 after 7 days 8,000 after 28 days
Bond strength, ASTM C882, psi	2,500 after 7 days
Linear length change, ASTM C157	+0.03% after 28 days (wet) -0.05% after 28 days (dry)
Thermal co-efficient of expansion, ASTM C531, in./in./°F	5×10^{-6}
Chloride ion permeability, ASTM C1202	< 1,000 Coulombs

The initial TPT forces were then applied on the box-beams after five days of curing of the shear-keys. The purpose of the initial TPT was to prevent any relative movement between the adjacent beams prior to casting the slab. An average force of 6 kip was applied to each steel strand, as shown Figure 5.2-34(a).

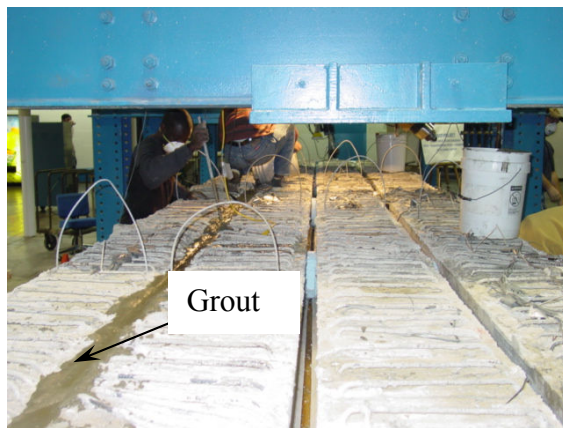


(a) Sealed keyways ends

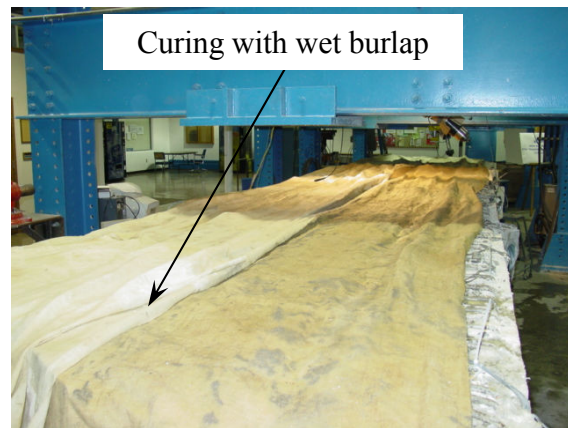


(b) Styrofoam gaskets attached to the ducts

Figure 5.2-32 Preparation of keyways before casting of shear-key.



(a) FSSC placed inside keyways



(b) Curing of shear-keys

Figure 5.2-33 Construction of shear-key using FSSC grout.

5.2.11.3 Deck Slab Reinforcement

The formwork for the deck slab was prepared. The reinforcement grid for the deck slab contained conventional #3 deformed steel bars spaced 6 in. center-to-center in the longitudinal and transverse directions of the bridge model. The deck slab reinforcement was attached to the protruded stirrups using zip-ties, as shown in Figure 5.2-34(b).

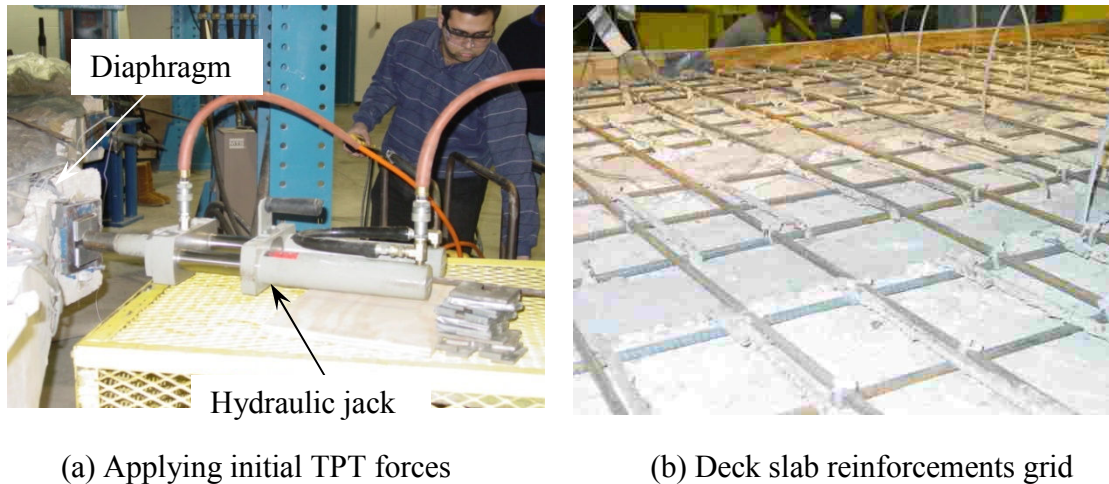


Figure 5.2-34 Application of initial TPT forces and casting of deck slab.

5.2.11.4 Placing of Concrete

The cast-in-place deck slab was 3 in. thick constructed using MDOT recommended ready-mix concrete supplied by the McCoig Concrete Products [Figure 5.2-35(a)]. This mix design was approved by Michigan Department of Transportation (MDOT) project manager. The proportion of the concrete mix used is shown in Table 5.2-9. The deck slab was then allowed to cure under wet burlaps covered with plastic sheets, as shown in Figure 5.2-35(b). The average compressive strength of the concrete used in casting of the deck slab after 28 days was 4,600 psi. Figure 5.2-36 shows the details of the bridge model cross-section after completing the deck.

5.2.12 Construction of Additional Exterior Box-Beam

An additional exterior box-beam was constructed and used as a replacement for the “assumed-damaged” exterior box-beam from the bridge model. The main objective was to study the process of replacing a damaged exterior box-beam of the bridge on the distribution of the applied vertical load in the transverse direction. The procedures used during the construction of the former box-beams were also followed to construct the new exterior box-beam (see Figure 5.2-37).

Table 5.2-8 Compressive strength of shear-key grout.

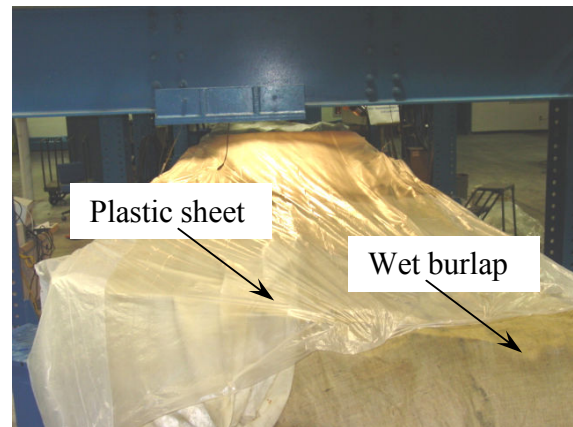
Time, Days	3	7	14	28
Average compressive strength of grout, psi	4,350	6,200	7,250	7,750

Table 5.2-9 Concrete mix proportions for deck slab.

Material	Design Quantity per Cubic Yard, lb	Total Quantity, lb
Fine aggregates	1,390	2,840
Coarse aggregates	1,741	3,564
Cement (Type 1)	342	680
Cementitious material	184	400
Water reducing admixture	1	16
High range water-reducer	8	84



(a) Casting of deck slab for the bridge model



(b) Curing of deck slab

Figure 5.2-35 Casting of deck slab concrete and curing process.

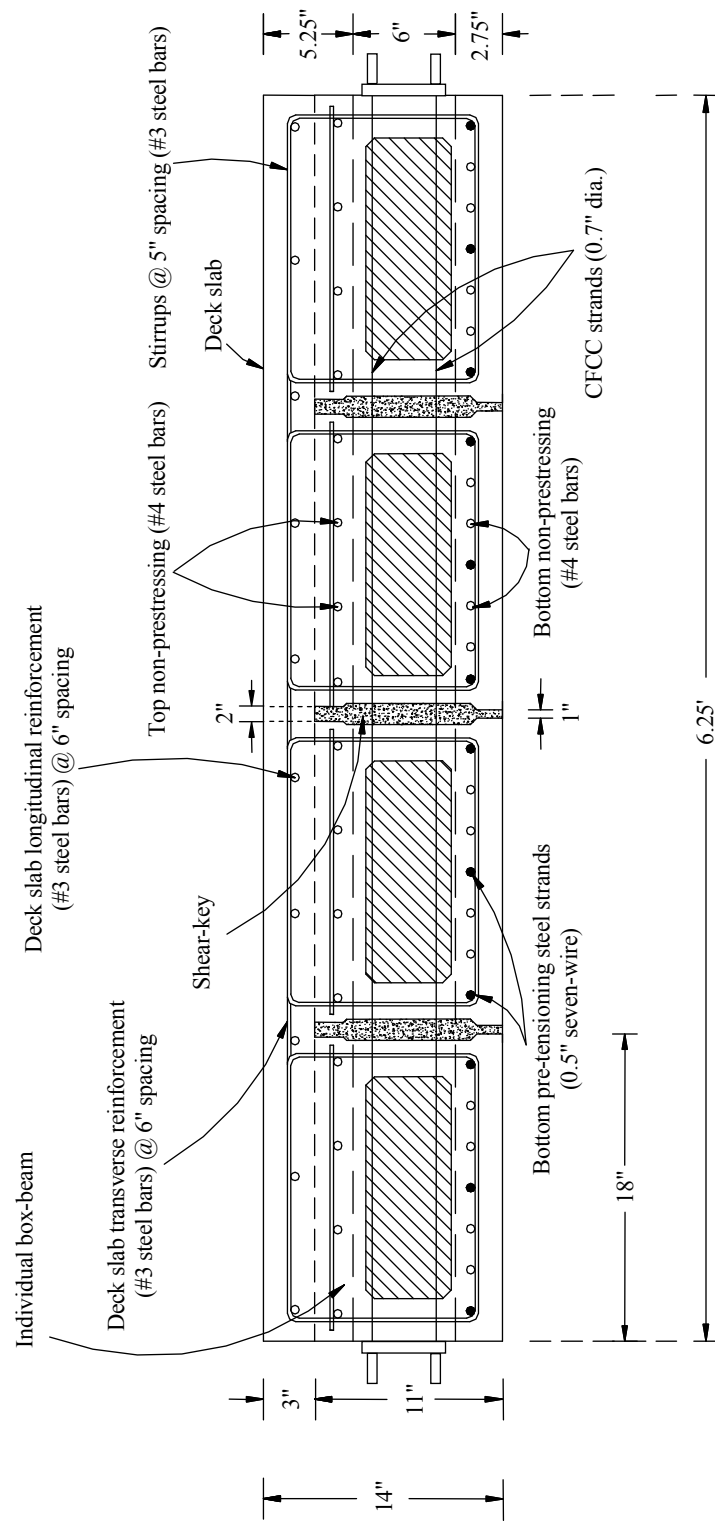


Figure 5.2-36 Cross-section of the completed box-beam bridge model.